

Copyright
by
Michael Elazar Legatt
2016

The Dissertation Committee for Michael Elazar Legatt Certifies that this is the approved version of the following dissertation:

An Experimental and Analytical Method for Assessing the Integration of Electric Vehicles into the Bulk Power System

Committee:

Ross Baldick, Supervisor

Michael Webber, Co-Supervisor

K. Suzanne Barber

Arthur Markman

Surya Santoso

**An Experimental and Analytical Method for Assessing the Integration
of Electric Vehicles into the Bulk Power System**

by

Michael Elazar Legatt, B.A.; M.A.; M.S.E.; Ph.D.

Dissertation

Presented to the Faculty of the Graduate School of

The University of Texas at Austin

in Partial Fulfillment

of the Requirements

for the Degree of

Doctor of Philosophy

The University of Texas at Austin

December 2016

Dedication

To my wife, best friend, and muse Caroline, and to our amazing children Caleb, Eliana and Zachary, parents Alan, Liz, Martha & Clif, and grandparents Herb, Lilly, Stanley and Edith, and siblings Joel, Rachel, Aviva and Will. Thank you for sharing me with this work, and for being so supportive and encouraging throughout this long process. Thank you for being a constant source of strength, and encouraging me to always learn and grow.

To my grandma Edith's memory: as a student and teacher of history, she would appreciate the amazing power society has to bring about a brighter future. To my grandma Lilly's memory: she always found ways to bring people together, and would appreciate the new ways people can connect to the world around them. To my grandpa Herb's memory: he would appreciate the ways our economy and energy continue to grow together, and the new opportunities that are coming available to the next generation of students, who will one day become a generation of teachers. To my grandpa Stan's honor: I hope you enjoy the work, and as many times before, see it as an opportunity to make the world a better place, even when it's not easy or requires thinking differently.

To the memory of my first boss, mentor, and dear friend John Lightstone, who always found in his background in physics a tremendous beauty in the world around us, and in his economics background, the ceaseless belief in people and society. As a person who loved and strived for building bridges and creating peace around him, I thank you for inspiring me to try and make a piece of the world a little better, and hope you would have been proud.

To the memory of my first ERCOT boss, mentor, and dear friend Gary Macomber, thank you for seeing the potential that a psychologist could have working in the energy world

and believing I had a potential to help. I am still shocked that, thirteen years after being in an emergency operations center after the 2003 Northeast Blackout, I have the joy of working to support the building of a resilient grid into the future, and supporting the crucial flow of electricity that our society so depends on. Thank you for your belief and trust in me, and for always encouraging me to grow and do more. I hope the work in this research, and in the work I strive to continue that we started together, would have made you proud.

To my amazing colleagues and friends at ResilientGrid, ERCOT, University of Texas at Austin, North American Electric Reliability Corporation, Department of Energy, Austin Energy, Electricity ISAC, Pecan Street Project, Circular Energy, Energy Thought Summit, Lightstone Capital Management and the Environmental Defense Fund. Thank you all for encouraging and supporting my research, and sharing me with it.

To my mentors and role models through the years: John Adams, Kelly Blackmer, Ross Baldick, Bill Blevins, Les Bronstein, Pam Butler, Earl Carnes, Sam Chanoski, Trip Doggett, Theresa Gage, Ron Henderson, Rachel Kobrin, Joel Koepke, John Lightstone, Gus Lott, Gary Macomber, Bill Magness, Art Markman, Jake Mazulewicz, James Merlo, Joel Mickey, Juliana Morehead, John Moseley, Diran Obadina, Jodi Heintz Obradovich, Lance Ransom, Woody Rickerson, Dottie Roark, Emek Sadot, Robbie Searcy, Rizwan Shah, Alison Silverstein, Bob Stoll, Dave Tuttle, Paul Wattles, Greg Woods, Michael Webber and Vance Zemon – just to name a few (there are so many more). Thank you for being continual sources of knowledge, inspiration and encouragement.

To Larry Alford – thank you for presenting about your research on electric vehicle emissions. Sitting in that audience back in April 2010 changed the course of my career,

and I've loved every moment of it. To everyone in Austin Energy's Electric Vehicles & Emerging Technologies group, Pecan Street Project, University of Texas at Austin and Electric Reliability Council of Texas who have worked with me on Electric Vehicles these past several years, thank you for so many opportunities to learn more, collaborate, and dream of a future together.

To the Human Performance Communities of Practice in the electric power sector, such as NERC's Improving Human Performance on the Grid, WECC Human Performance, and so many others: thank you for building a strong, sustainable community around the principles of empowering people in our industry to foster safety, reliability, resilience, and continuous improvement, all while recognizing the humanity in all the amazing people who do amazing things every day. It is an honor to be part of this family.

To Drs. Baldick and Webber, thank you so much for supporting me and this research, and for providing continual insights, encouragement, patience with my busy schedule and so many opportunities to learn so much. To my fellow students in Dr. Baldick's Energy Systems Engineering group and in the Webber Energy Group, thank you for so many stimulating conversations and opportunities to grow. Thank you in particular to Mahdi Kefayati, Dave Tuttle, and Robert Fares for always-fascinating discussions around electric vehicles and their potential futures. Thank you to Melanie Guilick, for your constant support, encouragement, great advice and patience through these past several years.

Acknowledgements

To Steve Grendel, Wes Holt, John Waters, Julie Ringling, Brittany Barcuch, Scotty Clifton, Robert Lopez, Anthony Barcuch, Rob Stanford, Ernie Gray, David Bailey, and Mark Sprowl, thank you so much for installing, supporting and growing the research platforms at our Taylor and Austin sites. Thank you to everyone at ERCOT who supported this research, provided encouragement, moral support, and even the opportunity to alter some of your cars' charging behavior.

To Scott Hinson, Brewster McCracken, Richard Smith, and all of Pecan Street Project, thank you so much for your never-ending support of this research project, for working together to develop the J1772 intercept board, and for support during its firmware development. This research would not have been possible without all of your support, insights, and time.

To Megan Germann, Marina Dultra, and Hunter Estes, thank you for sharing your internships with me, and for all of your hard work to get the ERCOT Electric Vehicle research project up and running.

To Dr. Calderon-Garciduenas, thank you for your years of work bringing awareness to the public health implications of ultrafine particulate in Mexico City, and for sharing your research and time with me to discuss UFPM.

Thanks to the National Science Foundation and its support of Pecan Street Project and the Electric Vehicles: Transportation Electricity Convergence groups who in turn supported this research.

“לא עֲלִידָהּ הַמְּלָאכָה לְגִמּוּר, וְלֹא אַתָּה בֶּן חוּרִין לַהֲבַטֵּל מִמֶּנָּה” - “It is not your responsibility to finish the work (of repairing the world), but neither are you free to desist from trying” -

Pirkei Avot, 2:21.

An Experimental and Analytical Method for Assessing the Integration of Electric Vehicles into the Bulk Power System

Michael Elazar Legatt, Ph.D.

The University of Texas at Austin, 2016

Supervisors: Ross Baldick, Michael Webber

In recent years, several trends are indicating a move towards a very different bulk power system. Increased integration of renewables, energy storage, synchrophasors, microgrids, Internet of Things devices, and electric vehicles are increasing the complexity of the system. While these changes have the potential to lead to significant reductions in environmental impact and peak demand growth, they also require significantly stronger, granular, and faster-moving controls to ensure reliability and resiliency.

Previous research shows that electric vehicles have the potential to significantly reduce global (e.g., CO₂), and regional (e.g., particulate) emissions associated with transportation. As fast-responding flexible loads, it was hypothesized that electric vehicles could participate in reliability-centric markets. To study the integration of these vehicles into the bulk power system, this project involved building an experimental charging system for electric vehicles with bulk modeling of the electric grid. This research test bed was developed in Taylor, Texas, to analyze real-world behavior of EVs in response to control signals.

The diverse group of participating vehicles provided rapid response between 1/6 and 1/2 second, suggesting a strong capacity for providing grid reliability services. Successful real-world tests of primary frequency response and dispatched load control highlight the scalability of this approach. Vehicle charging patterns (as measured by load ramp and current waveform at peak) were observed to be clustered by vehicle make,

indicating predictive value of high-resolution waveform measurement at the beginning of a charging session.

Simulation of a network with intermittent renewables shows that inclusion of these rapidly responding EVs can strengthen system stability in normal, black start, and islanded situations. It shows that controlled EV charging can provide reliable means for improved renewables integration. The aggregation of electric vehicle charging can certainly provide fast-responding services that provide frequency support, congestion management, synthetic inertia, and many other useful services of significant value to the reliability of the bulk power system.

Table of Contents

List of Tables	xvii
List of Figures	xviii
CHAPTER 1: INTRODUCTION	1
Motivations	1
Objectives	2
CHAPTER 2: BACKGROUND	5
Vehicle Electrification	5
Description and History	5
Electric Vehicle Charging Technologies	8
Psychological Factors associated with the bulk power system.....	10
Situational Awareness.....	10
Time differential disconnect between usage and payment	11
Disconnects from status of transmission, distribution, generation systems..	12
Range Anxiety and driver mental models.....	13
“Curse of the default”	14
Moral self-regulation and pro-environment / pro-reliability decisions.....	15
Social and Financial Domains	15
A Growing Dynamic System from the Holistic Perspective	16
Changing paradigms of control.....	18
Nano-and Micro-Grid islanding.....	18
Fast-responding local telemetry protocols	19
Modbus	19
DNP3 / IEEE 1815-2012	20
IEC 61850	21
Distributed (e.g., Blockchain) recordkeeping and settlements	22

Previous Research on Electric Vehicle to Grid Integration	23
Challenges with the Current State of the Art	24
Local response of electric vehicles	25
Synchrophasor integration: local and remote	25
On-peak charging.....	27
“Birthday cake” curve.....	29
“Duck” Curve.....	31
Research Goals.....	33
CHAPTER 3: ELECTRIC VEHICLE CHARGING MODELS	35
Introduction.....	35
Synchrophasor Measurements	35
Electric Vehicle Charging Strategies	36
Immediate charging	36
Delayed charging	38
Reliability-supported charging.....	38
Generation Data-linked charging.....	39
Renewable integration/offset Charging	40
EVSE Data-linked charging.....	40
Average Rate charging.....	41
Ancillary Services and Average Rate Charging	42
Local frequency response and average rate charging	42
End-user protections in EV aggregation.....	43
“Trust No One” EV charging concept	46

Conclusion	55
CHAPTER 4: ELECTRIC VEHICLE CHARGE CONTROL IN SITU	56
Introduction.....	56
Methodology.....	56
ERCOT Electric Vehicle Research Project.....	56
Participants.....	57
J1772 Intercept Board	58
Mobile Application Design.....	59
Server Hardware Selection	60
Server Software Design	61
Results.....	62
Early Experiments: eGauge and Chargepoint API with custom software....	62
Nissan Leaf with manual control signals	62
Chevrolet Volt under a PV envelope, cellular network only	63
Hardware Intercept Board and High-Speed Charge Control Experiments...66	
Charging under a PV envelope, local high-speed control.....	67
Local Frequency Response with droop control	68
Vehicle Charging Observations	72
Conclusion	74
Afterword.....	75
Service quality considerations	75
System stability considerations.....	76
Peak shaving considerations	77
Emergency responsiveness considerations	78

CHAPTER 5: SIMULATION OF ELECTRIC VEHICLE AGGREGATION FOR STABILITY SERVICES	79
Introduction.....	79
Methodology.....	79
Components	80
Neighborhood microgrid.....	80
Synchronous Machine.....	80
Photovoltaic array	81
Wind Turbine	83
Home.....	83
Electric Vehicle.....	84
HVAC Unit	86
Results.....	87
PID controller With Deadband	87
Droop Controller with Deadband.....	88
Blackstart Simulation with EV PID controller	88
Blackstart Simulation with Droop Controller	89
Control Simulation against an oscillating load	90
Conclusion	92
CHAPTER 6: DISCUSSION	93
Summary of key findings.....	93
Additional Considerations	95
Revenue-grade telemetry	95
Control/data integration point: EV or EVSE?	96
Electric Vehicle (EV) to Electric Vehicle Supply Equipment (EVSE) integration	97
Local control-and-report versus centralized control.....	98
Electric Vehicle Supply Equipment to Electric System Integration	99
Fast-responding services.....	101

Blockchain or other distributed accounting for System Operator/EVSE/EV integration	102
Committed Time to Charge/ Simplification for driver	103
Ultracapacitors and EV/PV buffering	104
Future Work	105
Hardware enhancements	105
Firmware enhancements	106
Software enhancements	106
Electric Vehicle Driver to Real-Time Energy Market Integration	107
Behavioral Economics of Electric Vehicle demand response services	108
Driver Situational Awareness and Altruistic Behavioral Change.....	108
APPENDICES	110
Appendix A: Emissions and Human Health	111
Particulate Matter.....	111
Smog	112
Internal Combustion Engine (ICE) engines	113
Bridge Apartments: Ultrafine particulates and neuropsychological functioning	114
Mexico City and Ultrafine particulate matter	116
Approaches to Emissions Reduction	117
Austin Energy and per-mile emissions reductions.....	117
University of Texas: Vehicle electrification impacts on emissions...	118
Appendix B: J1772 Intercept Board	120
Custom Hardware Layout	121
Voltage input and processing.....	122
Current input and processing	126
EVSE to board PWM signal input and processing	127
EV to board PWM signal input and processing.....	129
Printed Circuit Board Design.....	129
Firmware Design.....	129

Clock synchronization	130
Waveform Capture.....	130
Data computation	130
Finite State Machine	131
Appendix C: Institutional Review Board (IRB) Proposal	133
BIBLIOGRAPHY	155
VITA	162

List of Tables

Table 1 : J1772 Pilot Signal voltages and resistances [10].....	9
Table 2: "Swim lanes" for EV-EVSE-Aggregator communications	47
Table 3: ERCOT Test Bed Responsiveness to Emergency Energy Alerts (EEA)	78
Table 4: J1772 Intercept Board Finite State Machine (excluding diagnostic and test modes).....	132

List of Figures

Figure 1: Thomas Edison next to the 1914 Detroit Electric plug-in electric vehicle [9]	6
Figure 2: J1772 pinouts for Level 1 and Level 2 charging (Eric Tischer).....	8
Figure 3: A psychological framework of range anxiety [15].....	14
Figure 4: Growth of ERCOT Wind Capacity [25].....	17
Figure 5: Examples of ERCOT system and a home's load based on ambient temperature	27
Figure 6: The Birthday Cake Curve, with on-peak EV charging (red) and HVAC usage (blue).....	31
Figure 7: The California "duck curve" as a result of DER growth.....	33
Figure 8: The installation of components adjacent to the breaker panel (early installation)	60
Figure 9: Nissan Leaf response to varying levels of DR commands.....	63
Figure 10: An example of EVSE remote control to charge an electric vehicle under a PV envelope.....	65
Figure 11: Control loops involved in follow-solar strategy.....	66
Figure 12: Local EVSE control charging an electric vehicle under a PV envelope	68
Figure 13: Simulated droop Response with a deadband of 59.95 to 60.06.	69
Figure 14: Simulated droop Response with a deadband of 59.99 to 60.01.	70
Figure 15: Actual vehicle response to historic values, with deadband of 59.99 to 60.01	71
Figure 16: Current profiles for a 2014 Chevrolet Volt, 2013 Tesla Roadster, 2012 Ford Focus Energi, and 2015 Nissan Leaf.....	73

Figure 17: Current waveforms for a 2014 Chevrolet Volt, 2013 Tesla Roadster, and 2012 Ford Focus Energi.....	74
Figure 18: ERCOT hourly system load by season. Calculated from [42]	77
Figure 19: Dynamic Electric Vehicle charging to offset heavy renewables and limited microturbine ramp rate capabilities	89
Figure 20: An oscillating load whose demand is met through a microturbine only	90
Figure 21: A view of the Bridge Apartments, New York City [70]	115
Figure 22: Dog (left) and human (right) MRI studies in Mexico City participants	117
Figure 23: Austin Energy emissions comparison between tailpipe and smokestack	118
Figure 24: Anticipated coal-powered unit retirements 2014-2025	119
Figure 25: The pinouts of the Arduino Due.....	121
Figure 26: Circuit design for $9V_{AC}$ input and rectification to $12V_{DC}$ to power the hardware.....	123
Figure 27: Simulation of $9V_{AC}$ to $12V_{DC}$ Rectification	124
Figure 28: Voltage distortion shown in the initial design.....	125
Figure 29: Voltage distortion repair in the modified circuit, with inverting op-amp	126
Figure 30: Current measurements on the J1772 intercept board	127
Figure 31: Circuit design for the communications between board and EVSE	128
Figure 32: The PCB layout of the J1772 intercept board.	129

CHAPTER 1: INTRODUCTION

Motivations

Electric vehicle sales are on the rise, and under certain scenarios these vehicles offer environmental and security benefits to society. These electric vehicles also have the potential to offer fast-responding reliability-enhancing services to the bulk power system. This is an understudied topic; therefore, this dissertation seeks to address a few key aspects about their adoption. This includes a combination of experimental and analytical methods, and analysis of how intelligent EV charging could play a role in a “smarter grid”, based on a research test bed of hardware, firmware, and software that was developed for this effort.

In recent years, several different motivations and opinions have started to converge around the electrification of the transportation sector. 30.5% of CO₂ emissions between 1990-2013 are attributed to the transportation sector [1]. The fossil fuel contributions to electricity generation and thus electric vehicle charging are primarily domestic, thus transitioning from a perceived imported fuel (gasoline) to a perceived domestically sourced fuel (although this common perception is not entirely accurate). Certainly, though, local energy markets are less connected to international markets than gasoline, and thus less variable.

Adding electric vehicles also allows for greater contribution of intermittent renewable resources into the fuel mix, thus reducing the overall emissions per mile driven (e.g., [2], [3], [4]). Electric vehicles have, on average, fewer parts at risk of failure, with growing possibilities for non-vehicular uses of its primary cost component, the lithium-ion battery pack, when it is no longer suitable for vehicular use. Electric Vehicle (EV) prices have significantly dropped in cost from 2011-2015, indicating likely economies of scale, as well as continued innovations and economies of scale around its battery packs [2].

Since the 2011 release of the mass market Chevrolet Volt and Nissan Leaf, electric vehicle driving patterns, battery degradation, and efficiencies continue to be studied. These vehicles are far more than transportation devices, incorporating cellular connectivity, satellite navigation, and power electronics that could be leveraged to improve (or at least

not negatively impact) the bulk and distribution power systems to which the vehicles are connected. Studies indicate that at least 86% of vehicle trips can have their miles fully served by battery electric vehicles [5].

At the same time that electric vehicles are decreasing in cost (along with their primary cost component, the lithium-ion battery), the cost of photovoltaics are also decreasing. These factors have led to a promulgation of distributed energy resources throughout the state of Texas. If one has a goal of decreasing emissions, whether at the global (CO₂) or local (SO_x, NO_x, PM₁₀, PM_{2.5}, UFPM) levels, it may seem growing levels of wind and solar generation throughout the state would suffice. However, when one takes into account the differences in efficiencies between the internal combustion engine (ICE) and bulk power system, electric vehicle motor, battery and conversion systems (21% vs. 62%; [6]), shifting transportation to the bulk power system can produce a far more significant reduction in statewide emissions (e.g., [2], [4]). Of further benefit, this change would shift the emissions that are most harmful to human health farther away from major population centers, and offer both economies of scale and simplified scaled management of overall emissions.

Objectives

This proposal builds beyond the author's M.S.E. thesis work, in which it was demonstrated that electric vehicle charging, especially with intelligent and grid-interactive charging (avoiding peak, decision making on marginal units, etc.) and distributed energy resources such as rooftop photovoltaics, can reduce per-mile vehicle CO₂ emissions by over 80%, NO_x by over 41%, PM₁₀ by 73%, and UFPM / PM_{2.5} by 62%, and further distance the minimally-traveling particles from major population centers. It further highlights that at the neighborhood perspective (miles driven and electrical use), vehicle electrification offers greater than a 65% emissions reduction.

However, for society to reap these kinds of benefits, several different approaches to the management of the bulk power system can be employed. In some, infrastructure would continue to grow, both with massive growth in fossil fuel generation and

transmission towers (to offset consumer vehicle charging on peak), with exceptionally high internal and external costs to society. Hidden in this approach, one would anticipate actually a decrease in the reliability of the system, in the sense that an on-peak outage, especially when incorporating dynamic factors such as congestion and subsynchronous oscillation, could destabilize the centrally-fed system very quickly.

An alternate solution would instead to employ a new philosophy of grid management, one in which every device and individual on the grid is, in some sense, a participant, in the bulk power system as a whole. From that perspective, one can think of the distribution systems as becoming bidirectional in two fashions, first serving to push back from the distribution system onto the transmission system at times through distributed resources, and second serving to have a data conversation with the reliability coordinator¹ in terms of scheduling and participation in real-time and ahead-looking energy and ancillary markets. In this paradigm, therefore, all energy demands with flexible power requirements can work together, either in a small-local or global-grid fashion to avail themselves of the state of the grid, offsetting intermittent renewables, and dynamically working together to ensure the continual reliable function of the system. These metrics are the typical ones viewed by a reliability coordinator, such as the ERCOT Independent System Operator, which manages the bulk power system for approximately 90% of Texas' population.

These reliability metrics, such as measurements of frequency, voltage and transient stability, and N-1 contingency avoidance would still apply, but would be expected to need management at higher periodicity. One can also further extend this model by creating an intermediary between the transmission and distribution system, using a microgrid capable of providing internal and/or grid power to an area, and

¹ By NERC definition, a reliability coordinator is “The entity that is the highest level of authority who is responsible for the reliable operation of the Bulk Electric System, has the Wide Area View of the Bulk Electric System, and has the operating tools, processes and procedures, including the authority to prevent or mitigate emergency operating situations in both next-day analysis and real-time operations. The Reliability Coordinator has the purview that is broad enough to enable the calculation of Interconnection Reliability Operating Limits, which may be based on the operating parameters of transmission systems beyond any Transmission Operator’s vision” (North American Electric Reliability Corporation, 2015)

potentially aggregating real-time energy and power demands and supply to ensure maximum efficiency.

This research seeks to examine how the plug-in Electric Vehicle (PEV) as a core technology could be leveraged to create a more resilient energy system as it continues to grow more dynamic. At the time of this writing, PEV vehicles have been mass-market available for five years, and studied in a variety of contexts, both in Texas where the research is being conducted, and around the world. All mass-market EVs also fit the other requirements for a good candidate for this approach, namely that they have internet connectivity, often have energy requirements that allow for shifting of the power usage within a time window, and have the ability to leverage power electronics that can be further enhanced to lend additional informational “smart grid” support to the bulk power system. In addition to the experimental testbed to analyze charging patterns and the modeling work of the bulk power grid, this research also included analysis of human factors to estimate how users might engage with these systems, and investigated means of increasing participation in these systems.

This dissertation has the following four objectives:

- 1. Develop a research test bed to serve multiple classes and types of electric vehicles in ERCOT's Taylor, Texas facility, and track charging behaviors over time, and to*
- 2. Develop a custom hardware board to intercept the signaling between EVSE and EV, with millisecond-accuracy measurements and control of those signals and current/voltage measurements, and to*
- 3. Test several types of electric vehicles to determine the reliability and response time of response to changing control signals, and to*
- 4. Simulate frail power systems with EVs responding in a manner consistent with their real-world values from (3), and determine the vehicles' capacities to contribute to system reliability and resiliency.*

CHAPTER 2: BACKGROUND

Activities such as electric power generation and transportation usually create emissions that in turn affect human health. These can be near-term issues, such as extreme smog that increases short-term risks of cardiac arrest, and longer-term factors such as global climate change as a result of carbon dioxide and methane emissions that poses economic, safety, and societal risks. Electric Vehicles have been identified as a possible technological pathway to reduce these emissions. These issues are discussed in detail in Appendix A.

Vehicle Electrification

This section covers the electrification of transportation, starting with the early EV prototypes in 1895, different degrees of electrification, and the research being conducted in Austin on the emissions associated with electric vehicles.

DESCRIPTION AND HISTORY

Some of the earliest transportation vehicles used electric power, stored in batteries, to propel them. In 1895, Thomas Edison built a battery-powered front-wheel drive electric vehicle, and by 1913, he and Henry Ford produced several experimental and then production Ford electric vehicles. These vehicles were anticipated to cost between \$500 and \$750, and run between 50 and 100 miles per charge (albeit with a peak speed of 20 miles per hour). Much of these product's early failures were attributed to interpersonal factors, such as Ford demanding Edison's nickel-iron batteries to be used (which had high internal resistance and lower power density), and Ford's closing down the project when he found out that lead-acid batteries instead were being used in stealth [7]. Even Ford's wife, Clara Ford, had insisted on keeping her 1914 Detroit Electric vehicle, as opposed to moving to a model T, and marketing during that time highlighted

gasoline vehicles' propensities to “blow up” from time to time. At the time, her vehicle employed a wide variety of technologies still seen in EVs today, such as regenerative breaking, long-range driving (241 miles) and battery protection systems [8], albeit at much lower maximum velocity.



Figure 1: Thomas Edison next to the 1914 Detroit Electric plug-in electric vehicle [9]

Currently, electric vehicles can be thought of as a variety of technologies that utilize electric power to, in some way, contribute to the movement of the vehicle. Some of the simplest technologies leverage more powerful and reliable starter motors for internal combustion engines (ICEs), so that the vehicle engine turns off when, for example, the vehicle is stopped at a traffic light. Parallel hybrid technologies leverage batteries for energy storage, utilizing an electric motor and ICE connected together to the drivetrain. In such a vehicle (herein referred to as a “hybrid” vehicle), excess energy from the ICE or vehicle motion is shunted to the electric motor, generating electric power that is stored in the batteries. Similarly, in situations where additional power is needed (or in low-speed conditions where the ICE is not needed) the electric power is shunted from the batteries to the motor, enhancing or generating the vehicle motion. These hybrid vehicles also are likely to leverage additional energy saving technologies such as regenerative breaking, in which depressing the brakes leads the motor to extract excess energy to

charge the batteries, thus charging and slowing down the vehicle at the same time, and avoiding brake dust (a major contributor of ultrafine particulates). Examples of these vehicles include the Honda Civic Hybrid, Toyota Prius, Ford C-Max Hybrid, and a great many other hybrids currently on the market. These vehicles tend to have minimal electric-only ranges, small battery packs and a mix of chemistries, such as nickel metal hydride and lithium ion.

As the vehicle interactions move towards more electrification, the series hybrid electric vehicle or enhanced range electric vehicle (herein referred to as eREV) functions primarily as an electric vehicle; its primary source of propulsion and braking comes from electric motors. These vehicles tend to have larger battery packs using newer battery formulations such as lithium ion and nanoscaled lithium ion, and are capable of operating at any proscribed speed in electric only mode. Their primary mode of charging is through being plugged in, using connections such as the J1772 adapter. They have additional electric power generation capabilities utilizing another source, most commonly gasoline. Examples of these vehicles include the Chevrolet Volt, BMW i3 with range extender, and Ford C-Max Energi. Some of them, like the Volt, may under certain conditions (e.g., high speed) bring the gasoline generator's rotation in-line with the electric drivetrain in order to reduce conversion losses, but can function without gasoline provided sufficient battery charge. They tend to charge at 220 volts at 3.3kW for a few hours to reach full capacity from empty, with battery capacities typically in the 7-22 kWh range.

Completing the path towards electrification, the battery electric vehicle (BEV) eschews any secondary fuel source, and relies entirely on electric power stored in batteries charged from the grid (leveraging connectors like J1772, often at higher power at 220V such as 6.6 or 7.2 kW), and through regeneration. Due to their reliance on battery storage, they tend to have more batteries, with capacities ranging from 22 to 90 kWh, and many include the option for faster charging, via high-voltage and amperage direct current, through connectors such as ChaDeMo and J1772-Combo. Examples include the Tesla Model S, Nissan Leaf, Ford Focus Energi and the BMW i3 without range extender.

Electric vehicle adoption has been noted to growing since 2011 in the United States, and it is estimated that 87% of personal vehicle trips can be met with battery electric vehicle technology as it is presently available, without additional infrastructure needs, or high-speed charging, car/ride sharing, and others. Migrations towards increased electrification can further lead to more adaptability, and support of decarbonization [5].

ELECTRIC VEHICLE CHARGING TECHNOLOGIES

As a general rule, electric vehicle charging functions through the use of an EVSE (Electric Vehicle Supply Equipment), providing electric power to the vehicle while protecting the vehicle, power distribution system, and people around it. They provide electric power to the vehicle at distribution voltages at the residential level of $120V_{AC,1\phi}$ at low power (“Level 1” charging), $208/240 V_{AC,1\phi}$ (“Level 2 charging”) at higher power, and DC charging (“DC Fast”) charging, up to $500 V_{DC}$, at up to 200 A.

In the United States, most EV charging at levels 1 and 2 are done through the SAE J1772 connector. This connector has five pins, the largest two of which are AC Lines. In Level 1, one carries the hot and the other neutral, and in Level 2, both carry the hots of the split phase. The connector also adds a ground pin, and two extra pins, one for proximity detection, and one for the control pilot. The pinouts associated with this design are shown in Figure 2.

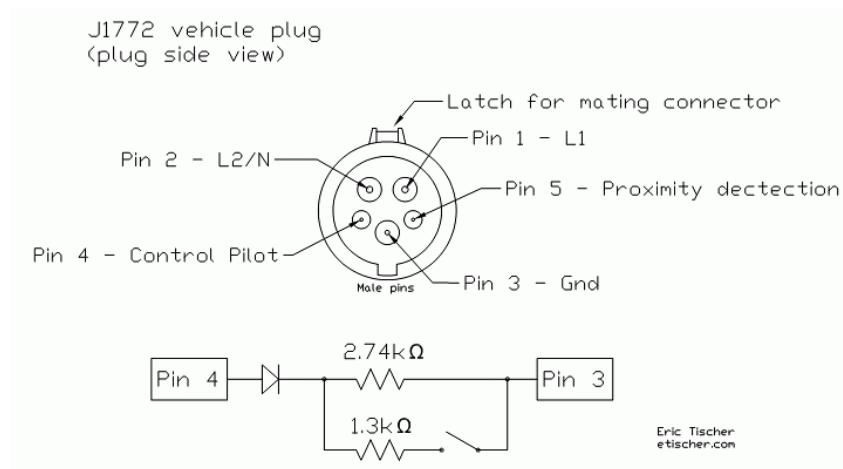


Figure 2: J1772 pinouts for Level 1 and Level 2 charging (Eric Tischer)

The technical specification for vehicle to charger was specified in 2001, first by SAE J1772, and later IEC 61851-1 and IEC TS 62763:30. The charging station provides a 1kHz PWM signal to the vehicle, whose duty cycle signifies the maximum charge rate at which the vehicle can charge (and thus, the vehicle has the autonomy to determine its actual charge rate provided it is at or below this maximum). For maximum charge rates between 6 and 51 amps, duty cycle is calculated as Amps / 0.6, and between 51 and 80 Amps, by (Amps / 2.5) + 64 [10].

This same wire is also used for the electric vehicle to provide different resistance levels, indicating the current state of the vehicle. Through the use of a diode, the low component of the pilot signal should always be -12 volts in normal operations, and the positive peak is used for state change. These states are shown in Table 1. It should be noted that some of these states are not typically seen; for example, State D (+3V to -12V) indicates an EV charging lead acid batteries (which produce hydrogen when charging), and thus indicate the need for ventilation. At present, no commercially available light transportation electric vehicles use lead acid batteries for the vehicle stack (although most do for the 12-volt accessory battery), and thus this implementation does not provide the relays for the 246 Ω scenario.

State	Positive Peak Voltage	Resistance Level seen by EVSE	Description
State A	+12 V (no PWM)	Open	EV not connected
State B	+9 V	2.74 k Ω	EV connected and ready
State C	+6 V	882 Ω	EV charging
State D	+3 V	246 Ω	EV Charging, ventilation required
State E	0 V to 0V		Error
State F	-12V to -12V		Unknown error

Table 1 : J1772 Pilot Signal voltages and resistances [10]

Within the J1772 connector, a series of resistors connects to the handle for the proximity detect signal. This signal is typically not relayed to the EVSE, and is used to

provide a signal to the electric vehicle when the driver depresses the handle, when they are about to remove the connector.

Protections from this scheme include a ground-fault detection within the EVSE, that when triggered, would open the AC lines via relays. The connection pins are physically isolated from the interior of the connector, so once inserted, no water can get inside. The handshaking process doesn't begin until the proximity detection signal is confirmed (handle securely connected), the appropriate resistance levels are seen by the EVSE, and then fault tests and PWM communications from EVSE to EV commence. Should the EV exceed the reported allowable amperage, or the EV fail to decrease amperage within a short period of time after a decrease in maximum charge rate, the AC line relays should trip and open.

This research focuses exclusively on the control of the unidirectional flow of power, from the bulk power system into the electric vehicle. There is a strong literature on bidirectional power flow (vehicle to grid; e.g., [11], [12]), that is considered outside the scope of this research. Furthermore, there is extensive research on DC fast charging (e.g., [13], [14]), which is also outside the scope of this research.

Psychological Factors associated with the bulk power system

Traditionally, the bulk power system was thought of as a “predict, command and control” system, in which electricity use was seen as being comprised of predictable and stochastic elements, but with the goals of the system operator simply being serving that anticipated load. To transition to a bidirectional relationship between grid operator and energy consumer (and thus in this case vehicle driver), a series of psychological factors must be considered and engineered into the system.

SITUATIONAL AWARENESS

Both at the ISO and at the end-user level, situational awareness is a key factor in decision making, as a loss of situational awareness significantly increases the probability of a decision that is to the detriment of the bulk system. Situational awareness is classically

defined as, “The perception of elements in the environment within a volume of time and space, the comprehension of their meaning, and the projection of their status into the near future.” Ultimately, situational awareness can be thought of as three components, from knowing the status of the situation and system (perception), to understanding the meaning of that status (comprehension), and ultimately being able to predict the direction of that system into the near future (projection) [15].

Strong end-user situational awareness would also support the idea that a small change by a single user with good situational awareness may be insignificant, a single point lost in the large noise of the system. However, if that situational awareness and thus improved dynamic behavior were to scale across a neighborhood or other large population of users, the effects could be quite dramatic.

At the energy consumer level, several new devices, such as the current transformer-based eGauge and CURB (circuit breaker-level energy meters), and advanced-meter interfacing displays can offer the potential for end users to have a much greater sense about their energy use. This increased understanding may change in turn lead to shifts in behavior, although the behavior change may not necessarily be the one in the best interest of the overall system. For example, giving end-users a meter measuring instantaneous whole-house consumption leads to the shifting of energy use towards off-peak, although not to significantly lower overall energy consumption [16].

TIME DIFFERENTIAL DISCONNECT BETWEEN USAGE AND PAYMENT

From the perspective of operant conditioning (a method of behavioral learning in which reinforcements and punishments determine the subsequent probability of the behavior), one of the major factors that lead to reduced perceived connection between customers and their electricity usage is in the large delays between consumption and billing. This concept, termed delayed reinforcement, has been theoretically and experimentally shown to make learning new behaviors, or changing existing behaviors, far more difficult [17]. Therefore, if one can imagine making a single energy decision, which, along with all the other energy decisions over a 30-day period, leads to a utility bill, it

becomes easy to conceptualize why they may continue making a series of disconnected decisions, given a reduced feedback loop.

However, minor changes in customer communications has been shown to produce significant behavior change. In a modern-day case, retail provider Direct Energy has shown that daily SMS messages to consumers of the prior day's electricity costs (in dollars, not kWh consumption) leads to approximately 18% decreases in consumption [18]. Therefore, by simply decreasing the time between the behavior and result, one can significantly induce behavioral change.

DISCONNECTS FROM STATUS OF TRANSMISSION, DISTRIBUTION, GENERATION SYSTEMS

Ultimately, residential energy consumers are generally unaware of the status of the generation, transmission, and distribution systems to which they are connected. One exception to this rule occurs at ERCOT, when physical responsive reserves drop below particular MW levels, leading to energy emergency alerts (EEAs). These EEA messages have been communicated from ERCOT to control centers for some years, and to the general public through media releases that are transmitted via radio, television, and online feeds. Since 2012, a smartphone application, the ERCOT Energy Saver, has been downloaded by over 20,000 users. The application allows both high-level information about the real-time status of the bulk system, and also allows for push notifications to end-users when ERCOT enters an EEA.

This certainly does not mean that all consumers would be willing to reduce their energy use continuously. In fact, experimental evidence indicates a "fatigue effect", in which continued messaging and behavioral change on the part of the user leads to an overwhelmed feeling, especially when the information is multimodal and about multiple aspects of life. Humans can be seen as able to thrive reasonably well on a dynamic system, but likely less so on a great many dynamic systems at the same time.

RANGE ANXIETY AND DRIVER MENTAL MODELS

Popular media frequently has used the term “range anxiety” to denote an electric vehicle driver’s fear that they will run out of charge, and end stranded or unable to take needed trips. Experimental data has found that range anxiety decreases with driver experience in their electric vehicle, due to improved mental models on the drivers’ part about the functioning of their vehicle [19], likely in the same fashion that all drivers get to better understand and predict the function of new vehicles over time. Generally, fairly new electric vehicle drivers tend to prefer electric vehicle ranges significantly in excess of their historic daily miles driven [20], and have concerns around limited availability and charging times associated with DC fast public charging stations. A framework of range anxiety is shown in Figure 3.

Based on measured patterns of electric vehicle driving between 2011-2014, it now also appears that EV batteries can be expected to support driver needs at or below 70% of nameplate capacity. This indicates a need to refocus on driver patterns and needs more than an abstract capacity figure [21], as well as potentially new inputs around the placement of EVSEs [22].

As is the case in the management of the bulk power system, human errors associated with EV driving can come from the application of the incorrect mental model. One recent example is with electric vehicle drivers in Atlanta, GA, near the North American Electric Reliability Corporation’s headquarters. Thanks to tax incentives at both the federal and state levels, there are a great many Nissan Leaf vehicles in Atlanta, and high speed ChaDeMo stations throughout the city. Some drivers are able to lease their Leaf BEVs for less than \$75/month, which when incorporated with fuel savings and potentially free workplace charging, becomes quite attractive as compared to ICE alternatives. However, one of the interesting noted phenomena in Atlanta is that, in the winter, several Leaf drivers run out of electric range, because they don’t expect a significant decrease in range using heating (which would be the case in an ICE vehicle).

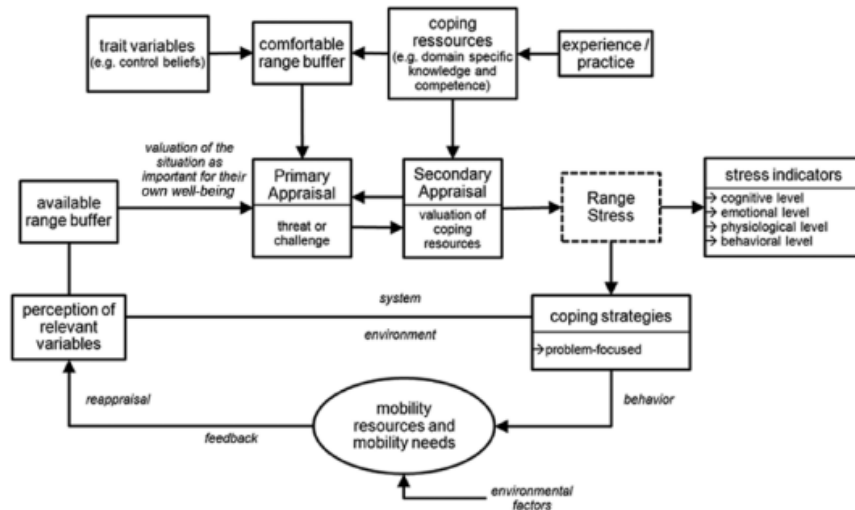


Figure 3: A psychological framework of range anxiety [19]

“CURSE OF THE DEFAULT”

One of the major challenges to adoption of any new technology has to do with the preponderance of users leaving the technologies in their original, or near-original configurations. In the early days of remote garage door openers, this meant that dip switch-based openers were set to ‘000000’ leading to several rashes of thefts, given off-the-shelf openers could open garage doors. When looking at web browser users, users who indicate that they would prefer not to be tracked as they browse across the web are not very likely to have enabled their browser’s ‘do not track’ header feature, which exactly accomplishes that function. That is why changes in defaults, like Firefox’s switch from Google to Yahoo as the default search provider, are seen as having tremendous market shifting power [23].

When applied to electric vehicles, this means that the vast majority of electric vehicles can be expected to behave exactly in the same configuration as they had when they first leave the dealership lot, meaning that today, they are likely to charge immediately on plug-in, which typically increases aggregate on-peak load for charging starting in the early evening, particularly in regions that have heavy early evening air-conditioning use. Therefore, if vehicle charging control is not seen as a near-term viability, it is strongly recommended that part of the final interactions with the dealership before leaving the lot

include programming the vehicle to charge off-peak, or programming to do so at the factory.

MORAL SELF-REGULATION AND PRO-ENVIRONMENT / PRO-RELIABILITY DECISIONS

One of the interesting facets of human behavior is that, while it's far easier to think of human decisions in an independent, probabilistic fashion, real-world behavior tends to be more linked between decisions. For example, the phenomenon of moral self-regulation describes a person making a decision they believe to be kind, moral, or environmentally friendly, which paradoxically increases the probability they will, in short order, make an unkind, immoral, or environmentally harmful decision. Interestingly, this seems to be heavily related to one's perception of self; affirmations to moral identity increase the probability of an immoral behavior, while threats to moral identity lead to more moral behaviors, presumably to re-acquire the sense of moral self-worth. Across many empirical and experimental studies, these phenomena are both observed and affected by these moral perceptions [24].

This phenomenon can be especially interesting moving towards a smart grid world, in which user behaviors on highly dynamic systems can cause instabilities and unexpected outcomes. For example, not all LEED-certified buildings use significantly less energy than their equivalent non-LEED counterparts [25], EV drivers with rooftop PV may be more likely to lower their air conditioner cooling set points or leave their doors opened. There are many other behaviors that lower the efficiency of a system from its theoretical maximum.

SOCIAL AND FINANCIAL DOMAINS

Furthermore, from a behavioral economics perspective, one can think of two separate domains of function, one social exchange, and one financial exchange. We tend to think of activities in either realm, but crossing from one to the other (especially social domain to financial domain) can also produce unexpected results. As an example, at a daycare center in Israel with frequently-late parents picking up their children, a late fine

began to be assessed after baseline tracking. While this was intended to curb lateness, it had the opposite effect, in that parental tardiness increased significantly and did not recede when the fines were removed.

While some view the fines as being insufficient, it appears a subtler shift happened with the parents: beforehand, while sometimes late, parents had a cognizance of the social factors associated with their tardiness. The teachers were not able to go home to their families as quickly, or were otherwise inconvenienced, and often late parents frequently apologized for being late. After enacting the fine, it appears that these parents shifted their thought process about their lateness from social exchange (being part of a society shared with the teachers and administrators) to a financial exchange domain (fee for service). Once in the financial domain, the parents were performing far simpler cost-benefit analyses around their behavior. Through that lens, a higher fine might produce less tardiness, but still weaken the empathy and sense of community that the parents had with their teachers [26].

A Growing Dynamic System from the Holistic Perspective

Electric Reliability Council of Texas, Inc. (ERCOT) serves as the grid operator for most of Texas (75% of its land mass, and 90% of its population). Over the course of the past several years, ERCOT has undergone many changes, including a new Nodal market system, new whole-grid CIM-based network modeling and management system, new situational awareness tools, and new series of protocols and procedures to support this growing system. At the same time a parallel series of major changes were occurring elsewhere on the grid.

Intermittent renewable generation grew drastically in the 2007-present range, growing from roughly 3,000 MW to 16,000 MW in nine years in an erratic growth pattern, as shown in Figure 4. In December 2015, ERCOT reached new wind-generation record levels, including wind supplying 48.28% of ERCOT's generation, and a maximum ever generation of 14,023 MW, in early 2016 [27]. ERCOT's peak load continues to rise,

with a peak of 71,093 MW on August 11, 2016 between 4 and 5 PM, at the time of this writing [28] .

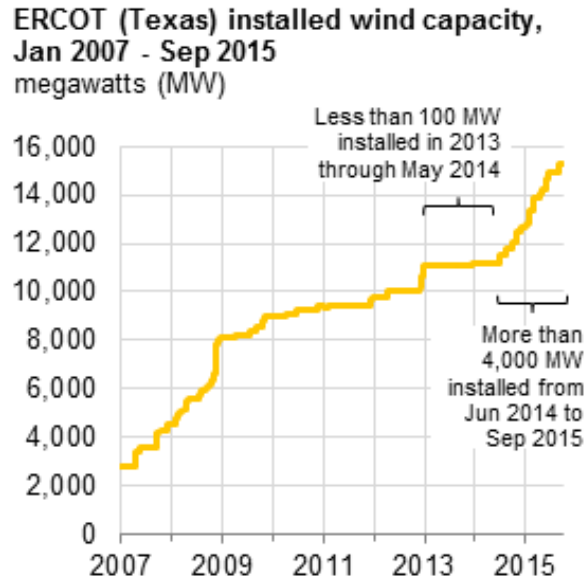


Figure 4: Growth of ERCOT Wind Capacity [29]

In addition to this growth at the high-voltage level (at the point of visibility to ERCOT’s operators), renewable generation has also grown significantly at the distribution level, including rooftop photovoltaics and small wind generation. ERCOT estimates that by 2030, 13 GW of solar PV generation is likely to come online, and possibly even more if EPA Clean Power Plan rules are enacted [30].

Under ERCOT protocols, distribution generation resources are defined to be generation at a point of delivery at 10 MW or less, or at 60 kV or lower. ERCOT requires registration of such devices with a capacity of 1 MW or greater if the resource would be accounted for in wholesale market settlements. ERCOT works to track DG installations also that provide 50 kW to 1 MW. As of October 2015, there were 130 units with a combined capacity of 21.77 MW, according to ERCOT estimates. However, there also are a great many PV installations at the residential level, which contribute significantly to some homes’ load profiles during the day.

Changing paradigms of control

One of the trends in the growing speed and depth of data around energy management is the transition of traditional SCADA communications technologies from the high-voltage substation to the distribution-level and premise-level areas. Several technologies are growing in this area, and it is anticipated that the same protocols, philosophies, and layout designs as seen in the transmission infrastructure will have value on the distribution side as well.

It is important to consider the evolution of the bulk power system, as it moves from a centralized control infrastructure from the perspective of state estimation and dispatch, to at least some degree of non-centralized control on certain areas of the grid, often termed the “grid edge.” There are several advantages to this approach, especially when one takes into mind both the computational complexity of state-estimating an entire energy system, and the response times associated with both larger-scale computations and control signal timelines.

NANO-AND MICRO-GRID ISLANDING

One of the critical changes towards a more distributed energy system is in the design of a microgrid, which contains both some generation and load resources inside it. In order for it to function as a true microgrid, it must have the capability to, at will, disconnect and reconnect from the bulk power system, and also to be able to consume from or supply to the bulk power system (BPS). Intrinsicly, then, a strong degree of information sharing and coordination is required between the microgrid and the bulk system upon which it is connected.

FAST-RESPONDING LOCAL TELEMETRY PROTOCOLS

Within the transmission substation, several technologies are used to transfer measurements taken (e.g., a CT around a wire indicating current flow), transducing to a convenient electrical signal and then transformed to digital signals that make their way towards core management systems. These protocols have been evolving in recent years, and new philosophies of distributed Ethernet wiring are replacing ones of direct-wired connection.

A great many protocols exist within the substation (e.g., Modbus, DNP3, and IEC 61850), as well as between substations (e.g., IEC 60870-6/ICCP). For purposes of this research, the within-substation components are highlighted, as the research presumes a fixed perimeter around a group of EVSEs, and secured communications between the charging stations and an aggregator/utility.

Modbus

Modbus, a common protocol for informational exchange, was developed by Modicon in 1979. Its core philosophy is of a master/slave architecture. It is a lightweight protocol, originally incorporating data transmittal through serial connections in a binary format (Modbus RTU) or text format (Modbus ASCII), both over either RS-232 or RS-485 protocols. It also has evolved to incorporate the same protocol over an Ethernet physical layer (Modbus TCP), which is identical save an additional 6 bytes in the header to support routing. It focuses on components having particular addresses, which are classified by type (e.g., digital inputs starting at 10001, analog inputs at 30001, and writable registers at 40001) [31]. It does not incorporate any levels of authentication or encryption (although third-party gateways provide such services), and thus works from the model that the substation network's security provides the only security layer for the substation automation. It is designed in such a way that the any device (e.g., human-machine interface,

SCADA concentrator) must have *a priori* knowledge of the device, its address, and associated meanings of all its variables. Due to the low bandwidth requirements for transmitting Modbus data, and for the low memory costs of implementing it in hardware, a great many devices, from transmission substation-level to building-level devices, use this protocol.

DNP3 / IEEE 1815-2012

Within the electric power field, the DNP3 protocol was developed to foster better interoperability between substation computers, remote terminal units (RTUs), intelligent electronic devices (IEDs), and master stations. It is based on the International Electrotechnical Commission (IEC) efforts around OSI layer 3, “enhanced performance architecture” for remote control applications. It was developed by Harris, and transferred to the DNP3 working group in 1993, and became an IEEE standard in July 2010.

Like Modbus, it is an open and public protocol, and is based on transit using the TCP/IP transmission framework. It includes a great many enhancements to Modbus, including a link layer responsible for ensuring reliable communications, enhanced checksum/validity checking, and request-response and event-driven information transmittal paradigms. It includes more intelligent handshaking, such as sharing the device’s *endianness* (the byte order in which data are transmitted), and the ability to share floating point numbers directly, rather than needing to spread across multiple 16-bit registers, as was the case in Modbus. In 2010, its IEEE ratification included pre-shared keys for authentication, but its 2012 enhancement moved towards use of public key infrastructure, thus incorporating appropriate security measures into the infrastructure that would protect a power system even with potential compromise into the substation’s Ethernet bus [32].

While commercially-available products are designed to support the layout, configuration, and linkages between end devices and SCADA concentrators, ultimately devices interfacing with DNP3 devices need *a priori* knowledge of the layout of the system, addressing, etc. Like Modbus, DNP3's design is built around fairly lightweight memory footprint requirements, making them suitable for a variety of different applications that can use low-performance embedded controllers. Also, like Modbus, DNP3 is primarily a serial protocol, with the capacity for packets to be wrapped in additional layers, such as the transport (TCP or UDP), internet (IP), and network interface levels (e.g., 100BaseT).

IEC 61850

One of the evolutions in substation and distributed SCADA philosophies is reducing complexity by creating common buses. While building a substation with several Modbus devices would likely require a great deal of wiring between each transducer and SCADA concentrator(s), an emerging philosophy has been growing of using a shared substation high-speed Ethernet bus (Gigabit or 10-Gigabit Ethernet, likely fiber optic) broadcasting high speed Generic Object Oriented Substation Event (GOOSE) messages. This architecture significantly simplifies substation design, and potentially can lead to lower costs, both through eliminating copper wiring runs between serial devices, and through the capacity to create emergent logic without the need for creating additional wiring pathways between existing devices.

GOOSE packets are defined as status/value updates transmitted to the network within 4 milliseconds, usually broadcast to many clients using X.255 addressing. In the event of a value change (e.g. an amperage reading off a CT), GOOSE broadcast packets are rapidly transmitted, and the rate of retransmission continues to slow over time, resetting to rapid retransmission should the raw read value change. These approaches lead to more

efficient usage of the Ethernet bus, but also create opportunities for a new client to quickly establish the present state of the system, and allows intelligent devices to read the states of other devices and provide its own, or exert other local, automated controls [33]. There are some cybersecurity concerns with the protocol (e.g., [34]), that likely will especially grow to be of concern in a distributed SCADA approach. However, at its strictest sense, it is likely the 4ms requirement may be difficult to meet using existing cellular and routing technologies, without dedicated fiber runs between sites, thus limiting the strictest adherence to the implementation in the “smart grid” world. When its high speed requirements are met, it also has the potential to more easily provide synchrophase measurements, if the GPS reference signals are broadcast across the same bus, and thus all devices are synchronized.

In addition to a new common bus and messaging philosophy, IEC 61850 also incorporates a new approach as well to the announcement and configuration of devices. Devices each present their object names to the bus, and the types of messages they are capable of receiving (commands) and sending (telemetry). All of these names are standardized, making integration easier. IEC 61850 devices, in addition to reporting value states and changing repeat rates, also can broadcast waveform samples across the bus, thus leading for more opportunities for synchrophase measurement, harmonics analysis, and testing between devices against a common time reference. [35]

DISTRIBUTED (E.G., BLOCKCHAIN) RECORDKEEPING AND SETTLEMENTS

One of the emerging trends at the grid edge involves the use of distributed means of information sharing and processing. One of these technologies, blockchain, is the foundation of several cryptocurrencies, including Bitcoin. The core philosophy behind blockchain is to create a distributed database architecture that is synchronized, distributed,

tamper-resistant, and self-correcting, such that all participants have a perfect data trail of information. Each block within has some data and/or program instructions, and reference (via hash) to a previous block. Blockchain technology leads to consensus-building of the database, consistency checking, confirmation of a block entering the block chain, high degrees of difficulty in altering the stream, and automated conflict resolution techniques [36].

While blockchain was originally developed as part of the Bitcoin project, its capacity as a distributed database is not limited to financial transactions. Within the energy space, there is growing interest in blockchain use in energy transactions (e.g., [37]). Some of its advantages are in maintaining anonymity of the participants, and by creating a distributed database that is shared by all participants, the capability to have market clearing, research analytics, and other functions run asynchronously across multiple parties without additional infrastructure. This would allow, for example, multiple entities to provide a market clearing recommendation to ensure validity of the solutions.

In a distributed system, especially with more grid edge devices, it is anticipated that weak cellular networks and routing, power outages and other factors may lower the reliability of telemetry, so technologies like blockchain may help distributed data sharing occur. Since the data placed within a block is focused on its particular application, it is also possible that anonymization techniques (e.g., using public key infrastructure cryptography to encrypt driver information) would help support consumer privacy.

Previous Research on Electric Vehicle to Grid Integration

During the earlier state of this research, an agent-based modeling system was built by the author, designed to analyze a simulated neighborhood (based on real-world hourly

load averages from a transmission-level load), with and without electric vehicles. Presuming the peak load of 1 MW as serving 200 homes, and the 2010 average of 1.7 vehicles per home, this led to roughly 5,700 homes and 9,781 vehicles per neighborhood. If each of these vehicles were to travel the 2014-average of 13,476 miles per year, that would translate to 131,808,756 miles driven annually.

Through analyzing the role of transferring these vehicles to electric vehicles such as the Chevrolet Volt, simulating charging at particular times of the day, and tracking the transmission-level marginal generators during those periods, a differential was computed between ICE and EV driving. In a simple scenario with 5% of the vehicles being electric, and 5% of rooftops having PV arrays (4 kW mean capacity), this led to an 80% reduction of per-mile by CO₂, and a per-mile efficiency of \$0.039/mile, as opposed to \$0.126/mile for the ICE vehicle. This also corresponded to a total-neighborhood reduction of CO₂ of 65%, based on the transmission-level marginal units at that point in time.

Further emissions reductions were achieved growing EV and PV adoption rates to 95%, with controlled charging offsetting the vehicle charging. Effectively, this could be seen as marginally inserting generation from PV that is withdrawn by timed EV charging, thus zeroing out the ICE emissions. This was particularly helpful in minimizing SO₂ emissions, which unlike CO₂, NO_x, PM₁₀, PM_{2.5}, and UFPM, tended to increase with vehicle electrification rates.

Challenges with the Current State of the Art

Within the framework of an increasingly dynamic power system, with intermittent renewables and roving, intermittently charging vehicles, several factors become increasingly critical in order to ensure the reliability of the power system. This includes maintaining power balance, alleviating congestion, and maintaining a capability to respond to dynamic urgent situations. It may further require additional telemetry to ensure improved functioning, and new types of algorithms and management system to detect potential concerns, such as subsynchronous oscillation, and intelligent dispatch of devices to prevents swings on the system.

Local response of electric vehicles

To ensure the reliability of the bulk power system, and in situations where control signals cannot reach the equipment, devices need to have the capacity to independently change their functionality based on local measurements of the state of the system on which they are connected. This can occur, for example, with a device that can detect when the system moves outside its normal range of function. For example, a charging electric vehicle that detects frequency drop below some set point (such as 59.8 Hz) should reduce or delay its charging, to give the system room as local generation is ramped up to rematch system-wide load. Local control services can provide grid stability in a more rapid fashion than dispatch from a central controller's AGC signal, and also provide additional resilience against communications disruptions. One could also imagine an EV or EVSE deferring charge when the system harmonics cross a certain THD threshold, thus protecting the vehicle from transients on the system, or be able to use power electronics to attempt to counteract particular harmonics, potentially extending capacitor lifespan.

Synchrophasor integration: local and remote

Modern-day electric vehicles are quite sophisticated and connected devices. Given the functionality that EVs have, including battery charging management, GPS navigation, and cellular data and voice connectivity, one could imagine utilizing these features with additional AC waveform analysis, providing GPS time-stamped synchrophasor measurements back to an aggregator or utility. Aggregation of these points could potentially build an interesting view of the overall status and health of the system, all the way from transmission to distribution level. This would also offer additional early-warning indicators about common distribution-level issues, such as transformer tap changer difficulties, and about other equipment that may be transmitting harmonic currents and voltages on the system.

While this information is likely not directly helpful (and in fact due to information overload potentially a risk) to the grid operator to maintain, a distribution system operator could serve to aggregate this data, and create automated behaviors based on multiple synchrophasor measurements. For example, a growing angular divergence between two electric vehicles connected to different transmission level loads could indicate a fault on the system, and thus lead to some automated action on the part of the vehicles, such as a 20 second pause of charging. Similarly, sudden changes in THD at one but not the other may indicate other devices on the system functioning poorly, or the transfer of a system from grid-tie to backup power generation. Of course, these same functions could also be carried out at the low side of the transformer, although leveraging the existing technologies already in the EV and many EVSEs may offer a reduced cost for acquiring that data.

Limited communications pipelines between vehicle, supply, and system

One of the concerns around integrating electric vehicles and the bulk power system is around the limited communications pipelines between the two. The current J1772 specification supports a very limited exchange of information between the vehicle and charger, namely safety and maximum charge rate in amps. Some vehicles and chargers are compliant with open standards such as OpenADR, but not most. Closed and proprietary systems at both the vehicle and charger levels further make integration across a wide area of devices far more difficult, and unknown black box systems, with multiple vendors with financial incentives to over-market their products may lead to unrealistic timing, reliability, or control estimates, thus damaging overall model accuracy. Ultimately, in order for these systems to connect to the power system from the market services perspective, reliability statistics need to be far better understood, and end-to-end testing with transparent data acquisition is needed. Ultimately, this data would lead to more accurate models (and thus

likely better compensation to the providers), as well as additional protections to the user, ensuring those vehicles have sufficient charge when needed.

On-peak charging

Generally, uncontrollable load systems are engineered to offer sufficient capacity at peak levels. Within the ERCOT region, Texas climate has yielded the primary predictive factor for system load temperature. As an example, as shown in Figure 5, a contrast is drawn on two days, one a mild day (Dallas temperature 64° F, March 9, 2011), and a hot day (Dallas temperature 109°F, August 3, 2011). In this example, the largest increase in load was from the residential sector, which increased fourfold. Similarly, when analyzed at the residential level on a hot August day, circuit-breaker level data indicates the vast majority of home energy use is associated with temperature control, with additional smaller components in the late afternoon associated with homeowners’ activities, returning home from work [38].

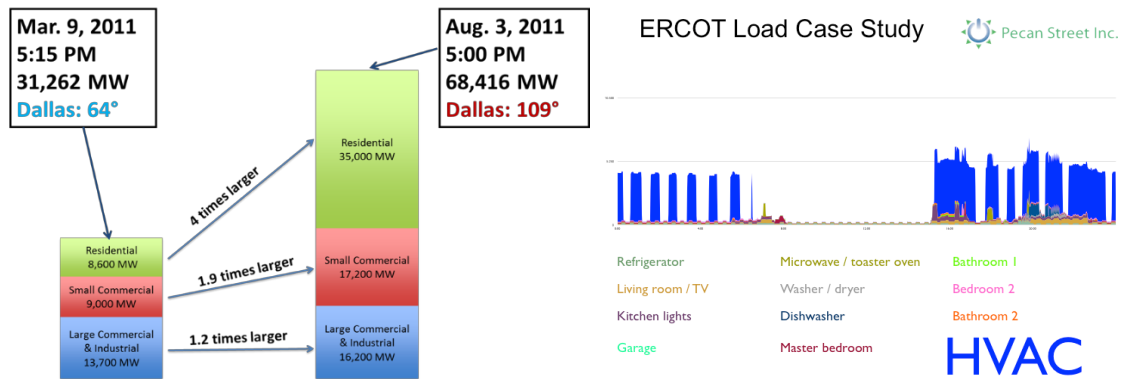


Figure 5: Examples of ERCOT system and a home’s load based on ambient temperature

Line Capacity issues on peak

In order to maintain the reliability of the bulk power system, the grid operator is directed to maintain the system to be able to withstand a N-1 contingency event, meaning that the system can maintain proper function after any single failure of generator, transmission line, transmission level transformer [39]. Security-constrained economic dispatch (SCED) ensures dispatch is cost-optimized giving the limited carrying capacity of the transmission infrastructure, and other systems conditions such as outages. Recently, in the ERCOT region, further modeling of loss of reactive support devices (capacitors, reactors and static VAR compensators) are also being studied.

When considering that a large scale growth of electric vehicles could affect the transmission system during a high temperature day with significant HVAC load, concerns about the security and economics of maintaining the bulk power system function need to be addressed. From a perspective of social equity, devices that can potentially be shifted (a vehicle charged starting at 6 PM or 12 AM, provided it has sufficient time to charge fully, is not differently charged in the early morning) should be encouraged to load shift, while other devices that are less easily shifted perhaps should be allowed to function. The impetus for this shift could come from differential pricing models from the market signals perspective, or grid or locally-controlled behavior from the smart grid perspective.

One of the interesting phenomena that occurs on a power system is that sometimes, increasing load at a particular point will actually reduce the flow on a particular transmission line. Therefore, controllable loads such as electric vehicles can be thought of as providing potential reliability-strengthening behaviors, both in increasing and in decreasing load, although proportionally, is it anticipated that the ratio is heavily tilted towards load curtailment, and away from load augmentation.

Distribution transformer overheating on peak/loss of cool-down off-peak

Typical distribution transformers are run as unintelligent devices, simply changing from higher distribution-level voltages to residential levels, whether as three-phase 480 volt, or single-phase split 240/120 volt systems. It seems as though the general trend is to see these devices as replaceable, with indication of device failure partially automated through its downstream advanced meters reporting outages. As passive devices, the transformers are expected to work by providing increased flow-through on peak, which include generation of waste heat from internal resistances and other losses. As with other devices, this heat can build up and shorten the lifespan of the transformer's coils, oil, core, or other components, and other factors, such as low oil levels, can exacerbate the problem. In a traditional system, on-peak use on hot days would lead to increased thermal loading on the transformers, with cool-down periods overnight as home energy consumption drops overnight. Shifting electric vehicle charging from on-peak to this cool-down period may in fact better support the transmission system or system-wide energy prices, but potentially at the expense of reduced distribution transformer life, as compared to non-EV serving transformers. However, this shifting behavior is still preferable to both on-peak HVAC and EV loads, for economic dispatch, emissions, and reliability concerns.

“Birthday cake” curve

If one were to supplement the household peak in the afternoon (approximately 6 kW) with a level 2 charging station (typically running between 3.3 and 7.2 kW), one can imagine a significant increase in distribution transformer loading at those peak times. Pecan Street Project studied such effects in the Mueller neighborhood, which has significant adoption of both photovoltaic generation and electric vehicles. EV charging tended to begin at approximately 4 PM, peaking approximately 8 PM on weekdays with flat-rate pricing. Interestingly, time of use pricing participants instead ramped at 12 AM, and peaked at 1

AM, attributed to the change in pricing tier at those points, creating an economic incentive for drivers to program their vehicles to defer charging to those times. More interesting, their neighbors on flat-rate plans tended start shifting their EV load, likely due to conversations with their neighbors on time of use plans [40] .

Given the cluster effect, an EV driver who is likely going to come home, turn on their HVAC and start charging their car, is also likely to have many neighbors who do the same. The example shown in Figure 6, is likely is an underestimation; it was collected by Pecan Street Project in 2010, and based on its 3.3kW load, is likely an early Nissan Leaf or Chevrolet Volt. At the time of this writing, many electric vehicles maximum charge rates are higher (7.2 kW or more for the Tesla Model S, 6.6 kW for the Nissan Leaf, Ford Focus Electric, and several others).

From the implications both to the distribution transformers and the overall grid during peak hours (especially summer heat-related peak), this on-peak charging has the risk of leading to significant issues from both grid reliability and distribution-level reliability. Given that EV charging tends to shift HVAC loads higher, it is often called the “birthday cake curve”, an example of which is shown in Figure 6.

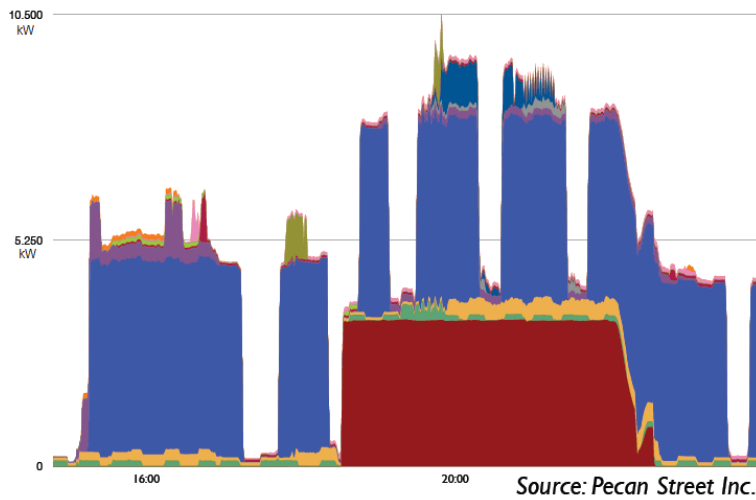


Figure 6: The Birthday Cake Curve, with on-peak EV charging (red) and HVAC usage (blue)

“Duck” Curve

A fascinating trend has started to emerge with systems in California and Hawaii, both with strong incentives and adoptions of distributed photovoltaics, which shifts total system load. This “duck curve”, as shown in Figure 7, leads to significant drops in system net load from late morning to early afternoon, due to large proliferations of behind-the-meter PV generation. In contrast to ERCOT, both Hawaii and California have more modest peaks of air-conditioning load. This can lead to issues at the distribution transformer level (e.g., heating due to real power upflow), potentially negative load at the transmission interconnection point, and at the transmission level changes in congestion patterns on the system, as well as leading to situations where base load plants do not have sufficient demand to stay online at minimum MW levels. These offlining units can lead to concerns about reliability support later in the day, or the possibility for needing rapid ramping of both real power flow and direction should clouds occlude an area. From the California

perspective, if the trend of rooftop PV panels continues at the current rate, it could lead to potential system over-generation by 2020, or over 13 GW of needed generation ramping within three hours.

This phenomenon also has interesting psychological questions associated with it. Energy users, especially in places like California, are used to receiving messaging about avoiding unnecessary load during peak times, instead delaying the load to off-peak times in the evenings. As these people are not home during mid-day, they are less likely to allow their washing machine to run (the clothing may sit for hours waiting to be transferred to the dryer), they cannot charge their electric vehicle, and they are encouraged not to use their pool pumps. Now, with this new issue, some of these messages to Californians may in fact begin to shift, although it is unclear that there is sufficient elastic load available in the system mid-day. This may lead to increased incentives for energy storage, or additional subsidies for research and development.

As with many intersections between the engineering of the bulk system, the development of its markets, government policies and incentives, and human behavior, the duck curve problem highlights the need to plan ahead for the proliferation of devices, and in an increasingly dynamic way, leverage the total of uncontrollable generation assets and controllable load and generation assets to balance the system. Furthermore, it highlights the need for a more holistic and anticipatory view into future system planning from an overall integration standpoint.

Generalizing from the examples above, one could imagine scaling out California's workplace EV charging, adding controls to have vehicles charge and modulate against the distributed solar resources in the state. This has an interesting effect in theory, though, as essentially it uses the distribution system as a generation aggregation asset, not just a load serving asset. While it may be a good solution in California, it is likely less viable in Texas,

given the additional exacerbation of peak load associated with EV charging on peak. Given Texas' ramp of wind generation from West Texas in the late evening/early morning, home charging may make more sense in those regions, at least with current levels of PV adoption.

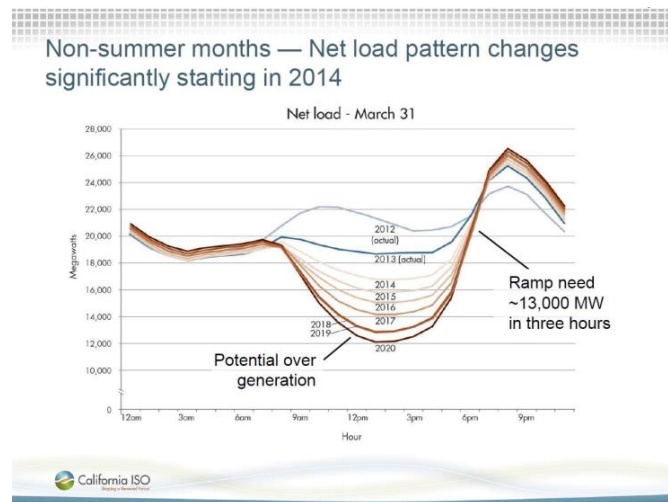


Figure 7: The California "duck curve" as a result of DER growth

RESEARCH GOALS

As discussed above, several facets of the bulk power system are changing and integration of new devices and faster-changing characteristics create challenges for the management of the bulk power system with current control methodologies. Current techniques for managing these new loads, such as dispatched demand response, lack the capacity to support rapid changes that may be associated with large-scale renewable growth. Ultimately, this research seeks to determine whether it would be possible for intelligent controlled electric vehicle charging to provide several capabilities to the power system to strengthen reliability and resiliency, rather than serving as yet another load that has the potential to destabilize the system on peak. If so, means of integrating these new

control structures and/or markets will be analyzed, and the behavioral aspects necessary to have drivers comfortable with participating in these markets are also analyzed.

CHAPTER 3: ELECTRIC VEHICLE CHARGING MODELS

Introduction

This chapter investigates theoretical issues around stronger integration of electric vehicles into the bulk power system. This includes incorporating emerging principles found elsewhere on the bulk power system, such as satellite-time referenced waveforms measured in synchrophasors, and different charging strategies, as well as their advantages and disadvantages. Given much of Texas offers competitive choice for retail electricity, a framework is proposed that supports drivers transacting with retail providers to select pricing models, both for the energy necessary for vehicle charging, and the services that the vehicle can in turn offer to support the system's stability. Furthermore, this is done through the lens of allowing drivers to transact while maintaining a greater degree of privacy than is currently afforded with existing charging infrastructures.

Synchrophasor Measurements

One of the emerging trends in grid management involves the capture of high-resolution waveforms, against a GPS time reference. This technology allows for detection of fine differences between frequencies in different, fully interconnected areas, something which was not previously possible. Furthermore, synchronization across multiple areas allows the generation of a point-in-time snapshot of the state of the entire system.

This dataset is growing increasingly important for grid operators. For example, integration of this data, even if collected at the distribution level, can provide highly accurate estimates of the locations of events at the sub-second level, views into the unanticipated interactions between geographically disbursed equipment, and the capacity

to perform, if tightly linked in a network, an approach to state estimation in which phase angles are known, leading to a simpler and more robust algorithm. In Texas, over 2,500 synchrophasors are IEEE C37.118 compliant, able to output data at a rate of 30 times per second (2 Hz) or faster [41].

Given that these devices are just beginning to be installed throughout the system, and that EVSE design is fairly new and growing, it may be beneficial to consider merging the two. Furthermore, in order to grow an EVSE to revenue-grade quality metering, the high accuracy of required current transformers (CTs) would provide measurements that could help aggregators and system operators to build wide-area views, and also additional confidence in the ability of the devices to participate in the market.

Electric Vehicle Charging Strategies

Several strategies for charging electric vehicles are discussed in the following section. Some of them have been tested, in simulation and/or against the ERCOT test bed, while others are offered to highlight theoretical strategies that could be implemented in the future.

IMMEDIATE CHARGING

Immediate charging is the most common electric vehicle charging strategy, as it is the default on all current commercially-available electric vehicles. Simply put, immediate charging corresponds to the vehicle, after proper handshaking, charging at 100% of its maximum rated load (e.g., 3.3kW for a Chevrolet Volt, 6.6kW for a Nissan Leaf, 7.2kW for a Tesla Model S), and continuing this behavior until the battery pack is deemed fully charged. Following this completion, some EVs may occasionally draw additional load to power the battery pack thermal management system, thermally condition the cabin, etc.

Generally speaking, this strategy implies a high immediate load that tapers quickly to zero upon completion, and is an autonomous action.

These strategies, while not posing major concerns to the system for an individual EV, can lead to many challenges with high EV adoption rates, or during the conjunction of EV charging with other heavy loads (e.g., EVs and HVAC cooling). Large numbers of EVs charging in this way could challenge the distribution system, affecting local transformers as drivers come home from work, and simultaneously plug in one or more EVs, turn on lights, air conditioners, pool pumps, etc. Thanks to the cluster effect, it is likely that these homes are surrounded by other homes with EVs as well, thus increasing loading on the distribution transformer. The same effect could occur on the transmission system, as the aggregate behavior of HVAC and EV loads coming online could create significant swings in demand. This could be expressed at any level in terms of congestion over lines as they approach capacity, and thermal/lifespan concerns about transformers, especially at the distribution level where real-time thermal monitoring rarely occurs.

Default configurations for charging are likely to be used in the absence of compelling reasons for drivers to modify their vehicle's charge settings, leading to full charge behaviors immediately on plug-in. In observations at the ERCOT electric vehicle test bed, all but the author's vehicle (n=22 over the course of five years) implement this immediate full-charging strategy, at least when engaging in workplace charging. Due to the early configuration of the test bed, only one-second eGauge telemetry was available, as opposed to the sub-second intervals offered by the J1772-intercept board. Visual observation of the eGauge data indicated some indications as to the vehicle type, based on its peak charging rate, and the behavior of the vehicle at the end of the charging session. Some vehicles, such as the Chevrolet Volt, tend to taper off towards zero load with occasional returns to full charging rate of 3.3kW for battery conditioning, while other

vehicles, such as the Nissan Leaf, tend to drop rapidly from peak charging rate (6.6 kW on newer models) towards 0 kW with newer models having lower-power to zero-power oscillations at the end of the charging cycle. Given that the Leaf does not have active thermal management, no significant additional load is detected unless the EV driver requests a cabin thermal conditioning, which is confirmed by consistent power factor across the charging cycle.

DELAYED CHARGING

Many EV and EVSE manufacturers offer the capacity to delay the vehicle's onset of charging, based on either a set start time, or departure time. This requires the user to configure their EV or EVSE outside of their default parameters, and tends to occur only when incentives, such as time of use pricing, leads to altered behavior [42]. There may be many potential reasons an EV driver may wish to change the charging time, such as environmental ones (e.g., aligning charging to the peak of West Texas' wind generation), reliability-based ones (e.g., avoiding summer afternoon peaks and winter morning peaks), financial ones directly affecting the customer (e.g., TOU rates at the charging station or home), and financial ones affecting their employer (e.g., lowering demand charges). Like immediate charging, these policies are set by the EVSE or EV owner, and do not require any interactions between the vehicle and the grid.

RELIABILITY-SUPPORTED CHARGING

Another potential charging method can maintain the autonomous behaviors of immediate and delayed charging, but offer additional reliability services to the grid (which also may protect the vehicle). One could imagine an EV's charge controller monitoring the voltage waveform provided through the EVSE, and should that waveform become heavily distorted (as measured in THD), or start to decrease in frequency (which indicates a

significant event on the grid such as a major loss of generation), or have a frequency approaching traditional underfrequency thresholds, the EV could immediately stop charging, and signal to the EVSE to open the charge relays. Similarly, if an EV were charging at less than maximum, and frequency was noted to start to increase, or become close to thresholds for overfrequency relays, the EV could move its charging to the maximum possible rates, and potentially even add additional loads, such as pre-cooling the cabin, to provide some load support to a grid in need of inertia. These strategies could be carried out without any remote information, and could be used to further enhance the system. If one were to consider a future of islanded microgrids with small inertial support, these kinds of behaviors might become increasingly valuable to the reliability of the system.

GENERATION DATA-LINKED CHARGING

Another strategy that involves simple point-to-point data connectivity could pair a particular EV to a particular renewable resource. This type of strategy could be used by a homeowner with both home PV resources and an EV, so that they can feel as though their EV charging load were virtually cancelled out by their PV generation, and thus they are driving on “green energy”. While this sounds theoretically intriguing, practical considerations make it less simple to implement. Certainly, the network latency of the system would lead to the need for prediction of a distant resource, and the farther the load is from the generation (especially if separated across multiple layers, with an EV at work and PV at home), shift factors on the system, losses, and other factors could prevent this working in the truest sense of its intent. In a closed system such as a workplace with rooftop PV and EVSEs connected to the same distribution transformer, this becomes more feasible

due to the elimination of topological distance and reduction of network latency effects because it could be carried out in a closed loop.

Also, if one were to investigate the environmental impact of EV charging, it is likely that in ERCOT, providing load reduction services on PV peak generation (e.g., allowing PV generation to compensate more for large summer HVAC loads) may have more effect from a neighborhood CO₂ perspective. This is largely due to the 85% difference between per-mile ICE engine and EV charged by a non-renewable generation fleet [2], thus allowing PV to offset traditional generation fleets in time, and shifting EV charging to lower-peak and higher-renewable rates. However, in areas with heavy PV adoption (e.g., Hawaii, California) where “duck curve” concerns are growing, having loads anywhere on the system to offset renewable generation can help provide the inertial support necessary for traditional power plants to ramp.

RENEWABLE INTEGRATION/OFFSET CHARGING

An extension to data-linked charging could involve pairing a group of electric vehicles with a group of renewable resources, and optimizing the charging of the EVs, pairing individual or groups of resources together, based on the shift factors of their associated buses. In theory, if done correctly, this could lead to EV charging offsetting distant renewable resources, although this could lead to increased system congestion. The less variability an aggregate resource has (e.g., a system-wide view of the aggregate of all wind turbines, as compared to an individual turbine), the more likely network latency issues will be less impactful, due to the need for lower periodicity of signals.

EVSE DATA-LINKED CHARGING

Another data-linked paradigm could involve pairing two EVSEs spread across distant sites with each other. Because the implementation of our hardware include GPS

time references, and 10-microsecond accuracy, public internet point-to-point communications between the two devices could share system frequency and phase angle reference. If the two EVSEs were to detect an increased angular divergence between the two of them (indicating a system fault in between the two charging stations), both could decrease their load temporarily to give the system time to recover, or provide a signal to an aggregator indicating the detection of this divergence. From this perspective, multiple interconnected EVSEs may help a system operator quickly locate faults, or provide a lower-resolution backup to grid-level synchrophasor networks.

AVERAGE RATE CHARGING

Average rate charging, as suggested by Kefayati & Baldick [43], requires inputs from the vehicle and its driver, including current battery state of charge, desired departure time, and charge goal (e.g., charge until full, or charge a set kWh to drive a set distance, which requires a kWh/mile efficiency estimate from the vehicle and destination miles from the driver). The charging pattern then simply becomes to charge at the power level given by $[\text{Total kWh}] / [\text{Total time in hours}]$. Due to the J1772 specification's discrete amperage maximum, the vehicle would then receive the next higher max amperage rating from that calculation in order to guarantee the targeted state of charge on time or earlier.

Conceivably, this could be accomplished without an interface to the vehicle, if the driver is able to present the vehicle's state of charge (kWh), or estimated electric range (EER) upon plug-in, intended departure time, and the vehicle make and model so that reasonable estimates of the vehicle's charging behavior can be inferred.

Modifications to this strategy can include a minimum estimated electric range (EER), during which period the vehicle charges at full power, and once obtained, then moves to an average rate modality. This may require additional polling of the vehicle's

state of charge over the course of the charging session. Given that EV estimated ranges can vary depending on a host of characteristics (e.g., driving downhill in one direction and uphill in another, changes in ambient temperature, HVAC behaviors, etc.), charging algorithms would need to be especially careful to ensure the driver has the needed state of charge at the intended time.

ANCILLARY SERVICES AND AVERAGE RATE CHARGING

Given that an electric vehicle using average rate charging is somewhere between the maxima and minima of its charge rate, there is also the capacity to offer load increases and decreases, to bid into fast-responding ancillary services or demand response markets. Care would need to be taken to ensure that the EV always has the necessary state of charge upon completion, so any load decreases or DR events would need to be compensated for later. That may also indicate risks that load reductions early in the charge session pose particular risks to the system, because demand flexibility will be exhausted towards the end of the charging session.

LOCAL FREQUENCY RESPONSE AND AVERAGE RATE CHARGING

The same characteristic behaviors of modulating charge rate around an average rate can be provided without signals from a grid operator or aggregator. These could be carried out using a traditional droop control system, a PID controller (utilizing proportional, integral and derivative gains to continuously support system frequency), or discrete functions. Given load modulation is a reliability-supporting service, and that the power electronics in the EV can change consumption very quickly, it would be appropriate to remunerate the EV driver and/or EVSE operator, or to adjust regulatory standards accordingly to have this as a default behavior. In order for remuneration to occur, communications, at least on a daily basis, would need to occur between the EVSE and

aggregator, and the EVSE would need to incorporate revenue-grade CTs and certifications to support payments across these changed readings.

If remunerations were to be given for local response, it may also be appropriate to consider the entitlements of both the EV which is actually offering the load modulation services, and the EVSE which is providing the revenue-grade measurements, information sharing, data connectivity, and signaling to the vehicle so that the vehicle could respond. While the vehicle could offer these services by enhancements to its own power measurement equipment and firmware, it would likely create many concerns. For example, it may lead to requirements for annual vehicle inspections including measurement of vehicle charging response to differing frequencies and THDs, validation of the measurement accuracy of system profile, and estimations of the vehicle's associated electrical bus at each plug-in.

While these charging strategies highlighted above have the potential to create reliability supporting/enhancing behaviors on the part of the electric vehicle, they are not likely to be heavily adopted unless the end-users (electric vehicle drivers) feel safe about participating in them, and thus end-user protections need to be considered as well.

End-user protections in EV aggregation

If one imagines a world in which there is vast adoption of electric vehicles, and these many EVs are providing services to support the reliability of the power system, one also must consider the large density and variety of data that are needed to reliably provide these services. Furthermore, to provide an improved user experience to the drivers, even further information may be necessary.

Some vehicle information is necessary in order to determine a vehicle's charging needs and response capabilities, such as its make, model, and year. In order to offer ancillary services to the grid operator, the vehicle's current location and state of charge would also be necessary. In order to ensure vehicles are charged on time, the aggregator or local controller would also need to know driver habits such as estimated time of departure, miles that would be driven, and even potentially geographic locations and driving destination (as topology, traffic, and temperature differences would lead to different per-mile efficiencies).

Perhaps, driver preferences, such as whether they would prefer their cabin to be pre-conditioned five minutes before departure, would be valuable to know as well and could lead to both improved user experience. Further, total energy consumption once unplugged can be improved with these variables. Vehicles with battery thermal management systems can pre-condition the battery pack leading to more efficient current draw, and further draw that preconditioning power over the EVSE rather than the battery pack once the vehicle is in motion.

From the technical perspective, some of this information can be already obtained using other protocols. For example, the ChaDeMo protocol, a DC fast charging paradigm developed in Japan, includes pins directly placing the charger on the vehicle's CAN bus. From that perspective, state of charge, or issuance of commands such as cabin conditioning are trivial. In the current Level 2 charging implementation, additional interfaces are required to the vehicle's telematics APIs (e.g., GM's Onstar, Nissan's CarWings) or across PLC or other communications techniques, which are not currently included in the ratified specification.

Protections of EV drivers can be thought of in multiple layers: protection of the driver's identity, separation between the vehicle's charging needs/capabilities and its

driver, per-event anonymity to ensure correlation attacks or pattern analysis attacks are more difficult, and separation of the EVSE (which is in a fixed location) from the EV and its driver.

Blockchain technologies, if properly implemented, may be able to help support these types of approaches, as could properly implemented direct communications systems. However, without a model incorporating anonymity, the aggregator may need to know both the information about the driver and about the charging station, and thus is the point in which data are aggregated, and drivers and behaviors identified.

Public key infrastructure can be used to create secure communications between multiple parties, protecting the identity of the driver. The following example demonstrates one potential implementation of this approach. Note that this model presumes one could be in a competitive choice area where multiple aggregators could compete with each other; as such, this approach requires no pre-established relationship between any party. In order to simplify this example, the only two data pathways used are between an electric vehicle and the EVSE to which it's connected, and between the EVSE and the internet.

This protocol is illustrated as a proof of concept below. Communications between EV and EVSE are presumed to be direct TCP/IP (e.g., over PLC), while communications between the EVSE and a collection of aggregators are presumed to be over two paths: aggregators offering potential charging/market opportunities for EV charging over a hashgraph, and direct TLS-encrypted communications between EVSE and the aggregator of the EV driver's choosing. Additional network security concepts, such as perfect forward secrecy, are assumed but not explicitly defined herein. These layouts are designed to attempt to adhere to the "trust no one" (TNO) model, in which each of the parties in the transaction provide validations to the others to ensure proper behavior [44]. The exception

to this rule is the lack of generated per-transaction bitcoin addresses for payment transfer, although these could be considered as well.

“TRUST NO ONE” EV CHARGING CONCEPT

This concept employs several actors. Within this example, each actor is bolded for clarity. The **driver** is the vehicle driver, and **EV** is their electric vehicle. They plug in or wirelessly interface with the **EVSE** to create both data and power transfer connections. The EVSE is a part of a hashgraph/blockchain network, which has multiple **aggregators** offering pricing options that they can offer the EVSE on its particular network (for example, in a competitive choice area, this would be multiple aggregators with relationships with the distribution service provider, while in vertically integrated areas this would likely be one aggregator, who is also the utility). Each aggregator offers one or more **pricing options** that are offered to the vehicle drivers.

For stronger security, it is assumed that the aggregator may be a large company, with different departments offering different pricing options. Therefore, communications are designed such that only the appropriate groups within the aggregator are able to communicate with the EV. Communications are based on public-key/asymmetric cryptography [45], and are denoted such that P_{Actor} corresponds to the public key for a particular actor, Q_{Actor} corresponds to the private key for that actor, and n_x corresponds to a nonce (randomly-generated number) that is passed between entities to ensure reliable security between the actors. It is presumed that the act of transferring an encrypted nonce leads to a validation event on the receiver against the receiver’s private key, and that within this context, the validation is assumed to be successful.

Table 2 provides a summary view of this proposed communications methodology. Green lines correspond to actions from the driver, whether with a plug or on the vehicle’s

display, or a mobile app. Blue lines correspond to encrypted powerline or direct packet communications between devices, using public key infrastructure. Red lines correspond to changes in the PWM duty cycle.

Step #	Driver	Electric Vehicle	EVSE	Aggregator	Information Relayed
3	Driver informs EV of charging parameters				Estimated time of departure, anticipated destination, lunch?
4, 5	Driver plugs their EV to the EVSE. Initiates communication.				Handshake, public key transfer, nonce confirmation
6		EV provides EVSE charging information			Maximum charge rate, multiple departure times (for each, minimum kWh, kWh estimated to full, estimated departure time)
7		EVSE provides EV charging options			Maximum charge rate, EVSE name and ESI ID, other capabilities (e.g., IEEE C37.118), and the list of currently available pricing options
8		EV Selects aggregator / pricing plan			
9 - 11			EVSE initiates communications with aggregator		Handshake, public key transfer, nonce confirmation. Transfer of EVSE system limitations. EVSE and aggregator bitcoin addresses
12 - 17		EV and aggregator handshake and share financial information			Pricing option identifier. Nonce
18-20			Aggregator informs EVSE that succesful handshake has occurred		Pricing option identifier, confirmation of handshake
21, 22		Charging commences.			Vehicle sees PWM duty cycle. EVSE provides signals locally as necessary.
24			EVSE provides 1-m telemetry		Time stamp (against GPS reference), set maximum rate, instantaneous rate
25		Aggregator provides dispatches as needed			EVSE provides 0,15,30,45,60 cycle after duty cycle change RMS power
26	Driver stops charging session				Driver depresses handle on button to indicate end of charging session. EVSE informed.
27			EVSE informs aggregator notification of session end.		
28-36		Payments are distributed to aggregator, EVSE owner, and EV owner			Bitcoin or third-party financial transactions
37, 38	Driver informed that payments complete. Driver unplugs.				

Table 2: "Swim lanes" for EV-EVSE-Aggregator communications

1. Initial staging:
 - The **EVSE** is connected to the hashgraph of all available EV-charging related services. Perhaps also, this hashgraph contains other offers for synchrophase data at different levels of reliability (e.g., revenue-grade, IEEE C37.118 compliance, etc.) although this is not considered in this example.
2. Use case begins.
3. **Driver** interfaces with **EV** (upon arrival at destination).
 - **Driver** informs **EV** of estimated time of departure, anticipated destination, and other behavioral expectations (e.g., driving to lunch).
 - **EV** calculates the requirements for state of charge necessary to meet the **driver's** requirements and comfort (e.g., cabin thermal conditioning prior to departure).
4. Driver plugs their **EV** to the **EVSE** (or using wireless inductive charging, a handshake occurs between the **EVSE** and **EV**).
 - **EV** generates a public/private key combination (P_{EV} and Q_{EV}) for use during this charging session.
 - **EV** transmits its public key P_{EV} to the **EVSE**.
5. **EVSE** completes initial handshake with the **EV**.
 - **EVSE** generates a public/private key combination (P_{EVSE} and Q_{EVSE}) for use during this charging session.
 - **EVSE** provides the **EV** its public key P_{EVSE} , and a nonce (n_0) encrypted by the **EV's** public key P_{EV} .
6. **EV** provides the **EVSE** (all encrypted by the **EVSE's** public key P_{EVSE})

- The same nonce (n_0)
 - Maximum charge rate (kW)
 - The number of departure times
 - For every departure time (e.g., lunch, end of day):
 - kWh minimum necessary
 - kWh estimated for full battery charge
 - Departure time
7. **EVSE** provides **EV** (all encrypted by **EV**'s public key P_{EV})
- Maximum charging rate
 - **EVSE** name and electric service identifier (ESI ID)
 - **EVSE** capabilities (e.g., IEEE C37.118 compliance)
 - For every **EV** pricing option
 - Pricing option unique identifier
 - Attributes of the pricing option (e.g., flat rate, ancillary services, price per kWh, price given to driver for charge control events).
 - The public key associated with this pricing option P_{PO} .
 - The public key associated with the aggregator offering this pricing option P_{AGG} .
8. **EV** provides **EVSE** (all encrypted by **EVSE**'s public key P_{EVSE})
- Selected **pricing option**'s unique identifier
 - Charging information (all encrypted against the **pricing option**'s public key P_{PO}):
 - A generated nonce (n_1)
 - Maximum charge rate (kW)
 - Vehicle driver's bitcoin address

- The number of departure times
 - For every departure time (e.g., lunch, end of day):
 - kWh minimum necessary
 - kWh estimated for full battery charge
 - Departure time
9. **EVSE** provides the **aggregator** (all encrypted by the **aggregator's** public key P_{AGG})
- The **EV's** selected pricing option unique identifier
 - A generated nonce (n_2), encrypted against the pricing option's public key P_{PO}
 - The **EVSE's** public key
 - The **EVSE** owner's bitcoin address.
 - Any system constraints currently in place on the EVSE
10. **Aggregator** provides the **EVSE** (all encrypted by the **EVSE's** public key P_{EVSE})
- The same nonce n_2
 - The bitcoin address of the **aggregator**
11. **EVSE** provides the **aggregator** (all encrypted by the **aggregator's** public key P_{AGG})
- The bitcoin address associated with the **aggregator**.
 - The charging information provided by the **EV** to **EVSE** as listed above in step 7).
12. **Aggregator** provides the **EVSE** (all encrypted by the **EVSE's** public key P_{EVSE})

- Information to be shared with the **EV** (encrypted by the **EV**'s public key P_{EV})
 - A generated nonce (n_4)
 - The bitcoin address of the **aggregator**
- 13. **EVSE** provides **EV** (all encrypted by **EV**'s public key P_{EV})
 - The information relayed from the **aggregator** in step 11
- 14. **EV** provides **EVSE** (all encrypted by **EVSE**'s public key P_{EVSE})
 - The nonce n_4 provided by the aggregator in step 12 (encrypted by the **aggregator**'s public key P_{AGG} and then by the **pricing option**'s public key P_{PO}).
- 15. **EVSE** provides the **Aggregator** (all encrypted by the Aggregator's public key P_{AGG})
 - The nonce n_4 provided by the **EV**, further encrypted by the pricing option's public key P_{PO} .
- 16. **Aggregator** provides the **EVSE** (all encrypted by the **EVSE**'s public key P_{EVSE})
 - A profile of planned charging setpoints: timestamps and maximum kW values
 - A cryptographic hash generated against the above profile, against the **EV**'s public key P_{EV}
- 17. **EVSE** provides the **EV** the data provided in step 16 (all encrypted by the **EV**'s public key P_{EV})
- 18. **EV** provides the **EVSE** a confirmation message accepting this pricing option (all encrypted by the **EVSE**'s public key P_{EVSE}).

- An approval message encrypted by the **aggregator's** public key P_{AGG} , and the **pricing option's** public key P_{PO} .
19. **EVSE** relays the information provided in step 18 (all encrypted by the **Aggregator's** public key P_{AGG}).
 20. **Aggregator** informs the **EVSE** that a successful handshake has occurred against a pricing plan and charging schedule, and that charging may begin (all encrypted by the **EVSE's** public key P_{EVSE}).
 21. **EVSE** receives the signal as transmitted in step 20, and alters the PWM duty cycle on the signaling pin, indicating the **EV** that it may commence charging at a particular maximum charging rate.
 22. **EV** initiates charging behavior.
 23. At targeted set points as provided by the charging schedule held in the **EVSE**, the **EVSE** modulates the PWM duty cycle as appropriate. Temporal accuracy is ensured due to the **EVSE's** GPS time reference.
 24. Every minute, the **EVSE** provides the **aggregator** (all encrypted against the **aggregator's** public key, P_{AGG}):
 - The last minute's **EV** charging energy (kWh)
 - For every modulation in maximum charge rate:
 - The time stamp (against the **EVSE's** GPS time reference).
 - The set maximum charge rate as set by the **EVSE**
 - The instantaneous power (kW) measured from the **EV** 0, 15, 30, 45, and 60 cycles after the dispatch.
 25. In the event of dispatch changes (e.g., ancillary services deployments):
 - The **Aggregator** dispatches to the **EVSE** (all encrypted by the **EVSE's** public key, P_{EVSE}):

- One or more charging events:
 - A time stamp for the associated event (or no time for immediate dispatch)
 - The target power (kW) intended for that point in time.
26. After the **driver** has completed charging, they press a button on the **EVSE** handle, indicating charge completion.
27. The **EVSE** communicates with the **aggregator** (all encrypted by the Aggregator's public key, P_{AGG}):
- A notification of charging session end
 - Total energy (kWh) consumed over the course of the charging session
 - Pricing option information (further encrypted by the **pricing option's** public key, P_{PO}):
 - The public key of the **EV**
 - Total energy (kWh) consumed over the course of the charging session
 - The number of received dispatch instructions from the **aggregator**
 - The % accuracy of **EV** response to those signals, as measured at 0, 15, 30, and 60 cycles out from an instruction point
 - The total amount of load flexibility offered to the aggregator during the course of this charging session (as measured as the differential between instantaneous actual charge levels and the **EV's** maximal charge rate)
28. The **pricing option** group within the **aggregator** receives the information from step 27.

29. The **pricing option's** group dispatches a payment to the **EVSE** owner's bitcoin address, based on both the value of the provided telemetry and a proportion of load flexibility offered.
30. The **pricing option's** group dispatches a payment to the **EV** owner's bitcoin address, based on a proportion of the load flexibility offered.
31. The **EV** dispatches a payment to the **pricing option** group for the energy (kWh) used during the charging session, as agreed to during the initial process.
32. The **EV** dispatches a payment to the **EVSE** owner for the energy (kWh) and/or usage of the parking spot during the charging session, as agreed to during the initial process.
33. The **EV** sends a message to the **EVSE** indicating it has completed its payments (all encrypted by the **EVSE's** private key P_{EVSE})
 - The bitcoin transaction ID of the payment to the **EVSE** operator
 - The bitcoin transaction ID of the payment to the **pricing option** (encrypted by the **pricing option's** public key, P_{PO}).
34. The **EVSE** sends a message to the **aggregator** indicating payments have been completed (all encrypted by the **aggregator's** private key P_{AGG}).
 - The bitcoin transaction ID from the **EV** from step 33.
35. The **aggregator** sends a message to the **EVSE** indicating payments have been completed (all encrypted by the **aggregator's** private key P_{EVSE}).
 - The bitcoin transaction ID associated with the payment to the **EVSE** from step 29.
 - The bitcoin transaction ID associated with the payment to the **EV** from step 30 (encrypted by the **EV's** public key P_{EV}).

36. The **EVSE** relays the bitcoin ID of the payment to the **EV** (encrypted by the **EV**'s public key P_{EV}).
37. The **EVSE** charging cord interfaces with the **driver**, indicating that all payments have been completed successfully.
38. The **driver** unplugs the **EVSE** cable from **EV**, and drives away.
39. The use case ends.

This use case demonstrates a potential means by which an electric vehicle driver can plug into the EVSE, select a pricing plan of interest to the driver, initiate charging, and ensure payments are properly transacted, without the EVSE or aggregator being able to identify the particular vehicle, driver, or driving destination. This approach certainly is complex, but could scale to a competitive choice area, in which retail providers could compete with each other for both cost effectiveness of EV charging, and in their ability to predict and control electric vehicle charging to provide ancillary services.

Conclusion

Integrating electric vehicles into the bulk power system can be accomplished in a variety of means. Ensuring that vehicles' charging behaviors support reliability, provide a positive user experience for the driver during their charging, and provide appropriate identity protections to the drivers is of importance. Success in these areas may lead to increased adoption of electric vehicles, investigations of new and advanced grid services, and better management of the system to which the vehicles are connected.

CHAPTER 4: ELECTRIC VEHICLE CHARGE CONTROL IN SITU

Introduction

In partnership between University of Texas at Austin, Electric Reliability Council of Texas, Pecan Street Project and EV-TEC, a test bed for electric vehicle to grid integration has been online since 2012. Over the past five years, this system has grown from four to eleven charging stations, added a 5 kW photovoltaic array, eGauge devices to measure circuit breaker-level telemetry at the one-minute interval, and J1772 intercept boards for millisecond-interval measurements and vehicle charge signal control. Several software designs have been developed since the project's inception, designed to answer various research questions of interest to researchers and ERCOT employees, as well as to provide necessary load shed behavior in the event of grid energy emergencies.

Methodology

ERCOT ELECTRIC VEHICLE RESEARCH PROJECT

Since 2012, ERCOT has participated in a research project to analyze the impacts of electric vehicle charging on the bulk power system, with the author as its primary investigator. The project began with four Chargepoint CT-500 EVSEs in the Taylor, Texas parking lot, funded through UT, Austin-based NSF I/UCRC EV-TEC, and Pecan Street Project. Additional ERCOT funds were used subsequently to add an additional four charging stations at the site, as well as a 5 kW photovoltaic array, and an eGauge breaker-level telemetry device, and cellular connectivity for transmission of telemetry. Additionally, three additional CT-1000 combination units (Levels 1 & 2) were installed in partnership with Austin Energy at ERCOT's Metro Center Drive offices, along with an eGauge and cellular telemetry transmission.

This project is designed to be ongoing, to explore electric vehicles (EVs) from the energy systems engineering, economic, environmental and psychological perspectives. EV Drivers have the capacity to opt in to the research project on a daily basis at the Electric Reliability Council of Texas (ERCOT)'s Taylor, TX campus. In exchange for participation in the study, drivers are given a reduced rate for charging their vehicles, with options tailored around their preferences. Much of this research was conducted by the author, and is highlighted in this dissertation, although other research topics and future questions are ongoing.

PARTICIPANTS

Since the research project came online in 2012, several different types of vehicles have plugged in to the Taylor, Texas EVSE infrastructure. The majority of these vehicles are the property of ERCOT employees, although infrequent use by ERCOT visitors were noted. The test bed is behind an access-controlled perimeter fence, and drivers, on interview, indicated strong knowledge of the bulk power system. As such, some results on driver behavior may not be generalizable.

Several ERCOT employees living in Taylor purchased electric vehicles, but did not consistently plug in. One employee is an early adopter (2011 Leaf), while the remaining (2012 and two 2014 Leaf) drivers reported becoming interested in electric vehicles after hearing their colleagues discuss the vehicles. At present, the following vehicle makes and years of manufacture were noted charging in the test bed.

- Chevrolet Volt (2011, 2012, 2013, and 2014 models)
- Nissan Leaf (2011, 2013, 2014, and 2015 models)
- Ford Focus Energi (2014 model)
- Tesla S (2013 S60 model)

J1772 INTERCEPT BOARD

To facilitate researching high-resolution electric vehicle to grid integration *in situ*, a device was constructed in collaboration with Pecan Street Project. The detailed design of the hardware is specified in Appendix B. The board was specifically designed to fit inside an EVSE housing, and to meet the following requirements:

- Reading an EVSE's charge control PWM signal
- Providing to the EVSE the appropriate resistance levels to correspond to the various states of charging
- Providing an EV a charge control PWM signal of our choosing
- Reading the EV's resistance levels to correspond to the various stages of charging
- Reading the voltage as it enters the EVSE
- Reading the current as it enters the EVSE (note, this includes a small parasitic load associated with the electronics of the EVSE itself, but is a far less invasive installation in some EVSEs than over the two line wires of the charging cable, which is inside the internal housing)
- Performing frequency detection on the voltage signal
- Performing power factor analysis, and computing real and reactive power components of the waveform
- Performing Fourier transformations on the current and voltage signals to determine total harmonic distortion (THD)
- Providing all of the above measurements and changes against a GPS timestamp reference, leading to the device functioning as a Synchrophasor.

These capabilities were chosen to ensure that a high resolution view of the electric vehicle charging handshake and subsequent charging process were observable, and that granular control of signal transmission, observation of signal change, and observation of vehicle behavior change were all tracked in a high resolution timestamp. Furthermore, oscilloscope measurements against the eGauge indicated that there are likely software features that lead to slower changes in current than are actually observed in real-time. Therefore, these boards were developed to not provide any software buffering, therefore providing a more accurate, albeit noisy, view of the vehicle behaviors.

MOBILE APPLICATION DESIGN

A mobile web application was developed for this research, as specified in the IRB proposal (as attached in Appendix C). A web-based mobile supported application style was chosen, as this paradigm avoids challenges and delays associated with mobile app review and deployment, as well as offering limited availability to only research participants. This was accomplished using QR codes and associated shortened URLs against the ev-tx.com domain, which was purchased for this research. Each of the eight charging stations has a dedicated URL, and local cookie storage on the mobile device is used to link drivers (and their associated vehicles and preferences) to their sessions. The mobile website application and its associated SQL database structure is included in the open source repository associated with this research.

SERVER HARDWARE SELECTION

To provide the appropriate controls and measurements for the research, an Intel NUC 5i5RYK was used, running Windows Server 2003, a 2.7Ghz Intel Core i5 processor, 500 Gb SSD drive, and 16Gb of RAM. The NUC, along with an eGauge providing voltage and current measurements at the breaker panel, and a network switch were installed at the Taylor EV research station. The interior of this enclosure is shown in Figure 8.



Figure 8: The installation of components adjacent to the breaker panel (early installation)

The server is provided high-speed 4G LTE internet via a Sprint USB modem adapter, and is configured to act as a NAT router and DHCP server, building a local network at 100-BaseT. The code is configured to interface with each of the J1772 intercept boards via a lightweight communications management protocol, as well as the eGauge's raw voltage and current readouts, in order to cross-validate the readings. The software leverages the USB cellular adapter's GPS to synchronize to a microsecond-accurate timestamp, after which it broadcasts the current time to all devices via UDP. The server

also utilizes Chargepoint's API to monitor and initiate demand response events through the charging station, in order to analyze the response times, from DR initiation to PWM duty cycle changes on the EVSE, as well as between the intercept board and the EV. All events are stored with millisecond accuracy in a database. The server provides APIs to link to third-party aggregator providers, to allow other optimization algorithms to be run in the future.

SERVER SOFTWARE DESIGN

As part of this research, a server application was developed by the author, designed to interface with several components, including the charging stations (via Chargepoint's API), the e-Gauge breaker-level telemetry (charging station, grid power quality, and PV generation) using that API, ERCOT-level data such as ancillary services capacity, and real-time system conditions, Google's SMS gateway, and the Smart Meter Texas network.

This research server is tasked with maintaining the relationships between all of the components in real time, and interfacing with command and control interfaces to assign max charging rate signals to the vehicle in response to conditions as they are programmatically specified. It has the capability to send SMS messages to EV drivers and respond to simple commands, detect new EVSE plug-in events, log real-time information and provide simplified interfaces to ERCOT facilities to respond to real-world grid conditions such as EEA events.

The server also provides an API to a future mobile application, designed to provide the interface between driver and the research project. It currently is being used by the research administrators to initiate manual charging and DR events. This API would continue to grow in future work, to support the additional functionality needed for the research. The code base is written by the author in C#, and will be provided to the open source community upon completion of this research.

Results

This section covers the results of the experiments conducted on the electric vehicle test bed, through various control methodologies. Early test results showed extreme variability in terms of time of response, and poor reliability, leading to the subsequent development of the hardware intercept boards. These experiments are grouped against the control methodology used during the research. Several additional experiments were conducted in the test bed; these examples are selected to highlight challenges with the current state of the art of electric vehicle load management.

EARLY EXPERIMENTS: eGAUGE AND CHARGEPOINT API WITH CUSTOM SOFTWARE

To validate the functionality of the server and its capacity to control electric vehicle charging, two simple experiments were conducted. The first experiment studied, the capacity of the server to receive information from an eGauge (monitoring PV production) and send max charge rate signals to the EVSEs in response, thus from the transformer perspective create roughly zero load, and the second, to look at the timing responsiveness of the entire system. Both preliminary tests show a fairly complex series of interactions that could affect the capacity of an aggregator to accurately predict, in high temporal and energy resolution, the behavior of a vehicle under its instruction.

Nissan Leaf with manual control signals

In July 2015, a simple experiment was conducted with a 2015 Nissan Leaf, analyzing its responsiveness to DR signals. It would appear, as shown in Figure 9, that internal vehicle controls may not behave as intended by the controller. In this example, a 2015 Nissan Leaf was instructed to charge at 10% (0.6kW), but instead chose to not charge at all. When instructed to charge at 25% (1.65 kW), the vehicle instead chose to charge at 1.5kW, but only after being first allowed back to the 6.6kW full rate for a brief period of

time. This is partially attributable to the J1772 specification, in which the EVSE is actually modulating a pulse width signal to indicate maximum charge rate, with some discrete set of values, but it also attributable to logic on the vehicle side, likely optimized to maximize battery life or some other function, which may not always align with rapid charge rate response to the maximum rate as specified by the controller. During this experiment, the vehicle's state of charge was unknown.

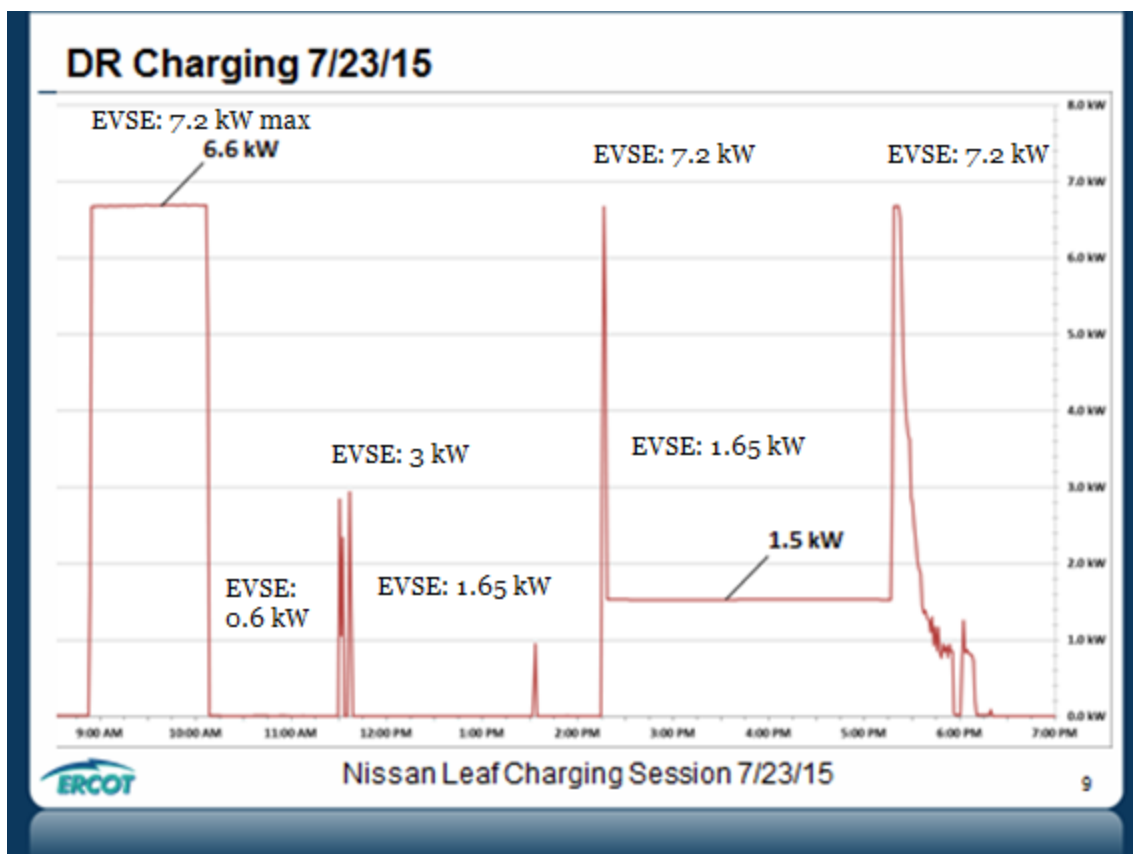


Figure 9: Nissan Leaf response to varying levels of DR commands

Chevrolet Volt under a PV envelope, cellular network only

The ultimate goal of integrating electric vehicles (at the vehicle and/or EVSE point) with the bulk power system is to provide the appropriate levels of controllability of EV

charging in order to support both economic efficiency and to enhance the reliability of the system. A very simple example of such a behavior was conducted at the ERCOT EV research test bed, during which over the course of a day, a 2011 Chevrolet Volt was sent (via EVSE) a one-minute max charging rate signal, based on the average generation levels from the test bed's 5 kW photovoltaic array over the prior minute's 60 sampled values. As shown in Figure 10, while overall charging trended towards the PV line, vehicle response tended to lag behind with high variability, attributed in part to the black box network surrounding the EVSEs and network lag. Furthermore, given the substantial variability of PV generation during the experiment (it was a day with some cloud covering and high wind moving the clouds quickly), a one-minute average failed to fully compensate for the variability of the generation curve, and additional network latencies led to the one-minute DR commands to expire prior to the next one arriving. In order to alleviate the generational variability, one might need to add ultracapacitor or battery storage on the DC side of the solar array, or use some other strategy to better smooth out the generation curves. Even in helping a building avoid demand charges or service amperage ratings not being exceeded, these kinds of techniques may be of value while simultaneously supporting increased intermittent resources.

For this research, a clearly significant effect was noted for EV charging rates in response to the PV rates, as is clearly visible. And unsurprisingly, the EVSE load and PV generation numbers are correlated (at $r=0.815$), but a regression model indicates a borderline significant result ($p=0.05$). As a light load in a heavily loaded system, this may be acceptable, but in dynamic conditions, or with mass adoption, these results indicate a level of performance that could pose concerns to the system.

Charging an EV under a solar generation envelope, Feb. 13, 2013

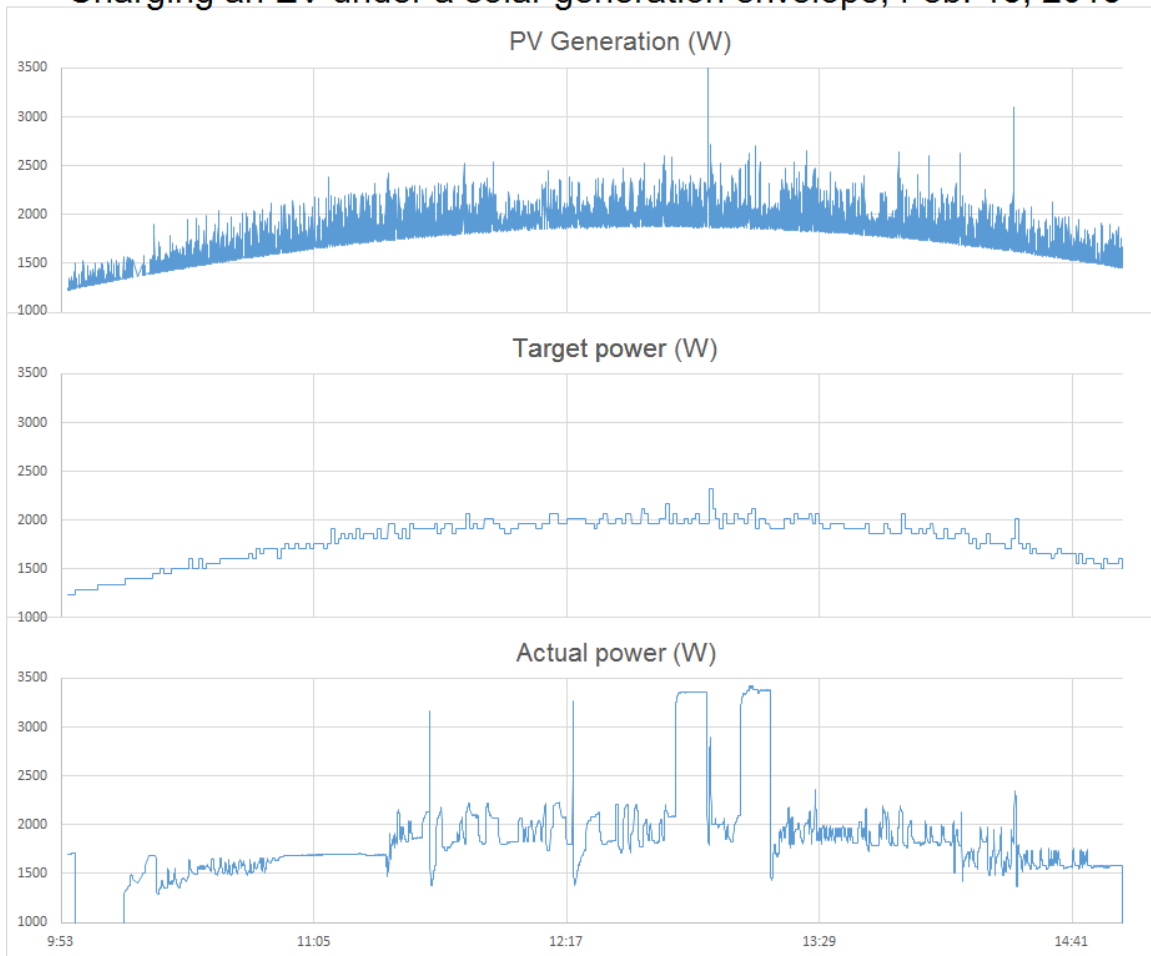


Figure 10: An example of EVSE remote control to charge an electric vehicle under a PV envelope

In this study, a server located in Austin read from an eGauge in Taylor (over a Sprint data connection) to determine the last minute average generation, which in turn led to a signal being sent to a control center in California, which is then rebroadcast back to Taylor via an AT&T cellular connection. This topology, as highlighted in Figure 11, details the several communications pathways which contributed to highly variable vehicle response to the EV load curtailment signal, including several instances of packet loss and the default reversion to a full 30-amp maximum charging rate signaling.

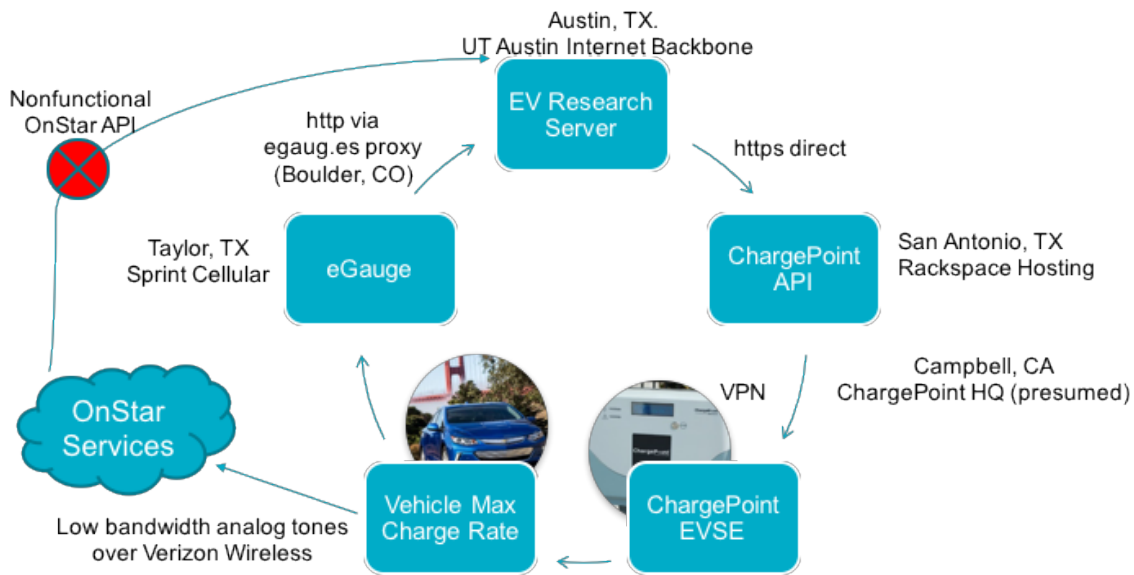


Figure 11: Control loops involved in follow-solar strategy

The response characteristics in this loop are less than ideal, especially considering the default behavior for the EVSEs, in the absence of a load curtailment signal, was a reversion to maximum amperage rate. In a scenario, such as a parking lot, where the sum of all EVSE's maximum capacity exceeds the service rating, communications loss could lead to service interruptions, equipment failures, or at very least, demand charges. Therefore, a much shorter control loop was investigated, to determine if more reliable signal responses could be observed.

HARDWARE INTERCEPT BOARD AND HIGH-SPEED CHARGE CONTROL EXPERIMENTS

The above results of the electric vehicle charging indicated significant challenges to reliable charging. High latencies indicated challenges that might occur with fast-changing situations, such as large PV arrays on days with significant wind and clouds. After the J1772 intercept board was developed and integrated, several experiments were

run to determine what, if any, increases in reliability and response time were achievable with these direct control devices.

Charging under a PV envelope, local high-speed control

Given the results of the above charging paradigm, the hardware boards and control software was run against the same PV output profile, to determine whether local control would provide better results. The research was conducted with a 2014 Chevrolet Volt (similar to the 2011 in the prior research), simply by modifying the setpoint to the J1772 intercept board at the appropriate times. As shown in Figure 12, vehicle responsiveness was significantly improved, in its ability to follow the same EV signal as used in the prior research. This figure shows both the one-minute and one-second average results against the 2013 PV data, and the original Chargepoint data for reference. By moving to local controls, both in terms of eGauge reads and signal dispatches, the latencies of the system were significantly improved.

Using the same approach and data set from the original research (simulating PV generation in real-time as though it were Feb. 13, 2013), the model became significantly more reliable, due to the lack of communications losses that led to the EV resuming full charging ($r=0.93$), and offered a more reliable regression against the real values ($p=0.04$). This infrastructure also allowed for far faster responses than Chargepoint; using the one-second approach (in which the EV was set to the prior second's output), the results fit the load curve almost perfectly ($r=0.981$), and the regression model was an even better fit ($p < 0.01$). Therefore, the abilities of the EV to match a load curve have dependencies on network latency, network reliability, and periodicity of signal change.



Figure 12: Local EVSE control charging an electric vehicle under a PV envelope

Local Frequency Response with droop control

In order to test local response, the Arduino firmware was enhanced to include an option of droop control, using a 5% droop factor. The firmware is configured such that, upon charge commencing, the vehicle is allowed to charge for 30 seconds at 100% of capacity (under the presumption that it will charge at the maximum rate for that particular vehicle). Then, the charge rate is adjusted to a set value (tested at 75% of the maximum rate), and updated using the formula $I_n = \max(I_{min}, \min(I_{Pk}, I_{n-1} + (I_{Pk} * \frac{1}{\% \text{ droop}} * \dots$

$\frac{f_{nom}-f_n}{f_{nom}}$), bounded between $I_{min}=5$ A and the maximum observed charging rate of the vehicle.

Initial testing, 59.95 to 60.05 Hz deadband

When tested to include a deadband between 59.95 and 60.05 Hz, against a previously recorded frequency signal, the output of the EV was predictable, and fairly infrequently diverged from its target output, at 75% of its peak 3.3kW (99.5% at 75% of maximum charge rate). When scaled against the amperage ratings of the J1772 specification, this lead to consistent results, with 99.5% of the time spent at the equivalent maximum amperage of 2.475 kW (75% of the Volt’s 3.3 kW). When the limits of the J1772 specification were applied, this led to even more rounding, and thus 99.7% of the charging occurred at the 2.448 kW level. The 59.95 to 60.05 Hz results of these simulated results are shown in Figure 13.

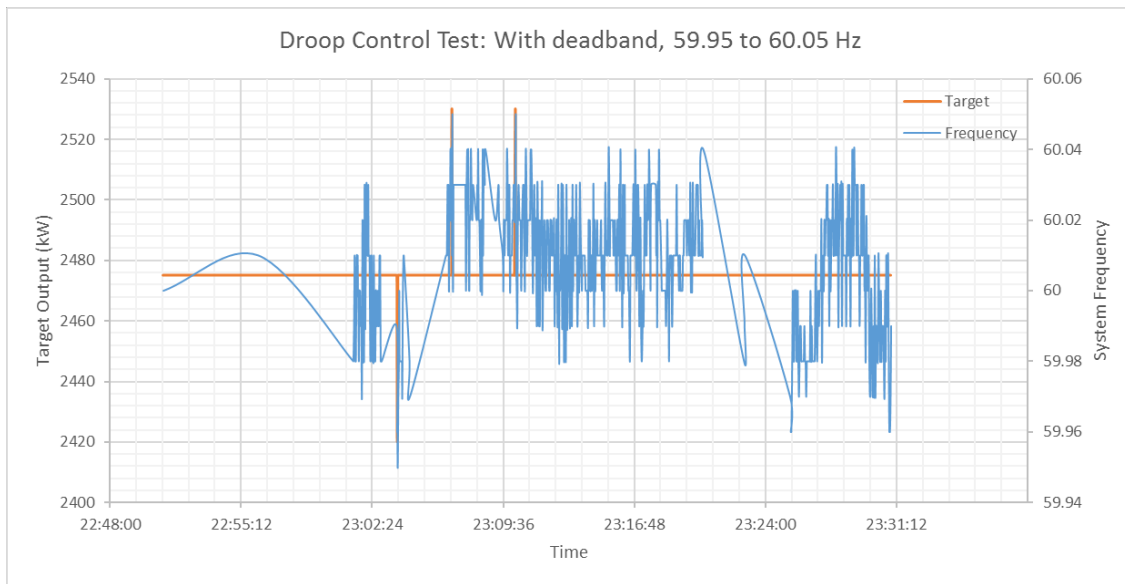


Figure 13: Simulated droop Response with a deadband of 59.95 to 60.06.

This type of droop controller, while it may scale well into an interactive system, did not provide a large observable behavior in the EV response. Therefore, a tighter was tested, in order to test theoretical and actual vehicle responsiveness.

Initial testing, 59.99 to 60.01 Hz deadband

Changing the droop controller’s deadband to 59.99 to 60.01 was anticipated to create significantly greater variability on the part of the maximum amperage, which would in turn lead to more stringent tests on an electric vehicle’s responsiveness. During this experiment against the same previously-recorded frequency signal as above, maximum amperage signals ranged from the maximum 3.3 kW to a minimum of 2.046 kW. When applied against the discrete maximum amperage ratings as per the J1772 specification, this led to a range of 2.016 to 3.3 kW. During this test, as expected, the vehicle spent less time in the 75% maximum charge rate, at 16.8% for absolute values, and 48% for J1772 discrete amperage values. The ideal values of this simulation are shown in Figure 14.

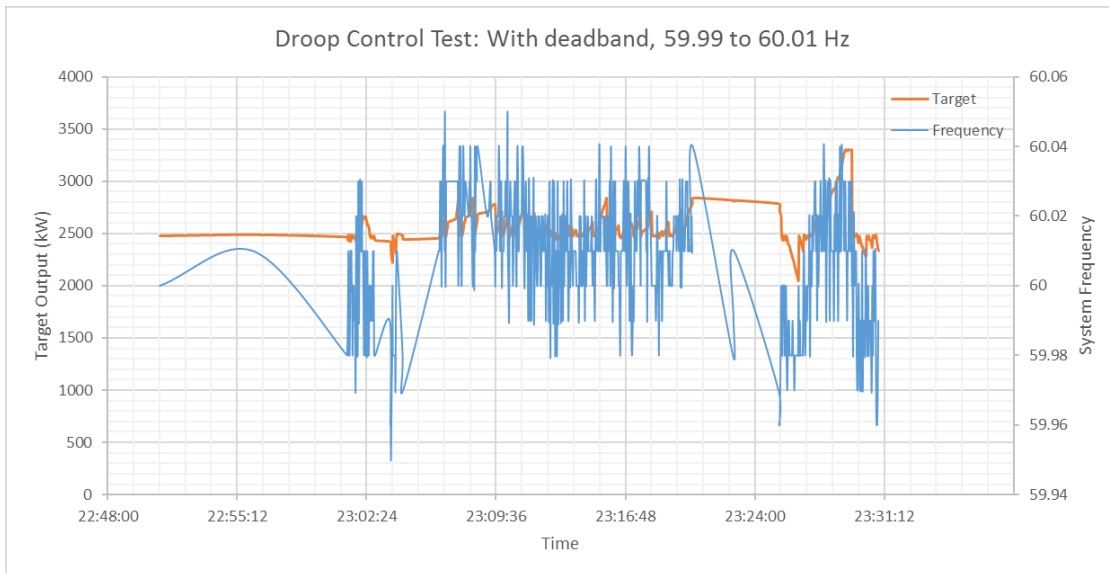


Figure 14: Simulated droop Response with a deadband of 59.99 to 60.01.

These results indicated significant variability in max charge rate, and thus were deemed appropriate for testing an actual vehicle's rapid responsiveness.

In-situ testing, 59.99 to 60.01 Hz deadband

These simulated values generated above were assigned to the owner's electric vehicle (2014 Chevrolet Volt), and set maximum amperage ratings were applied. The actual vehicle's power consumption tended to trend higher, which was attributed primarily to the differential between the nominal voltage assumed in the computations (220 Volts) to the actual system voltage, which fluctuated over the course of the testing, and thus lead to both an offset and response variability. The results of this experiment are shown in Figure 15.

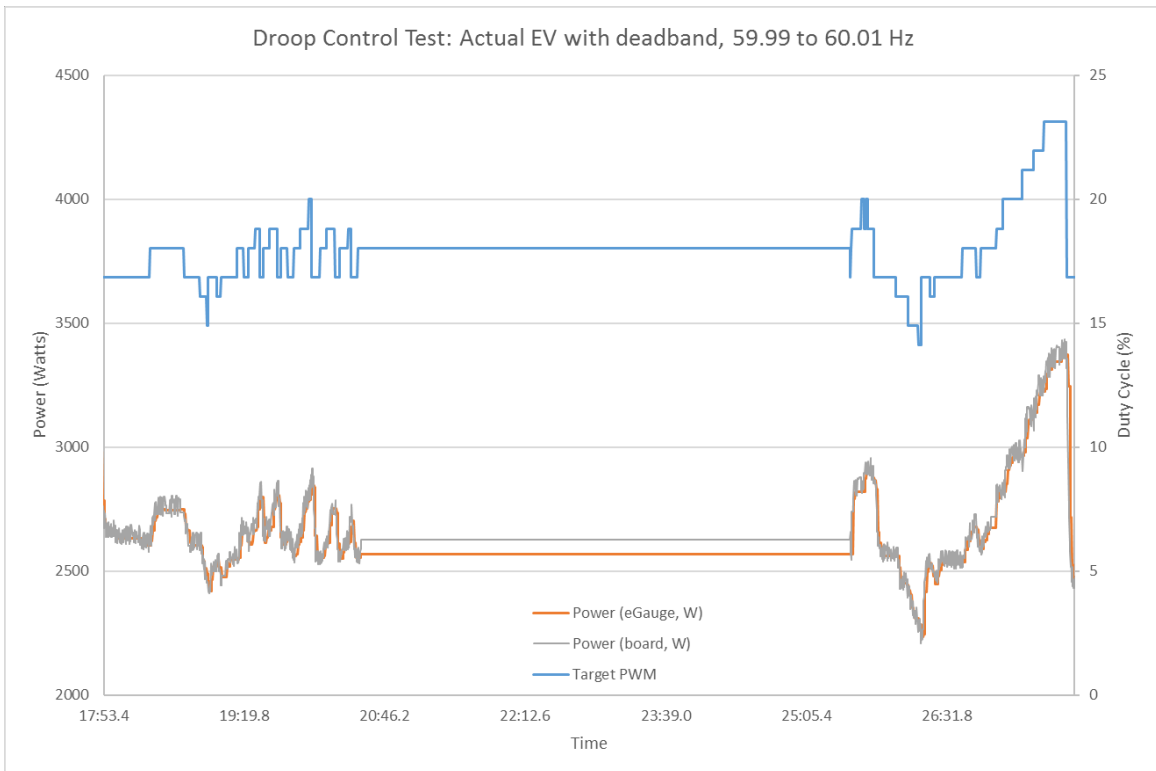


Figure 15: Actual vehicle response to historic values, with deadband of 59.99 to 60.01

These results are quite promising, as they show strong correlations between the idealized and actual values ($r=0.837$), and indicate the capability of local, direct, high-frequency control of EV charging, with the vehicle and its power electronics responding well to these kinds of control signals. It should be noted that this experiment attempted to apply pre-computed values which were calculated from the prior studies, which meant the server software dispatched UDP instructions over a network (which had to bridge a wireless gap between the router and the Wi-Fi-to-Ethernet bridge adjacent to the vehicle controller). Even so, the responses were reliable and consistent.

Furthermore, this incoming data set was applied at periodic intervals (scans every 250 ms, and dispatch every second), which differs from the original data set, which was extracted from the eGauge, with roughly 2 second periodicity. Therefore, this EV response time was double that of the original experiment, and it still faired quite well. It is anticipated that proper calibration (and perhaps, even an initial parameters testing when an EV plugs in) would further improve the accuracy of the system. Observations of the eGauge also show significant debounce on incoming signals (while the custom hardware has none), and thus further variability was detected between the two.

VEHICLE CHARGING OBSERVATIONS

With the completion of the ERCOT Electric Vehicle Test Bed, several additional tests were conducted to determine the real-world response characteristics to electric vehicle charging, in order to determine the response characteristics of many vehicles. Vehicles participating in this research included three Chevrolet Volts (2012, 2013, and 2014), four Nissan Leafs (2011, 2013, 2014 and 2015), a Tesla Model S 60 (2013), and Ford Focus

Energi (2014). Observational analysis of the waveforms as measured by the J1772 intercept boards indicates harmonic differences between the various EV charging types.

Representative samples of vehicle current growth upon the J1772 intercept board reaching state 8 (when the vehicle is provided a PWM duty cycle) are shown in Figure 16. Note that both the Ford Focus and Chevrolet Volt initiate an upfront large current draw before ramping up, while the Tesla and Leaf do not do so.

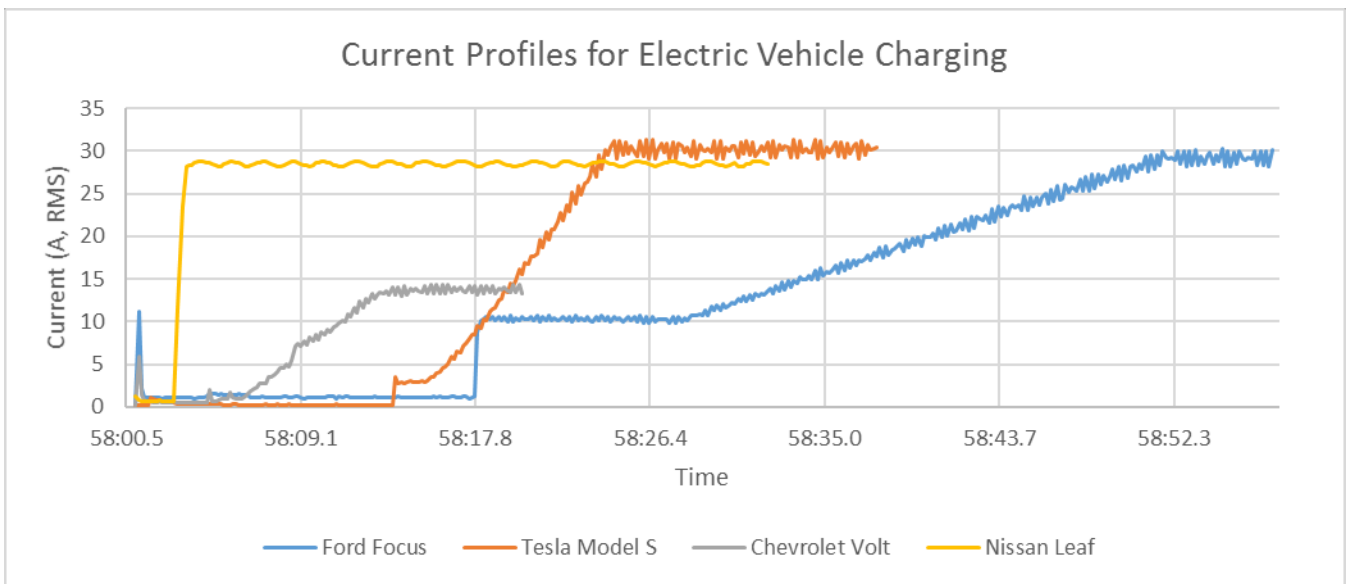


Figure 16: Current profiles for a 2014 Chevrolet Volt, 2013 Tesla Roadster, 2012 Ford Focus Energi, and 2015 Nissan Leaf

Current analysis also indicates that the Focus tended to produce the least distorted current waveforms relative to the other vehicles, as measured by total harmonic distortion. The aggregate of peak amperage and waveform shape tends to indicate that, generally, detailed waveform analysis can likely provide reasonable estimates of vehicle type, and thus patterns of response. These waveform examples are shown in Figure 17. Waveforms were selected to be off-center to highlight the differences in the waveform, and system

frequency varied between the three waveforms, leading to slight differences between the peak-to-peak lengths. This information could also be used forensically, if needed, to estimate the vehicle type during a charge event, especially in the event that a fault had occurred on the system at that time.

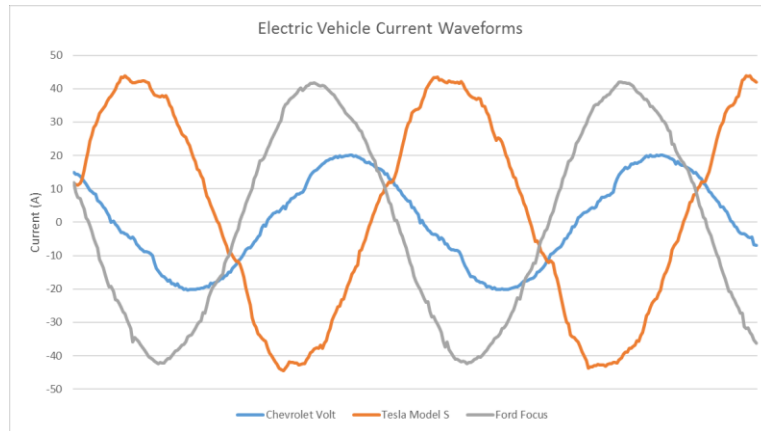


Figure 17: Current waveforms for a 2014 Chevrolet Volt, 2013 Tesla Roadster, and 2012 Ford Focus Energi

Conclusion

This research indicated that electric vehicle charge control was certainly possible; simple demand response or load shed signals were achievable through existing commercial products. Using the custom developed hardware, it was determined that the vehicles appear to have the capability to rapidly respond to load control signals, often faster than 30 cycles. In order to harness this rapid response, the architecture of EVSEs would need to support very low latency signals, or be configurable to behave rapidly against set parameters, much as is done with generator droop control parameters. With hardware providing rapid response to external signals, these vehicles are able to respond well within the 2-second

FRRS requirements, and should be able to respond even faster to support more rapidly changing, lightly loaded systems. Observations of the vehicles at the start of the charging session may also provide hints to the vehicle type, and as such, estimates of their battery capacity and potentials to provide ancillary services.

Afterword

Once the J1772 intercept boards were validated and functioning well in the charging stations, several vehicle charge control strategies were discussed for use in the test bed for non-research scenarios. These include strategies that preserve service quality, system stability, peak shaving, and emergency responsiveness. Code was written and tested to support each of the use cases, and the ERCOT facilities group has the ability to activate the various strategies as mentioned below.

SERVICE QUALITY CONSIDERATIONS

One of the challenges of building out additional EVSE infrastructure has to do with the limited capacity of the distribution transformer and service connection to the main breaker panel. Like the bulk power system, in which infrastructure is utilized near peak for only a small percentage of the time, the financial implications of building out local infrastructure to support EV growth are large, including transformer and primary service connection updates, and potentially further upstream investment requirements. Therefore, this research was conducted to determine if the maximum power as seen at the breaker mains could be controlled intelligently. Three strategies were tried for this approach. In all three approaches, the duty cycle directly at or below the target amperage rates were selected, ensuring the total power consumption never exceeded the target limits.

- Prioritizing BEVs: Allowing electric vehicles without range extenders to charge at full first, and then range-extended EVs.
- Shared capacity FIFO: Allowing EVs to charge at full until the maximum capacity of the mains are reached, and holding others until additional capacity becomes available, in a first-to-appear modality
- Shared capacity: Determining a common percentage of maximum charge rate to be applied to all EVs, such that the total power consumption does not exceed the capacity. Therefore, each EV is given a proportional share of the system capacity.
 - When an EV plugs in, the maximum charge rates of all other vehicles are reduced for a short period of time, such that there is 40A of capacity on the system.
 - The new EV is allowed to charge for thirty seconds, during which time its maximal charge current $I_{Max,Vehicle}$ is determined.
 - Then, each vehicle's proportion of load is calculated, and every vehicle's maximum charge rate is set to the floor of $I_{Max,Service} * I_{Max,Vehicle} / \sum I_{Max,Vehicles}$, relative to the discrete amperage values as per the J1772 specification.

SYSTEM STABILITY CONSIDERATIONS

In order to support the reliability of the system, a droop controller with a 5% setting, and deadband between 59.95 and 60.05 Hz was requested to be added. This would provide additional support to the system should any significant over-generation or under-generation events occur. Unlike the simulations and testing earlier in the research, these vehicles were

set to charge at 90% of their charge rates, as this was considered to offer some load increase potential should overfrequency occur, but not significantly decrease vehicle charging times.

PEAK SHAVING CONSIDERATIONS

Given concerns about the system peaks observed during the summer and winter seasons (as demonstrated in Figure 18), avoiding heavy loads in the summer after 4 PM, and in the winter between 7 and 10 AM and after 4 PM. This was accomplished by a notification to the EV driver that no charging would occur during this time period, and the intercept board providing a 1A (needed power electronics and pumps only) signal during that range. Outside that range, the EVs were given a 30A signal, and allowed to charge at a full rate.

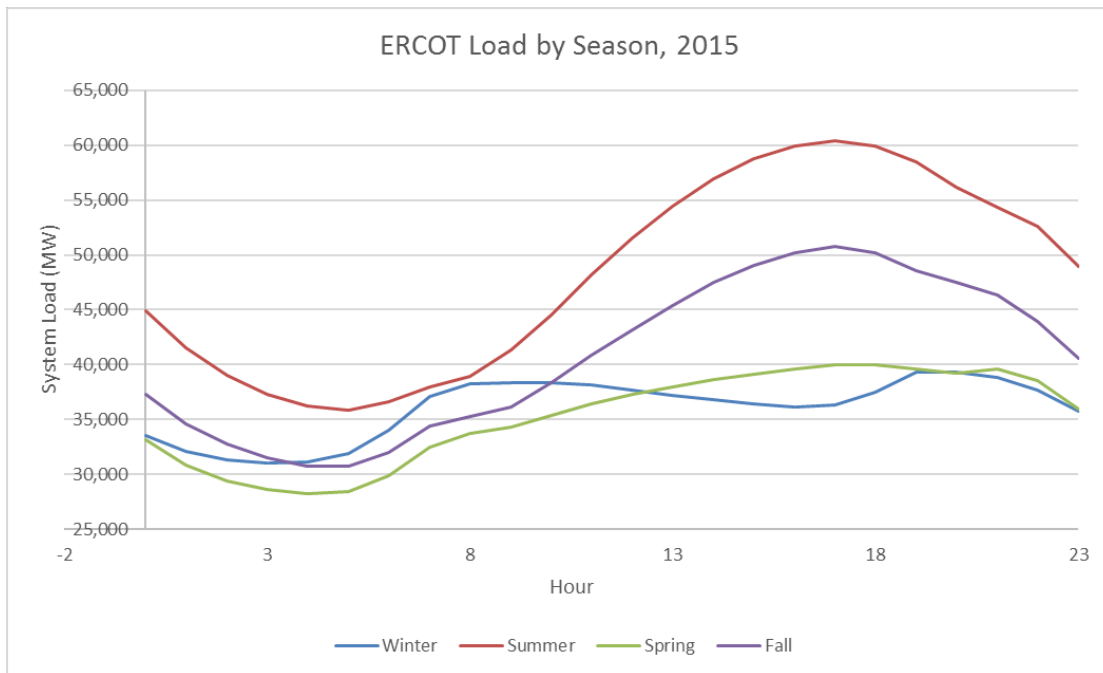


Figure 18: ERCOT hourly system load by season. Calculated from [46]

Emergency responsiveness considerations

As a policy, when an ERCOT control room operator determines the need to declare an Emergency Energy Alert (EEA), several signals are sent to the public, through interfaces such as Twitter (@ERCOT_ISO), Facebook, over the mobile Energy Saver application, through mail to the EmergencyAlerts listserv at <http://lists.ercot.com>, and on ERCOT's website, at <http://www.ercot.com>. On the website, a small JavaScript at http://www.ercot.com/content/alerts/conservation_state.js. This JavaScript applet is pinged by the test bed server every second (with a unique ID appended to the suffix to prevent caching), and regular expressions used to determine the EEA level of the system, if any. These values are presented in Table 3. In order to also protect the drivers, drivers do have the ability to indicate a personal emergency situation, which will move their vehicle to the maximal charge rate.

System Status	Test Bed Charging Behavior
Normal Operators	Vehicles allowed to charge normally, depending on other operational parameters.
Power Watch – EEA 1	Vehicle Charge rates reduced by 10% to what their normal rates would have been. Drivers notified via email.
Power Warning – EEA 2	Vehicle Charge rates reduced by 25% to what their normal rates would have been. Drivers notified by email and text message
Power Emergency – EEA 3	Vehicle charge rates set to 1A (presumed to support only needed loads such as battery thermal management)

Table 3: ERCOT Test Bed Responsiveness to Emergency Energy Alerts (EEA)

CHAPTER 5: SIMULATION OF ELECTRIC VEHICLE AGGREGATION FOR STABILITY SERVICES

Introduction

Given that a high-speed hardware intercept board was able to demonstrate rapid electric vehicle response to changes in the maximum charge rate signal, a simulation was developed by the author to determine how a large scale adoption of these vehicles could help provide stability services. For these experiments, unstable power systems were chosen for simulation, under the presumption that if a fleet of electric vehicles could help stabilize an otherwise destabilizing system, they can also help maintain system stability in normal operations, and offer the rapid, autonomous recovery characteristics associated with strong resiliency.

Methodology

Based on the input parameters derived from the hardware design in Taylor, an agent-based model was developed to test several scenarios in which high-speed electric vehicle charging load control could improve the stability of the grid. To provide a realistic proxy for varying conditions, this simulator was designed to approximate the mechanical and electrical responses of a synchronous generator, provide electric vehicle charging behaviors in accordance with the response characteristics derived from the research test bed, and simulate a variety of additional components on the system. The tool set is written in C#, and available in the open source repository associated with this research, under the MIT-style license. In order to create a simpler simulation, this initial research presumed a community microgrid currently islanded from the bulk power system. This allows for a small fleet of generation and loads, with both controlled and uncontrolled resources that can be configured to determine interplay.

COMPONENTS

In order to facilitate the simulation of a small power system, several components are simulated. These include wide-area, generation, load, and relay components.

Neighborhood microgrid

The neighborhood microgrid is designed to be the sole serving entity to its connected loads, due to its current islanded state. This approach was also selected for ease of a conversion to a blackstart simulation, in which a single turbine (with limited ramp rate capabilities) can be used, in concert with controlled and uncontrolled load and generation resources, to build a fairly stable small power system.

Synchronous Machine

The synchronous machine component simulates a microturbine or other synchronous machine. The simulation presumes an infinite fuel source (e.g., functional natural gas pipeline), and focuses primarily on the mechanical aspects of the generator and its relationship to frequency and load supply. The synchronous machine can be connected only to the neighborhood/microgrid.

Input Parameters

The synchronous machine's behavior is computed based on the following parameters:

- Speed of the generator, at no load (RPM)
- Speed of the generator, at full load (RPM)
- The number of poles on the generator
- The mass of rotation within the unit (kg)
- The vibrational sensor threshold.

- Parameters for the proportional-integral-derivative (PID) controller. These parameters provide the functional requirements for the unit's governor. Traditionally, isochronous mode zeroes out the integral and derivative components (providing instantaneous response because it is the primary frequency driver), while droop control zeroes out the derivative components (to prevent oscillations between multiple synchronized generators).

Computations

The synchronous machine, at every time step, has its inertia adjusted based on the changes in the system load (load/generation imbalance). The PID controller can choose to maintain or change the flow of fuel into the generator, which in turn affects the future inertia of the rotating mass. Based on the current speed, the system frequency is determined using the formula $f = \frac{P \cdot n_s}{120}$, where P is the number of poles, and n_s is the unit's speed in rotations per minute. The microturbine is presumed to solely determine the system frequency, in response to the change in load from the previous time step. The microturbine's regulation constant R is rated at 0.05 per unit, and the relationship between steady-state frequency and power is $\Delta p_m = \Delta p_{ref} - \frac{1}{R} \Delta f$ [47]. Losses within the microturbine are ignored, and the relationship between the mechanical torque in the microturbine and its output is modeled as $P = \frac{2 \cdot \pi \cdot RPM}{60} \tau$, where P is the power in watts applied to the generator, RPM is the speed of the microturbine in rotations per minute, and τ is the torque within the unit in Newton meters [48].

Photovoltaic array

The photovoltaic array object is intended to simulate an array of multiple photovoltaic panels and their associated inverter, designed to be grid-tied. They can be connected to either the microgrid (indicating they are on the same electrical bus as the high

side of the generator's step-up transformer), or on the rooftop of homes. Homes that have PV generation are also adjusted for HVAC parameters, as a decreased per-square-foot HVAC demand is anticipated with the additional PV shading on the roof.

Input Parameters

The photovoltaic array's behavior at a point in time is based on the following parameters:

- Nameplate capacity – The maximum anticipated generation of the array, from the output of its inverter
- eGauge inputs – The real-time PV generation levels tracked at the EV research test bed
- Frequency response bands – The upper and lower ranges of frequency in which the inverter will function. Outside this band, the inverter is anticipated to go offline for a period of time.
- Grid Support mode – This mode provides an extended range of function to the inverter, such that when frequency is too low, the inverter will attempt to continue generation for an extended period of time, hoping to help provide additional inertia and/or voltage support to the system. This mode also includes timing parameters for how long the inverter can operate in this mode.

Computations

At every time interval, the previous step's PV generation, and the eGauge's recorded generation numbers around the time period are determined. Based on the simulation parameters, the change of generation to the eGauge's next period is either linear, or linear with an additional randomization component.

Wind Turbine

The wind turbine component is based on scaling down telemetry from either a western or coastal wind farm, to the level of an individual turbine.

Input Parameters

The wind turbine's behavior at a point in time is based on the following parameters:

- Nameplate capacity – The maximum anticipated generation of the turbine
- Telemetry inputs – The real-time wind generation levels read from historic wind data at a particular location

Computations

At every time interval, the previous step's wind generation, and the telemetry's recorded generation numbers around the time period are determined. Based on the simulation parameters, the change of generation to the telemetry's next period is either linear, or linear with an additional randomization component.

Home

The home object simulates the behaviors of a house, and uses several parameters to estimate real-world activities. Because it follows real-world behavior scaled from eGauge results, it provides fewer simulations than other home energy consumption models (e.g., [49]).

It can house photovoltaic generation and one or more electric vehicles, but does not have to. Based on the simulation being conducted across a Texas summer day, all are required to have HVAC units. It leverages a home's eGauge data to determine load behaviors (outside EV charging and HVAC load, which are calculated separately).

Input Parameters

The home's behavior at a point in time is based on the following parameters:

- Ambient temperature and humidity – The conditions inside the home
- Square footage – The size of the home
- Number of people – The number of residents in the home
- Whether the kitchen is being used – Whether additional heating may be occurring in the home due to ovens.
- Non-HVAC/EV load – The whole house load provided from the home eGauge data, with the exception of that home’s real-world EV and HVAC loads.

Computations

At every time interval, the HVAC and EV loads, and PV generation are calculated for that home. The total household load is then considered to be the sum of the house’s HVAC, EV, and other loads, minus its PV generation.

Electric Vehicle

The electric vehicle provides our primary point of research intervention, allowing for a vehicle to ramp its charging load rapidly in order to support system stability. The EV model’s input parameters are based on the results of the Taylor, Texas research test bed.

Input Parameters

Several parameters determine the electric vehicle behavior in the research study.

- Battery capacity – this corresponds to the full usable range of the battery’s capacity. For example, the 2014 Chevrolet Volt has a total battery capacity of 16.5 kWh, but the usable capacity is 10.9 kWh. This differential occurs due to the charge controller’s protecting the battery pack.
- Maximum charge rate – this corresponds to the maximum instantaneous charge rate the EV can have

- Charge mode – This determines the vehicle’s behavior
 - Maximum charging – This is the traditional setting for electric vehicles, charging at the maximum rate until the battery capacity is reached.
 - Average rate charging – This input additionally requires departure time, and leads to a charging rate of $\text{Min}([\text{Total kWh needed}]/\text{hours}, \text{Maximum charge rate})$.
 - Average rate charging with frequency response – This input utilizes average rate charging, but utilizes a PID controller to self-generate frequency-responsive load changes to support the reliability of the system.
 - Average rate charging with ancillary services – This input utilizes average rate charging, and then allows for deviation from the average rate in response to ancillary services dispatch signals.
 - Time response to PWM signal change – The average and standard deviation of response time to the EVSE changing the PWM duty cycle. These parameters are derived from the values collected at the Taylor test bed. For the Chevrolet Volt, this translates to 15 ± 2 cycles.
 - Droop response – utilizes an average rate charging with a set droop mode (defaulted at 5%) to determine EV charge rates. This ostensibly has the effect of reducing load when frequency is below nominal (60 Hz), and increasing it when above. For the Chevrolet Volt (3.3 kW maximum charge rate), for example, this has the effect of 1.1kW/Hz.

Computations

The computations for the simulated electric vehicle focus mainly on battery charging behaviors, modeled on observed behaviors of the vehicles that participated in the ERCOT Electric Vehicle Research project. These included maximal charge rate, response characteristics to PWM signals (particularly the thresholds at which charging is stopped), and total available battery capacity). This was computed for the following electric vehicles:

- Chevrolet Volt (2011, 2012, 2013, and 2014 models)
- Nissan Leaf (2011, 2013, 2014, and 2015 models)
- Ford Focus Energi (2014 model)
- Tesla S (2013 S60 model)

HVAC Unit

The HVAC unit models a simple unit in air conditioning mode (as the research is conducted across summer months). Its behavior is modeled after observed HVAC usage (as measured by both compressor and fan at the author's home eGauge), scaled to computed per-home size values.

Input Parameters

The HVAC unit requires a SEER rating, and the home's square footage, number of occupants, and whether it has PV panels.

Computations

The per-hour BTU measurement for load is based on the formula $L_{H,BTU} = 20.0 * s$, where s is the square footage of the house. If the house's kitchen is frequently used, an additional 4,000 BTU are added. For every person after the second occupant, an additional

600 BTU are added. If the home does not have PV panels (and is presume to therefore have direct roof exposure to sunlight on peak), the BTU demand is increased by 10%. The final number is divided by the HVAC's SEER rating to produce a watt/hour measurement [50]. The eGauge data from the author's HVAC provides the reference data, and the peak HVAC hourly usage is scaled against this number, in order to determine a realistic and scaled view into the output.

Results

Based on the parameters derived from the ERCOT Electric Vehicle Research test bed, several simulations were conducted to determine scaling potentials of a great many electric vehicles in an aggregator model. They are described in the following sections, including a PID controller with deadband, blackstart simulation, and multiple generators with droop control.

PID CONTROLLER WITH DEADBAND

To create a straightforward local frequency-based control mechanism, a PID controller with deadband functionality was developed. The equations governing PID functionality are $u = K_p e + K_i \int e dt + K_d \frac{de}{dt}$. The proportional component, $u = K_p e$, generates a control action proportional to error (the differential between the current frequency and nominal frequency). The integral component, $u = K_i \int e dt$, reduces steady-state error at the cost of stability, and the derivative control $u = K_d \frac{de}{dt}$ attempts to predict the system behavior and respond more rapidly to the state of the system, often by increasing the variability of system stability.

Tuning parameters for the PID controller were developed by scaling the load of an individual EV up to a level where it could have a significant effect on system frequency, presuming constant load. The generator's governor controls were also disabled for the

initial tuning, to ensure that the electric vehicle was the primary driver for frequency control.

DROOP CONTROLLER WITH DEADBAND

The droop controller algorithm built on the J1772-intercept board was also included as an option for the EV and generator responsiveness. This same formula, $I_n = \max(I_{min}, \min(I_{Pk}, I_{n-1} + (I_{Pk} * \frac{1}{\% droop} * \frac{f_{nom} - f_n}{f_{nom}})))$, was validated, with the default deadband between 59.95 and 60.05 Hz.

BLACKSTART SIMULATION WITH EV PID CONTROLLER

The first experiment involved the development of a blackstart simulation, in which a very lightly loaded power system, containing a microturbine, PV panel, and electric vehicle running PID controller were run together. The governor controls on the microturbine were disabled, and thus the primary responsibility of the EV was to use its local frequency detection in order to modulate its load and maintain frequency within a narrow bandwidth of 59.5 to 60.5 Hz. The electric vehicles were assumed to be performing rapidly (15 cycles) locally to system frequency. Under and over-frequency relays were also simulated to test these parameters and ensure system stability. This approach was intended to mimic a very difficult, highly dynamic scenario in which the PID controller implementation of the vehicle could be tested. The simulation was constrained such that the PVs had to always ensure the system load was positive and respected the ramp rate capabilities of the microturbine. These vehicles were simulated to be in fixed locations, and charge at half their maximum charge rates, to provide sufficient ramping capabilities in both directions.

As shown in Figure 19, the simulation indicated that 200 Chevrolet Volts (at a maximum charge rate of 3.3 kW, usable battery capacity of 10.8kW, and average response

time of 15 cycles) were able to maintain system frequency (as represented by the green line) within this wide band for several hours during the morning, ramping up load as the PV panel generation (as represented by the white line) increased. However, as the vehicles' states of charge rose due to time and increased load to offset the renewables (as represented by the red line), the capabilities for load increases in response to overgeneration became limited, and eventually an over-frequency relay tripped the generator offline due to the excess generation that hit the system when the vehicles could no longer draw sufficient current.

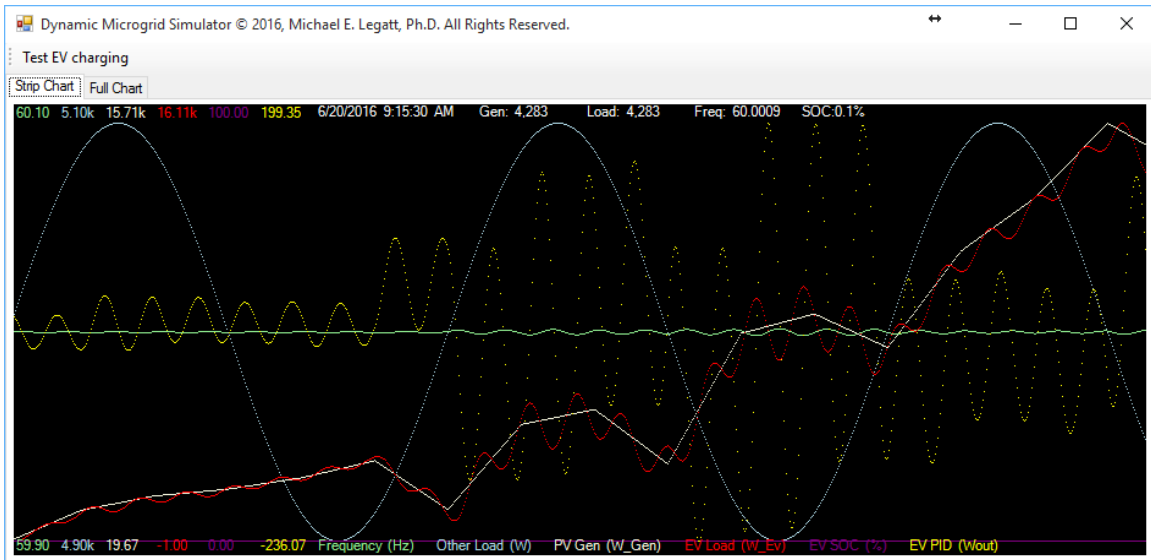


Figure 19: Dynamic Electric Vehicle charging to offset heavy renewables and limited microturbine ramp rate capabilities

BLACKSTART SIMULATION WITH DROOP CONTROLLER

The same test was conducted replacing the EV's PID controllers with the more traditional 5% droop controller. This approach yielded better results, as the swings on the system were responded to in a more predictable manner. The EVs did not provide any frequency response as long as frequency was within the deadband, but when the frequency

went outside the range, frequency restoration occurred more quickly. As expected, as the vehicle's batteries approached SOC, the capacity to respond to frequency changes became limited, and thus eventually an overfrequency relay tripped due to over-generation as it did in the PID controller case above.

CONTROL SIMULATION AGAINST AN OSCILLATING LOAD

In order to determine the ability of multiple scaled electric vehicles to support the reliability of a more dynamic system, a simple load profile was generated, comprised of two sinusoids; a lower- (1x) and higher-frequency (8x) oscillation, simulating some dynamics on the system. Without any electric vehicles, this load/generation profile looks misshapen, and is only stable due to its being within the ramp rate profile of the microturbine. This waveform is demonstrated in Figure 20. Scaling this load's oscillation amplitudes outside the range of the microturbine led to either over- or under-frequency relay trips quickly.

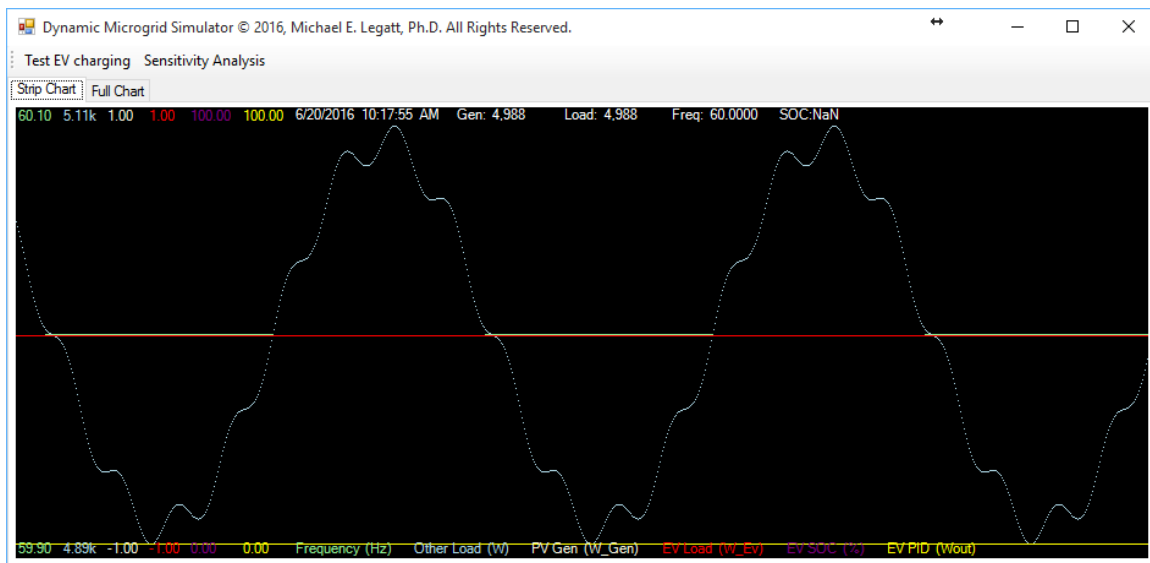


Figure 20: An oscillating load whose demand is met through a microturbine only

Adding electric vehicles with PID controllers to the environment significantly improved the frequency profile of the region. One of the noted effects was the risk of oscillations occurring between the microturbine's governor and the group of electric vehicles, leading to some competition for frequency regulation. Effective use of the integral and derivative components improved responsiveness within this configuration, although it is presumed to not be a generalizable effect. Generally, though, short-term factors associated with the response rates of the electric vehicles were noted to affect frequency, while longer-term, vehicles approaching their maximal state of charge led to reductions in frequency response capabilities, leading to overfrequency relays tripping during sudden growth in PV output, due to insufficient load resources remaining.

In the real world, however, there are several factors that could limit the effective responsiveness of electric vehicles. In the local frequency control mode, frequency detection algorithms (especially zero-crossing analysis means) could fail in high-harmonics environments, leading to misoperations on the control circuitry's part [51]. Furthermore, as the observations in the research test bed showed, electric vehicles that approach the end of charge have typically different patterns of ending their sessions, and their capability to respond to frequency diminishes as its state of charge approaches 100%.

Conclusion

This simulation demonstrates that the aggregation of electric vehicles, with proper set parameters for vehicle behavior, can lead to improved stabilization of an unstable power system. However, electric vehicles are shown to be unable to maintain these behaviors beyond their batteries achieving a full state of charge, or in the event of the driver choosing to disconnect their vehicle. This paradigm does assume a one-way power flow from the power system to the electric vehicle, so potentially a bidirectional power flow may have less of these constraints, but may not be acceptable to drivers, due to concerns of warranties being voided, and full vehicle ranges being unavailable in emergency situations.

This simulation indicate that controllable electric vehicle charging could play a role in the home “nano-grid”, mixing electric vehicle charging, energy storage, and local generation to support off-grid applications. There may be several features supported by these activities, such as alternating HVAC loads and EV charging loads, to reduce “birthday cake” issues. The vehicle’s capability to respond to these signals also indicate they may be able to provide dispatched load control (presuming the vehicles are plugged in and needing to charge) to better control load growth approaching peak hours, which may alleviate “duck curve” issues.

CHAPTER 6: DISCUSSION

Summary of key findings

This research demonstrates that electric vehicles can, with reliable low-latency connectivity to an aggregator, or ability to respond to local frequency or other control signals, and in a simulation, help to provide significant reliability services to a power system. These services could be provided at the bulk, micro- or nano-grid levels.

In the simplest scenario, EVs or EVSEs with intelligent, tightly-controlled (e.g., droop or PID) frequency response can be seen as helping to provide additional grid stabilization services, but in order to be effective, EV adoption rates would need to be much higher, or EVs would need to work closely in lighter-loaded scenarios, such as in micro- or nano-grids, or in areas with significant frequency variability, such as in Hawaii.

Electric vehicle charging patterns were noted to be clustered around vehicle make and year, which was unanticipated. This data could offer increased confidence for an aggregator or utility, if vehicles of similar profiles also have similar response characteristics to control signals. This data could also be used to provide early warning measures, so waveforms that begin to deviate may indicate damaged power electronics components, or other proxies to vehicle health.

Provided robust network communications and the appropriate revenue certifications, an EV that is capable of responding within 250 ms to a signal that arrives quickly and reliably, could easily participate in grid-wide fast-responding ancillary services, and a host of other services. Such services could, for example, be designed to alleviate congestion, offset intermittent renewables, and protect distribution level equipment. Further integration of hardware in the EVSE to measure THD, frequency,

voltage, and current, all against a GPS time reference, has the capability of providing distributed synchrophase data to a utility or aggregator. This data could further help grid operators to maintain system stability, and offer redundancy to system measurements, rapidly help locate system faults at any part of the system, through integrating a large number of these distributed, locational measurements. These same time stamps could help build highly reliable, integrated ledgers of transactions using technologies such as hashgraph, leading to decentralization, consumer privacy protection, and robustness due to decentralization. Because the point of system interconnection must be known to provide proper models and integration, and the value of distributed synchrophase measurements to the overall system, it would appear that additional use cases to system reliability are possible with the control hardware, telemetry, and aggregator interfacing occurring at the EVSE level, not the EV.

Certainly, none of this technology will work at all without participation at the consumer, educational, and regulatory levels. Drivers are likely to not configure their EVs to maximally support the reliability of the bulk power system unless they are taught how to do so at the point of purchase, and understand the benefits of doing so. They will likely not be willing to participate in services that could compromise their security or privacy, and thus need strong consumer protections in place. Certainly, a great many other concerns, such as vehicle cybersecurity, while not covered in this research, provide additional concerns around EV adoption.

Additional Considerations

This research indicates there may be several integration points between electric vehicles, their drivers, and the bulk power system, which have not fully yet been explored. These include integration points between the electric vehicles and the charging stations, the EV/EVSE combination and grid operators (at the NSO, MSO, DSO, and ISO levels), integrations of new and fast-responding market signals and EV drivers, and exploration of different control paradigms. This research focuses exclusively on the J1772 charging paradigm at Level 2 (240 Volts) and thus does not include Level 1 (usually wall outlet home, 120 Volt) or DC fast charging. It is anticipated that many of these hypotheses would transfer well to those paradigms, and likely, in terms of real-time market participation, altruistic demand response, and others, be even more critical in DC fast charging environments should high adoption rates of that style of EV charging occur.

REVENUE-GRADE TELEMETRY

Currently, time of use EV charging programs, such as SDG&E's EV TOU rate [52] and Austin Energy's EV 360 [53] rates, all require installations of additional revenue-grade advanced meters, in order to section off the EVSE onto a separate metered instance. This adds significant cost, in terms of permitting, installation, and monitoring to the utility. Furthermore, should a homeowner move, these meter/EVSE infrastructures are likely to become fixed and immovable, and not guaranteed to be captured in the home's sale price.

Therefore, this research indicates that a better approach may be an integrated EVSE with revenue-grade current transformers (CTs) and an overall certification of revenue-grade accuracy. This EVSE would be configurable to incorporate several different plug-in modules to support connectivity back to the utility, including, but not limited to, cellular, AMI backhaul, Wi-Fi, Ethernet, Modbus, DNP3, IEC 61850, etc. The goal would be to

create a device that can transmit data to the utility and/or management system through whatever paths are appropriate, in an open configuration that is able to find the lowest-cost pathway to reliable data transmission at any moment. These systems should also in turn be able to receive data across any of the pathways, which would include the receipt of real-time market signals, dispatch signals, energy alerts, etc.

CONTROL/DATA INTEGRATION POINT: EV OR EVSE?

One of the main questions currently in debate between EV and EVSE manufactures (even within companies, like Nissan or Tesla, that do both) is as to whether the primary control point should be the EV or the EVSE when electric vehicles interact with the bulk power system.

The results of this research suggest that a paradigm of advanced EVSE-EV communications, with the EVSE serving as the integration point, may offer several advantages. In order to improve the experience of provisioning and installing an EVSE, revenue grade certifications may lower installation costs. That guaranteed accuracy may also make the device, capable of synchrophase measurements, able to provide new reliable informational services to the utility. Because the EVSE is in a fixed location, its connectivity on the system remains the same, while tracing algorithms can rapidly determine the electrical bus to which the vehicle providing services is connected, which may change in mesh networked areas. This allows for the EVs to provide services not only for global frequency (as current fast-responding ancillary services address), but also for congestion, which requires focal understanding of interconnection points. Should a future of EVs transferring power back to a grid (from islanded nanogrid to interconnected BPS) become a reality, well-known control points for ERCOT-Polled Settlement (EPS) metering would need to be in place for both monitoring and control, and likely new integrations

between the EV and wider-area management system would need to be established. This is most likely to occur with fixed assets in place, fully under the ownership of the property in which they are connected. An electric vehicle, except perhaps as a fleet vehicle, does not have this capability.

However, it is also recognized that a second EVSE to EV communication would need to occur, which would have to do with the transfer of critical information that would allow an aggregator to determine target state of charge and trajectory, and to dispatch the EVSE/EV appropriately. Should such an interface grow, such as the J1772 P1902.1 powerline communications (PLC) addendum as recommended [54], additional limited subsets of commands, such as initiating a cabin pre-cool/pre-heat for maximizing driver comfort, would be recommended.

ELECTRIC VEHICLE (EV) TO ELECTRIC VEHICLE SUPPLY EQUIPMENT (EVSE) INTEGRATION

Current commercial EVSEs have quite limited communications with the EV, namely the handshake around charge initiation, proximity detection (which typically is limited between the handle of the charging cord and the EV), and PWM signaling from EVSE to EV to indicate maximum amperage to the vehicle. Current draft specifications for revisions to the J1772 specification include using additional technologies, such as powerline communications (PLC), to relay more information between EV and EVSE [54].

In order for the EVSE to function as a proper integration and control point, it would likely require several pieces of information, and also would need to have the ability to communicate downstream to the vehicle and simultaneously upstream to a central system. The following data are some examples of information needed to flow from EV to EVSE:

- EV Battery nameplate capacity (both original and derated as needed)
- EV Battery estimated state of charge (SOC)

- Minimum load required by EV (e.g., for thermal management of batteries)

In order to provide a higher quality of service to the EV driver, the following data points may enable the EVSE and its core system to provide a higher quality of service:

- Exterior ambient temperature/humidity
- EV Cabin ambient temperature/humidity
- EV Battery temperature
- Estimated efficiency, miles per-kWh

LOCAL CONTROL-AND-REPORT VERSUS CENTRALIZED CONTROL

One of the growing challenges in a more dynamic and distributed electric system is that of local versus centralized control. In the ERCOT region, for example, the grid operator dispatches units every four seconds with a Load Frequency Control (LFC) signal specifically designed to maintain the system balance at 60 Hertz. However, this central control paradigm does not function downstream of islanded systems (e.g., micro- and nano-grid), and does not support reliability in sub-second events. Therefore, this research indicates that while the EVSE would respond to real-time signals such as LFC, it should be able to leverage the EV's sub-second response capabilities, and thus immediately change the vehicle charging behaviors when local waveform analysis detects concerns (e.g., over-frequency, under-frequency, excessive THD on the voltage profile, etc.).

In that paradigm, therefore, the EVSE would engage in sub-second load behavior shaping activities, while notifying the aggregator about reliability-supporting behaviors that have been completed, with the expectation that a system operator would in turn remunerate the EV for those behaviors. This would require some additional communications between the EVSE and EV, or a market settlement function that

incorporated the EVSE providing the measurements and relaying the signals (which would imply remuneration owed to the EVSE owner) and the EV changing behavior (which would imply remuneration owed to the EV owner). Ultimately, this approach could add to the value propositions for a site owner to install an EVSE, and for an EV driver to allow load control of their vehicle.

ELECTRIC VEHICLE SUPPLY EQUIPMENT TO ELECTRIC SYSTEM INTEGRATION

The experimental results of this dissertation suggest that the EVSE may need to receive and transmit several pieces of information to a system operator or aggregator. For purposes of this research, the presumption is made that the EVSE communicates simply with an aggregator, which in turn relays all the appropriate signals to the building energy management, utility, distribution, transmission, and grid operator levels. The following information points are hypothesized to be necessary:

- From EVSE to aggregator (containing a GPS-synchronized timestamp)
 - At set intervals (e.g., every second)
 - Frequency
 - Voltage RMS
 - Phase angle
 - Voltage THD (%)
 - Voltage harmonics analysis
 - Current THD (%), if charging
 - Current harmonics analysis
 - Vehicle state:
 - Remaining kWh to full
 - Remaining kWh needed for next trip, estimated

- Maximum charge rate
 - Current charge rate
 - Responsiveness reliability metric
- In response to events:
 - Voltage THD alerts (when harmonics grow beyond an alert threshold)
 - Local frequency and voltage THD responses
 - Time of initiation
 - Time of return-to-normal
 - Total kWh change (positive are increased loads during time in question, negative decreases).
 - Vehicle plug-in
 - Vehicle plug-out
- From aggregator to EVSE
 - At set intervals (e.g., every 30 seconds):
 - Spot market prices for the current electrical bus
 - Total system load
 - Percentage of generation from non-CO₂ generating sources
 - System frequency
 - Grid-dispatched AGC signals
 - In response to events:
 - Demand response dispatch signals
 - Fast-responding ancillary services dispatch signals
 - Fast-response congestion management alleviation dispatch signals

Providing frequent information from the EVSE to utility may provide information valuable to maintaining system stability; much as state estimation at the transmission level can create rapid situational awareness for maintaining reliability, so could synchrophase data from distributed electric vehicles create a power flow map for the distribution system. When mixed with distribution SCADA telemetry, this may lead to ongoing views into the functionality of the distribution system, fault detection and localization, and a variety of other stability-supporting services.

FAST-RESPONDING SERVICES

To strengthen EV-to-grid integration, the future bulk power system would likely benefit from a variety of new services. These services would all be based on sub-second responsiveness. With the presumption of GPS time-reference synchronicity across the system, these dispatch instructions would be provided with GPS time stamps, and EVSEs (and other devices) would respond with time stamps for message receipt and action completion. For services that require an understanding of the provider's location (e.g., congestion management), the optimal locations for dispatch (load increase and decrease) would be determined using the shift factors between equipment's electrical buses and the support-needing electrical buses. The following are examples of fast-responding services these loads could provide:

- Maintaining system frequency through rapid load increase/decrease anywhere on the system (akin to ERCOT's fast responding regulation service [55], but faster than one second).
- Reducing system congestion nearby to a particular electrical bus, through rapid controlled load increase/decrease at particular points on the system.

- Buffering the system in the event of generator outage, supporting power electronics providing synthetic inertia, through modulated rapid load increase/decrease.
- Providing locational support, to a generator unable to achieve its ramp up/down time, by shifting load supply to other generators or decreasing load to support reasonable ramp up times (in order to alleviate “duck curve” issues).

BLOCKCHAIN OR OTHER DISTRIBUTED ACCOUNTING FOR SYSTEM OPERATOR/EVSE/EV INTEGRATION

One of the main advantages of a centralized accounting system is that it can maintain an integrated, time-synchronized log of all activities. As intelligence moves towards the grid edge, part of the challenge becomes the synchronization across multiple devices, potentially without a central authority. One of the means for achieving this is blockchain technology (e.g., [36]). Such technologies could enable peer-to-peer communication across multiple EVSEs or aggregators, and thus be segmentable in separate networks, and more fault-tolerant due to the lack of reliance on a single centralized infrastructure. Technologies such as hashgraph [56] can ensure all transactions and interactions between the EVSE, EV, and aggregator, are archived in a contiguous ledger that is third-party auditable and public, while at the same time, if designed properly, protecting customer privacy. Furthermore, with appropriate certifications for revenue grade accuracy, the hashgraph could also include local telemetry, such as system frequency, in order to create a centralized and auditable energy to market interaction view.

COMMITTED TIME TO CHARGE/ SIMPLIFICATION FOR DRIVER

If one were to imagine an exceptionally dynamic system, in which generation and load resources needed to be balanced rapidly (e.g., 15 cycles or less, in a situation such as a lightly loaded microgrid with intermittent and uncontrolled load and generation), power balance becomes more complex. In order to maintain a perfect power balance, the computational and operational requirements will increase significantly, especially in terms of the speeds of communications networks. From the perspective of electric vehicle charging, it is easy to imagine that constant demands for minor load increases and decreases could, in theory, affect the process of EV charging. For example, most algorithms to determine estimated time to charge use simple formulae for instantaneous charge rate, projecting out to the end of the charging cycle at that rate. While the aggregator or EVSE, provided it has the needed information, can provide these estimates, the question as to driver comfort and participation is a crucial one; without driver involvement, these new technologies will not be adopted. Therefore, the idea of the EVSE/aggregator committing to a “charge by” time, or providing limits around the degree of load shaping it can undertake, may lead to improved user confidence. It is likely acceptable to customers to offer an “urgent override” function to increase locus of control, and that should a true urgency arrive, with sufficient time, the driver could opt out of providing DR, or agree to pay spot market prices to complete the charge.

Unfortunately, constant exposure to real-time prices on the other hand, creates an exceptional deal of complexity which would likely significantly degrade the driving experience. Therefore, the user experience benefits of an autonomous trusted agent acting on the driver’s behalf increases the likelihood of adoption.

ULTRACAPACITORS AND EV/PV BUFFERING

The more one imagines the power system consisting of fewer controllable generation resources, and more dynamic loads, the more one can imagine that fast responding loads that are controllable, such as electric vehicles, can play a major role in maintaining system stability. However, drivers of electric vehicles may be less comfortable with the idea of constant, rapid transitions of their charging load on those unstable systems. It may also be the case that areas that have rapid dynamic swings on the system, such as Hawaii, may also have higher gasoline prices, and therefore vehicle drivers may still choose electric vehicles for cost savings purposes. Therefore, means of addressing high load variability should be addressed.

It may be beneficial to consider an enhancement to electric vehicle design that includes an ultracapacitor on the DC bus, allowing from the perspective of the power system, more ancillary services to be provided, without the battery seeing as much of a constant deviation during a charging cycle. This ultracapacitor could also provide an enhanced driving experience, leading to faster acceleration times, and greater degrees of energy capture during regenerative braking events, if in parallel with the battery stack or bridged together through power electronics. Given that a significant proportion of the ultrafine particulates that are associated with ICE driving are in fact fragments from friction braking, shifting to more electrical regenerative braking can lead to further reductions in per-mile emissions.

Similarly, that same approach could be considered for photovoltaic generation, as that additional buffering may perhaps offer a more stable generation profile on days with significant clouds and wind. One could imagine a small ultracapacitor connected to each PV panel (likely on the upstream side of the maximum power point tracking; MPPT) equipment, or on the DC bus side of the inverter, serving this role. These technologies

would not be able to provide long-term sustainable load shaping, but at least help reduce the rapidness of swings often seen on less robust power systems.

Future Work

Thanks to an ongoing collaboration with ERCOT, this research will continue, and subsequent results are intended to be presented in conference proceedings and peer-reviewed academic journals. This includes a great many psychological factors (e.g., altruistic load shedding, behavioral economics, etc.) which are part of ERCOT's EV research planned timeline.

HARDWARE ENHANCEMENTS

From the J1772-intercept hardware board perspective, many challenges were noted during the development and testing phases, and there are some additional enhancements that would lead to higher reliability levels. First, a redesign that isolates the 12-volt references as provided to the board from the voltage signaling measurements would be beneficial for cleaner input signals. Second, the board design presumes a balanced voltage input, and thus essentially multiplies the voltage and current measurements by two. Given the lack of a neutral and ground-fault protection in this particular EVSE implementation it is an appropriate decision, but in more real-world applications with greater potential phase-imbalanced systems, it may be beneficial to measure, at least, each voltage measurement against a common neutral bus. If one considers this EVSE as potentially the most advanced voltage sensing device within the household, it certainly would have value to detect distortions on one leg relative to the other, potentially indicating equipment malfunctioning

within the home. Furthermore, neutral-reference would allow additional technologies such as broadband over powerline (for network connectivity) and lower bandwidth powerline communications (e.g., X-10, for home energy management).

FIRMWARE ENHANCEMENTS

From the J1772-intercept firmware perspective, several enhancements would lead to improved integration in household and building systems. First, standardization around a common communications modality, such as Modbus or IEC 61850 (providing communications with a local building energy management system), or ICCP (providing communications with an aggregator) would lead to additional utility. Integration with other protocols, such as OpenADR 2.0 would ensure their ability to function in multiple use cases. Also, because of the Arduino Ethernet 2 board's SDHC capability, local GPS-referenced logging would also ensure additional forensic capabilities, and the ability to upload to an aggregator valuable information following a communications disruption.

SOFTWARE ENHANCEMENTS

This research built on the author's master's thesis work, which used simulations to determine the emissions reductions associated with higher photovoltaic and electric vehicle adoption. That work showed the capability of EVs to, in near-real time, to offset PV panels, and thus theoretically, further change the dynamics of emissions on a system. There is the potential to integrate the two research projects, and simulate the effects of charging behaviors designed to specifically minimize emissions, such as CO₂ or UFPM. This could range from EVs offsetting intermittent renewables to reduce secondary emissions, as have been observed in Texas [3]. Furthermore, simulations of synthetic inertia, or intelligent load management to reduce "duck curve" challenges could be run on this system.

The aforementioned updates are underway at the time of this writing, and updates to the hardware design, firmware code, sever code, and mobile application code will be added to the open source repository as they are completed. The following sections cover specific areas of human behavior as it relates to driving an electric vehicle and participating more actively in the bulk power system.

ELECTRIC VEHICLE DRIVER TO REAL-TIME ENERGY MARKET INTEGRATION

Given that electric vehicles can be one of, if not the greatest instantaneous peak loads on the home, some service territories (e.g., in SDG&E's footprint) have already chosen to expose EV charging to time of use or real time prices. There is evidence that providing these price signals to end users shapes behavior change in reliability-centric ways (e.g., [42]), and thus is beneficial as the proportion of EV charging load continues to grow on the system. However, it is also noteworthy that exposure to constantly changing pricing can induce significant anxiety on the part of an individual, in part due to the inability to form consistent, reliable mental models on the relationship between an act and its associated cost [57].

Given that high electric vehicle adoption can create new effects on system load curves, a move towards dynamic pricing could, from an economic standpoint, create proper incentives to shift charging behavior. However, this type of pricing model, as it is different from what both ICE and EV drivers currently expect, and would require constant monitoring in order to respond to changing system conditions, may not be attractive to drivers if they must participate actively. However, it is hypothesized that an autonomous agent, trusted by the driver to work towards their values, would be more likely to be acceptable. Therefore, should large EV adoption require exposure to real-time market

prices, trusted autonomous agents may be required to avoid significant degradation in vehicle ownership experience.

BEHAVIORAL ECONOMICS OF ELECTRIC VEHICLE DEMAND RESPONSE SERVICES

It is further hypothesized that electric vehicle drivers may choose to make different decisions as to whether to participate in particular load shaping services, depending on the framing of the messaging, particularly in gain vs. reduction of loss, internal vs. external locus of control, and in social exchange-domain vs. financial exchange-domain signaling. It is hypothesized that traditional behavioral economics principles that have been observed across many domains, would work similarly in the EV pricing model domain.

It is also important to consider in this approach that interfacing with drivers about EV charge pricing presents several unique opportunities. Given that the vast majority of residential consumers are on flat-rate plans with at-most monthly, low-resolution information on consumption and costs, electricity tends to be thought of largely as undifferentiated (with the exception that some customers differentiate on the emissions associated with generation source). The vast majority of customers tend to think little about electricity when its reliability is quite high; at best, one could expect to see some cultural effects as far as energy decision making (e.g., keeping old appliances vs. purchasing more efficient new appliances, leaving lights when not home [58]).

DRIVER SITUATIONAL AWARENESS AND ALTRUISTIC BEHAVIORAL CHANGE

As a driver shifts their mental models around the fueling of their vehicle, there also is a greater opportunity at that time to shift their mental models around electricity as well. As an example, this could include a growing perception of electricity as a commodity over a limited-capacity pipeline, leading to behaviors such as voluntary peak shaving/load shifting. This change could also then enable them to entrust these kinds of behaviors to

agents acting on their behalf, thus approaching a modality where the system usage is maintained below its capacity with reasonable safety margins, instead of behaviors that would lead to increased infrastructure needed to handle infrequent peaks.

Another opportunity that could include a shifting mental model has to do with individual behavioral response to a grid-level event, such as an altruistic demand response event. An example of this was observed on January 6, 2014 in the ERCOT region. Freezing conditions, along with associated generator outages, derates, and failures to start led to insufficient levels of physical responsive capability (PRC), which is the primary driver for energy emergency alerts (EEAs). As part of the EEA process, public appeals were distributed on the ERCOT Energy Saver mobile app, and on television and radio, messaging about the need for conservation to support the reliability of the system [59]. A large number of users who received the mobile alert brought up the energy saver application, and 46.7% of them clicked the 'I did this' button in response to conservation recommendations. Looking at primarily residential load transformers randomly selected across the ERCOT region, significant dips in load were detected within a short period after the public messaging. Due to the multiple paths across this message, it is difficult to determine the individual effect of each outreach method, but in aggregate, it was observed that residential customers were willing to altruistically lower their load in order to support the whole electricity system to which they were connected [60]. It is therefore hypothesized that users, sensitized to the needs of the bulk power system (as these users likely were following the February 2nd, 2011 load shed) will be willing, at least within some reasonable limits, to alter their energy consumption behaviors in order to support the overall reliability of the system.

APPENDICES

Appendix A: Emissions and Human Health

PARTICULATE MATTER

The term “particulate matter” generally serves as a catch-all term for extremely small airborne particles and droplets. Typically, PM consists of a variety of different components, including nitrates, sulfates, organic chemicals, metals, soil, and dust particles. One of the main factors to consider when analyzing PM is its size, as different sizes of PM behave in different fashions. The primary concern from a human health standpoint is around the inhalable particles, including the fine particles (2.5 μm to 10 μm), and ultrafine particles (<2.5 μm). Both particle types, when they enter the nose, are inhaled into the lungs, and can pass into the blood stream. The ultra-fine particles are sufficiently small as well to traverse the blood-brain barrier, and thus enter the brain and spinal cord, potentially causing damage to the blood-brain barrier and increasing the admittance to subsequent larger particles in the bloodstream.

Particulate matter inhalation has been associated with premature death in people with heart or lung disease, increased risk of cardiac arrest for healthy people, cardiac arrhythmia, and increased risk of asthma exacerbation, decreased lung capacity, and increased difficulty with respiration [61]. Estimates of mortality due to particulate matter are significant. The World Health Organization estimates 800,000 premature deaths per year due to PM_{2.5}, ranking it as the 13th leading cause of worldwide mortality.

Unfortunately, monitoring of particulate matter emissions is rather sparse, both at the vehicle and electric power generation level. For places where emissions are measured, they tend to be far more at the PM₁₀ level, rather than the UFPM level, and not as directly linked to power plants as CO₂, SO_x or NO_x sensors. Several source-level methods have been employed to track emissions from coal plants, and are affected by a variety of factors, including combustion temperature, coal type, effectiveness of scrubbing technology, and generation output variability.

The particle emissions from vehicles are also highly variable. Analysis of emissions near a London major roadway between 1998 and 2001 indicate that particles > 60 nm in

diameter tend to be emitted by heavy-duty (primary diesel-fueled) vehicles, while smaller particles between 30 and 60 nm are primarily emitted by light duty traffic. As wind speed increased, or distance from the roadway grew, the overall particle counts reduced significantly, in an inverse-square distribution. However, the smallest particles, between 11 and 30 nm in size, tended to be moved less by wind, and also showed an inverse association with temperature, peaking in the early morning [62].

Overall, a great many significant relationships between particulate matter exposure and human health have been noted. These included increased pediatric emergency room visits, type II diabetes, obesity, hypertension, depression and anxiety even when accounting for socioeconomic status, sex, age, tobacco use, education, BMI and occupational exposure e.g., [63].

SMOG

Simplifying a very complex series of interactions, smog is formed through the combination of emissions and sunlight. There are a great many studied interactions between smog and human health. For example, a person who has already had a heart attack is three times more likely to have a subsequent one on a high-smog day, as compared to a low-smog day. Similarly, patients with implanted cardioverter defibrillators had roughly an 80% increase in probability of a defibrillation event two days after a high smog day in China [64].

One of the most significant high-smog days recorded was on January 12 2013, in Beijing. There, the Air Quality Index (AQI; measured by ozone, O_3 + fine particulate matter, $PM_{2.5}$) was at a level of 755, well in excess of the formerly theorized limit of 500 when the EPA generated the index. $PM_{2.5}$ was measured at $886 \mu\text{g}/\text{m}^3$. The event was described as, "... all of Beijing looked like an airport smokers' lounge." This had the effect of reducing visibility to less than 50 meters. [65].

Based on hospital intake records, this high AQI event corresponded to a 16% increase in emergency room visits, a 12% increase in outpatient visits, and a 69% increase in hospital admissions. As the event ended, there was a heavy decline in these factors, as

was also noted in London's severe 1952 smog event. When analyzing hospital records against air quality metrics in Beijing between December 2012 and January 2013, each $10 \mu\text{g}/\text{m}^3$ increase in PM_{10} was associated with a 1% increase in ER visits, a 0.7% in outpatient visits, and a 3.9% increase in hospital admissions [66]. Another analysis on particulate inhalation in China concluded a linkage of roughly a three-year life expectancy reduction for every $100 \mu\text{g}/\text{m}^3$ average daily air particulate levels. When scaling this number to the Chinese population, the authors conclude an aggregate loss of 2.5 billion years of aggregate life expectancy for its 500 million residents, due to cardiopulmonary disease [67].

INTERNAL COMBUSTION ENGINE (ICE) ENGINES

Traditionally, road-based transportation has relied on the internal combustion engine, burning a petroleum variant to power movement. These vehicles typically emit several different classes of molecules, including carbon monoxide (CO), unburned hydrocarbons, oxides of nitrogen (NO_x), partial oxidation products, and particulate matter of varying sizes. Between 50 and 80% of urban air pollution has been attributed to these vehicle-generated emissions. Some emissions, such as carbon monoxide and hydrocarbons, are the primary byproduct of an idling vehicle, while at high speeds or accelerating, other byproducts such as nitrous oxides, with lead [68], or other additives now found in gasoline [69] as the predominant emissions.

However, vehicle emissions are also a far more complicated issue, as are the environmental factors associated with the vehicle's manufacture and disposal. Many newer internal combustion engine (ICE) vehicles are tending to outlast their emissions limiting equipment (e.g., engine life vs. catalytic converter life), leading to a question about the overall lifetime emissions associated with an ICE vehicle.

It is certainly the case that vehicles have grown in their capacity to self-monitor emissions of increasing types and accuracies. However, these technologies rely on the driver as an integral part of the control circuit, in the sense that it is the driver's decision to get the needed vehicle maintenance in response to the "check engine light", should one come on. The driver's decision would therefore affect the emissions output, and often

drivers may defer maintenance until the need for the next legally mandated inspection, or even after if one fails to get the inspection by its deadline. Driving vehicles with expired inspection stickers is a noted issue in law enforcement. For example, 21,000 citations for expired inspections (plus an additional 700 for no inspections) were issued by the Austin police department in 2010 [70]. Furthermore, human behavior on the part of the automotive manufacturer has recently been shown in Volkswagen “Dieselgate” and other vehicle manufacturers to create tampering and bypasses on these vehicle emissions control systems for long periods of time, further calling into question the efficacy of these control systems (e.g., [71]).

Behaviorally, this means that, aggregated across all high-emitting vehicles, emissions reduction equipment is of concern to society, while to the individual driver the “check engine light” is perceived as a non-immediate concern, and economically it likely more affordable to them in the short term sense to continue driving a higher-emitting and less efficient vehicle, rather than paying for the needed work to reduce emissions. With the Volkswagen “Dieselgate” and related emissions alterations, it is also possible that the individual driver may not even receive the appropriate notifications, either while driving or during inspection.

This behavior is also accentuated by the variability among vehicles and the differentials between the “average” vehicle emissions between different areas. For example, one study measuring PM_{2.5} and UFPM emissions from ICE engines found that over 50% of emissions came from 13% of vehicles in a neighborhood with low average socioeconomic status (SES). Emissions vary depending on a variety of host factors, including maintenance and the state of the vehicle, ambient temperature, the quality of the fuel, altitude of the vehicle, and a great many other factors [72].

BRIDGE APARTMENTS: ULTRAFINE PARTICULATES AND NEUROPSYCHOLOGICAL FUNCTIONING

One of the early long-term health psychology studies was conducted on residents of Brown and Guenther’s 1963 Bridge Apartments complex, over Interstate 95 in New

York City, adjacent to the George Washington Bridge. Between 1974 and 1991, over 8,000 residents were followed and studied for health, air quality, and neuropsychological functional measures, across the apartment's 32 floors.

As early as 1973, children participating in the study were noted to have significant impairments in auditory discrimination (ability to determine a signal sound from noise) and delayed reading skill, for children living on the lower floors, as compared to children living on the upper floors. Initially, this effect was attributed to simple noise levels [73]. Over time, additional analyses indicated that while noise was a major factor at lower levels, additional factors such as higher carbon monoxide and PM₁₀ levels were far more dangerous. For example, CO was measured peaking at 22 ppm on the third floor, averaging 14 ppm throughout the day. Unlike the noise factors, CO levels were not significantly reduced at the 30th floor. Other factors, such as particulate counts, were noted to significantly decrease at higher floors and thus were determined to be the root cause of the neurocognitive differentials between different-floor dwellers.



Figure 21: A view of the Bridge Apartments, New York City [74]

MEXICO CITY AND ULTRAFINE PARTICULATE MATTER

Much of the history and importance of poor air quality have been learned through studies in Mexico City over time. While on the uptrend now, air quality was so poor prior to 1992 that children, when asked to draw a picture with the sky then, tended to use green or yellow crayons instead of blue. Even back in the 1940s, air quality was sufficiently poor to obscure visibility to a mile or less, often occluding the snow-capped mountains. Particulate matter was traced back to a variety of sources, including industrial manufacture, electric power generation, and sewage being pumped into open air areas. It is one of the few places in the world that diseases that are typically fluid-borne (e.g., hepatitis, dysentery) can be inhaled [75].

Studies on both children and dogs living in Mexico City showed several signs of neurological trauma, including increased neuroinflammation, amyloid plaques, and neurofibrillary tangles. For example, 56.5% of the children studied showed white matter lesions in the prefrontal cortex, as compared to 7.6% of controls in a nearby town. The dogs showed a similar rate of neurological trauma (57%), and dog autopsy studies indicated the presence of ultrafine particulate matter (UFPM) in their brains, comprised of equivalent particle types to airborne ultrafine particulates. These studies are particularly alarming for human health, as the prefrontal cortex is responsible for higher-order and abstract reasoning, and thus a key structure used by members of a society striving to improve complex situations such as this one. Children followed who moved to Mexico City showed growing brain injury on MRI, corresponding to equivalent decreases in IQ, with significant performance decreases on tests measuring frontal lobe [76].

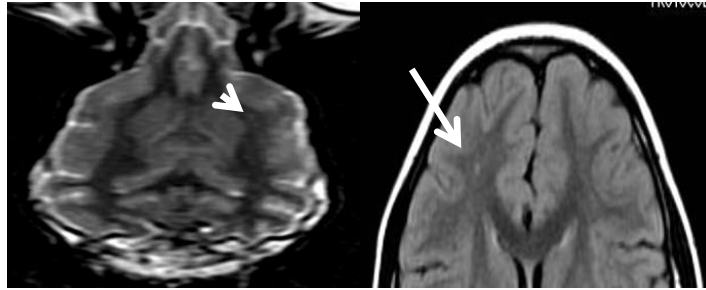


Figure 22: Dog (left) and human (right) MRI studies in Mexico City participants

APPROACHES TO EMISSIONS REDUCTION

Austin Energy and per-mile emissions reductions

Austin Energy owns a large fleet of vehicles, including non-hybrid ICE vehicles, parallel hybrid vehicles, and some early converted Prius vehicles that were capable of running in electric-only mode. In 2009, Austin Energy analyzed tailpipe emissions from their existing gasoline-only fleet vehicles, as compared to the emissions from their fossil-fuel generation fleet. Based on analysis of their driving patterns and emissions, transitioning emissions from the tailpipe to smokestack yielded a 95% reduction in NO_x , and 54% reduction in CO_2 . This early research indicated a strong potential overall improvement to society in transitioning to electricity as a fuel source [4]. However, these studies did not look at the myriad complex factors associated with energy demand, such as the time of day when the charging occurred and state of power flow on the system (and thus what plants contributed to that vehicle charging, along with its associated emissions).

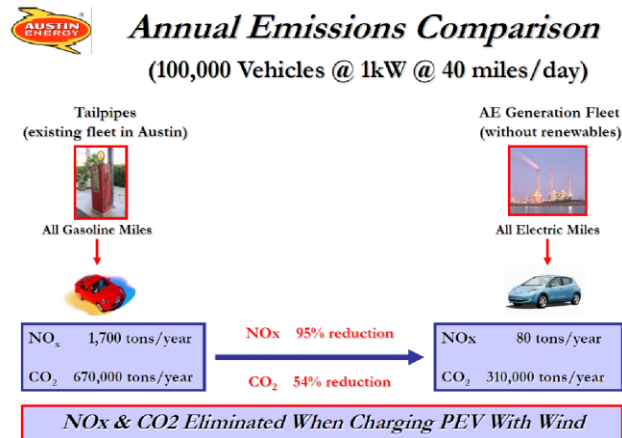


Figure 23: Austin Energy emissions comparison between tailpipe and smokestack

University of Texas: Vehicle electrification impacts on emissions

Previous research at University of Texas at Austin also looked at the emissions implications of vehicle electrification. These analyses included multiple scenarios looking at various charging patterns for both the Chevrolet Volt and Nissan Leaf. The research further highlighted the emissions reductions due to renewable generation, despite leading to slight increases in fossil fuel plant emissions due to ramping. Overall, the models indicate vehicle electrification leads to significant reductions in CO₂ emissions, a trend that holds until ICE vehicles achieve an efficiency of around 58 ± 8.3 mpg. According to the model, the cross-over point for NO_x is around 39 ± 9.5 mpg, while SO₂ emissions favor ICE vehicles generally at 0.6 ± 0.4 mpg, indicating a societal cost for SO₂. However, when taken in balance, from both public health and climate change concerns, the reductions in CO₂ are likely more valuable to society than the marginal increases in SO₂ emissions. For example, a recent analysis on the health impacts associated with coal plant emissions indicated a cost to society of \$0.214/kWh due to CO₂ emissions, and \$0.012/kWh for SO₂ emissions. [77]

The research further noted that the generation that would serve vehicle charging would be primarily served by combined cycle natural gas units, and then coal units. The increased generation of the coal units was identified as the primary cause of increased SO₂ emissions [3]. However, considering that in 2014, the Government Accountability Office

(GAO) significantly increased its 2012 estimates of the number of coal plants that would have retired by 2025, with the expectation that the bulk of retirements will occur in 2015, it is possible that in a few years' time, the SO₂ impact would be reduced by changes in the generation fleet, as shown in Figure 24 [78].

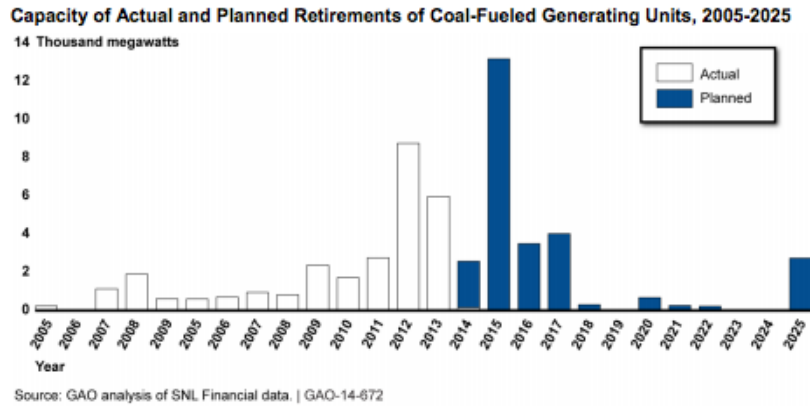


Figure 24: Anticipated coal-powered unit retirements 2014-2025

Appendix B: J1772 Intercept Board

In order to facilitate this research, a custom hardware development was built in collaboration between the author, Electric Reliability Council of Texas, Inc., and Pecan Street Project. The purpose of this custom hardware was to intercept the PWM/voltage signal between the EV and EVSE, and allow the board to inject its own messaging to the EVSE and EV. It is based on the Arduino Due, a 32-bit, 84 MHz ARM-based platform. It was selected because of its fast processing speed, 12 bit DAC, multiple digital I/O including pulse width modulation (PWM) generators, large internal memory, clock reference accurate to 10 microseconds [79], and ability to interface with Arduino's Ethernet Shield 2, which provides 100 Base-T Ethernet connectivity and an SD/SDHC card interface for offline storage and data logging [80]. The Due's PWM generator pins are defaulted to 1kHz, which is also the PWM frequency for the J1772 specification, and thus it is a good fit for the project.

The design for the J1772 intercept board contains three components stacked on top of each other using the Arduino pin layouts: The Arduino Due (central controller), intercept board (custom developed hardware for this purpose), and Ethernet Shield 2 board (for communications and data logging). The pinout diagram of the Arduino Due is shown in Figure 25.

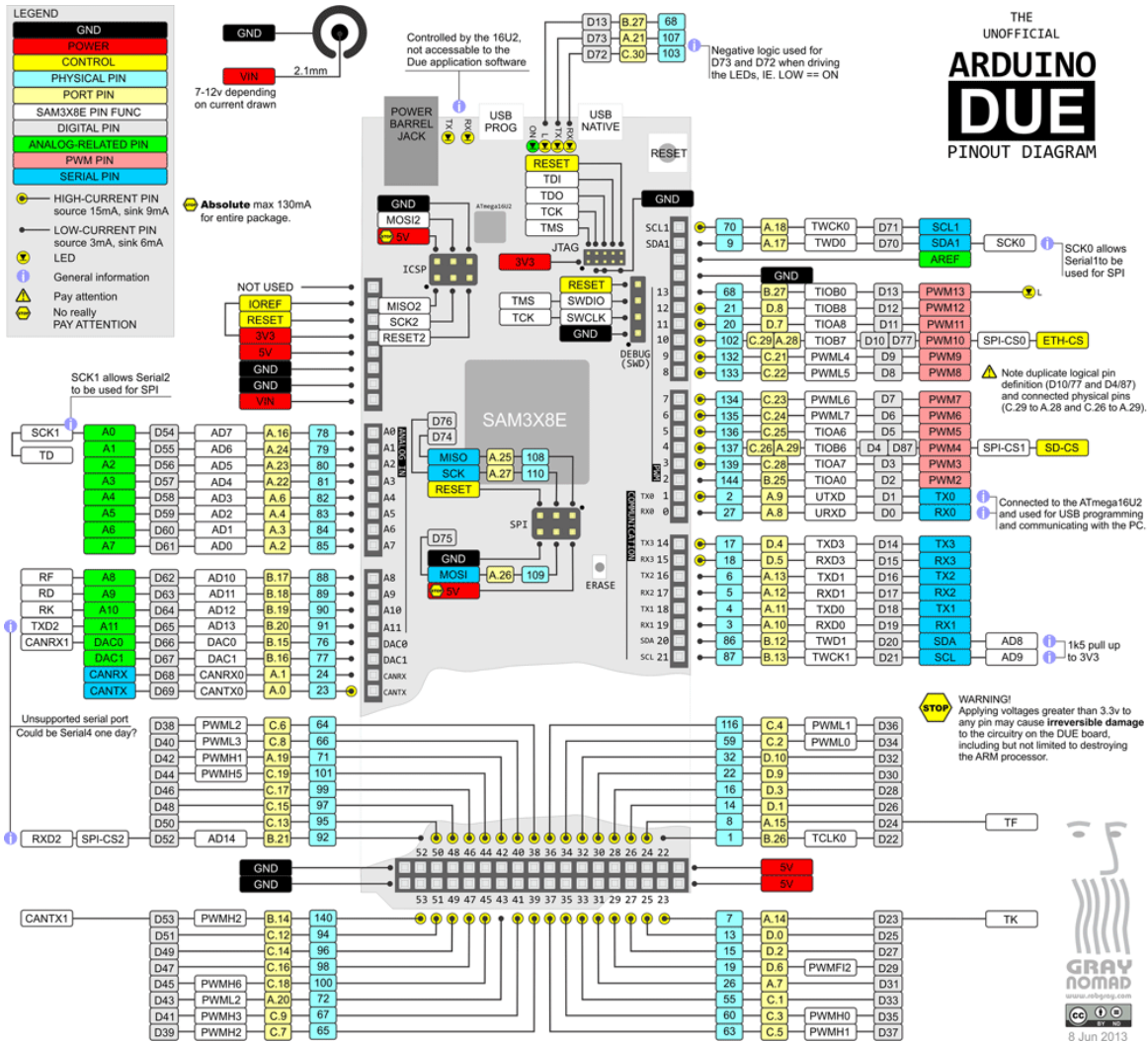


Figure 25: The pinouts of the Arduino Due

CUSTOM HARDWARE LAYOUT

The custom layout board carries out several functions. It has interfaces to the EVSE’s PWM signaling pin, as well as to the EV’s PWM signaling pin. It further has inputs for a 50-amp current transformer (CT) to be connected to one of the voltage legs, and an input for a 9 VAC input, to be provided by a toroidal transformer connected to both the L1 and L2 inputs entering into the EVSE. The board was originally designed to also incorporate the proximity detection pins as well, should the board want to bypass this

feature that is usually carried out in a resistor switching network in the EVSE's handle, but this bypass was not used in this research.

Since the suite of Arduino hardware boards run at either voltage references of 3.3 or 5.0 volts, the hardware is configurable by jumper for its scaling references, enabling it to function across multiple boards.

Voltage input and processing

The hardware design uses a toroidal transformer, designed to convert the $240V_{AC}$ from the EVSE's L1 and L2 inputs to $9V_{AC}$ out. Installation involves connecting the transformer in parallel with the EVSE's $220V_{AC}$ input. From there, one of the two $9V_{AC}$ legs are used to provide both power to the board (which utilizes power electronics to convert the $9V_{AC}$ to the $12V_{DC}$ needed by the board), and also serves as an analog input to the board, from which the voltage profile is analyzed. A future redesign is underway to instead use one of the $9V_{AC}$ legs to the DAC for voltage measurement, and the other through a rectification circuit to provide a stable $12V_{DC}$ that is galvanically isolated from the voltage signal.

The circuitry is designed so that diode D4 provides half-wave rectification of the input voltage, and thus two parallel $47\mu F$ capacitors provide buffering to reduce the V_{DC} ripple. This results in an ideal V_{DC} peak value of $9(\sqrt{2}) - V_{Diode} = 12.73 - 1.10 \approx 11.63 V_{DC}$, well within the 7-12 V_{DC} input ranges for the Arduino 8-pin power connector specification. The circuit layout for this component is shown in Figure 26, and a simulation of the $9V_{AC}$ input and $12V_{DC}$ output are shown in Figure 27. This $12V_{DC}$ output provides power to both the Arduino board and Ethernet Shield 2.

This component of the circuit also includes a voltage divider, providing to AC_MON, which is later scaled up to provide the scaled analog voltage. It incorporates

two parallel $100\ \Omega$ resistors connected to a series $1\text{k}\Omega$ resistor, thus scaling the input voltage down to $1/21$ its original input, or $0.429V_{AC,RMS}$, or ranging from $+0.606$ to -0.606 volts.

This circuitry was specifically designed for the Taylor, Texas installation which uses 220-Volt single phase inputs, and is not intended for use in other locations, such as ERCOT's Austin, Texas installation which uses 208-Volt three-phase inputs.

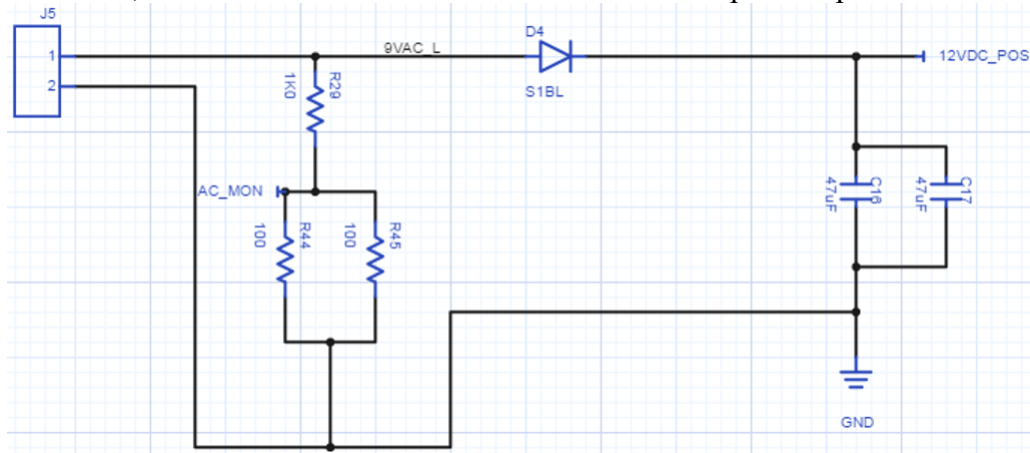


Figure 26: Circuit design for $9V_{AC}$ input and rectification to $12V_{DC}$ to power the hardware

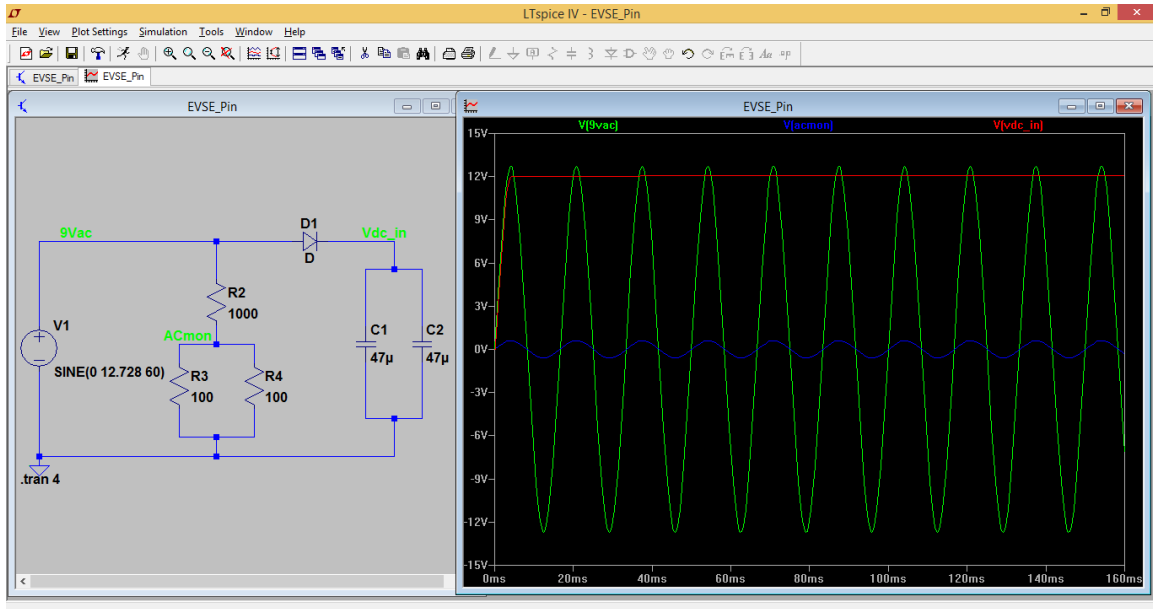


Figure 27: Simulation of $9V_{AC}$ to $12V_{DC}$ Rectification

The voltage input is then provided to a non-inverting op-amp buffer circuit (originally LM358ADR) with a gain of 2, and biased up to the midpoint of the reference voltage (1.65 volts of 2.5 volts). Given that the EV has a balanced input current at 208/220 volts (EVSE's GFCI circuitry protecting against unbalanced current, and no neutral wire), this voltage measurement can be multiplied by 2 to derive the voltage. For this implementation, this would include a voltage input to the Arduino's DAC, centered at 1.65 volts, ranging from 1.044V to 2.256 volts.

During the initial design and testing of the circuitry, it was noted that the voltage waveform was highly distorted, due to the nature of the op amp chosen and implementation (a simulation of the distorted voltage is shown in Figure 28). In order to repair this issue, the op amp was swapped for an inverting op amp, the LMV358IDR with the expectation that the custom firmware would need to invert the waveform about the 1.65V reference signal, in order to properly compute real power, power factor, etc. Aside from its inversion,

this circuit produces little distortion on the voltage waveform, and thus reasonable inputs for FFT analysis and harmonic detection, as well as power measurements.

The scaled and properly-biased voltage input is connected to the Arduino's analog input A5.

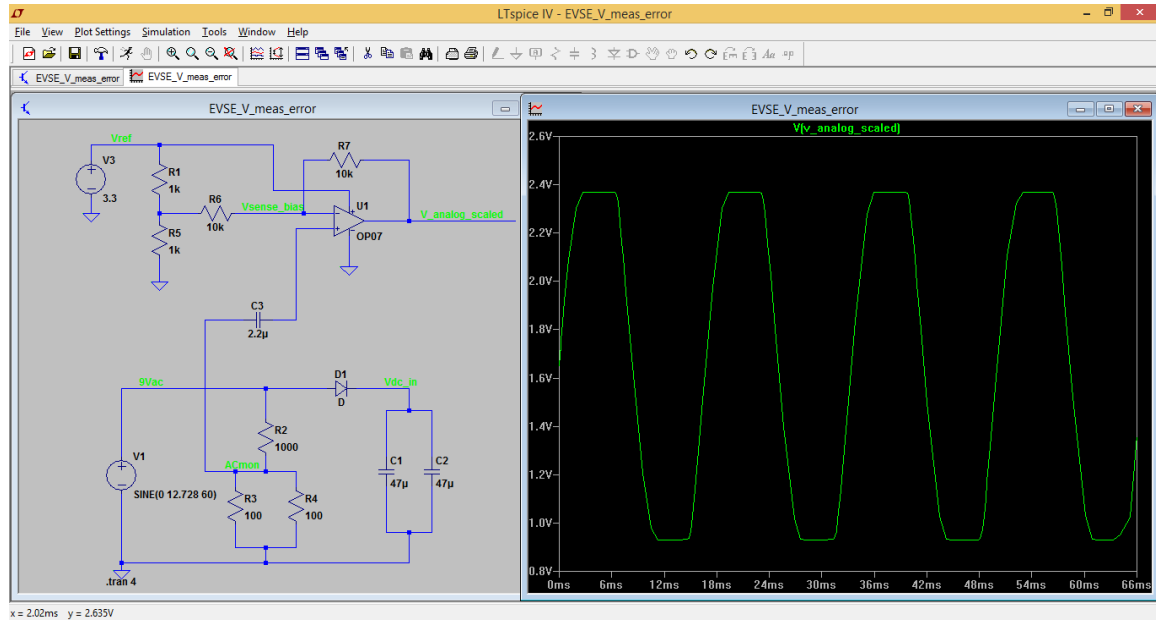


Figure 28: Voltage distortion shown in the initial design

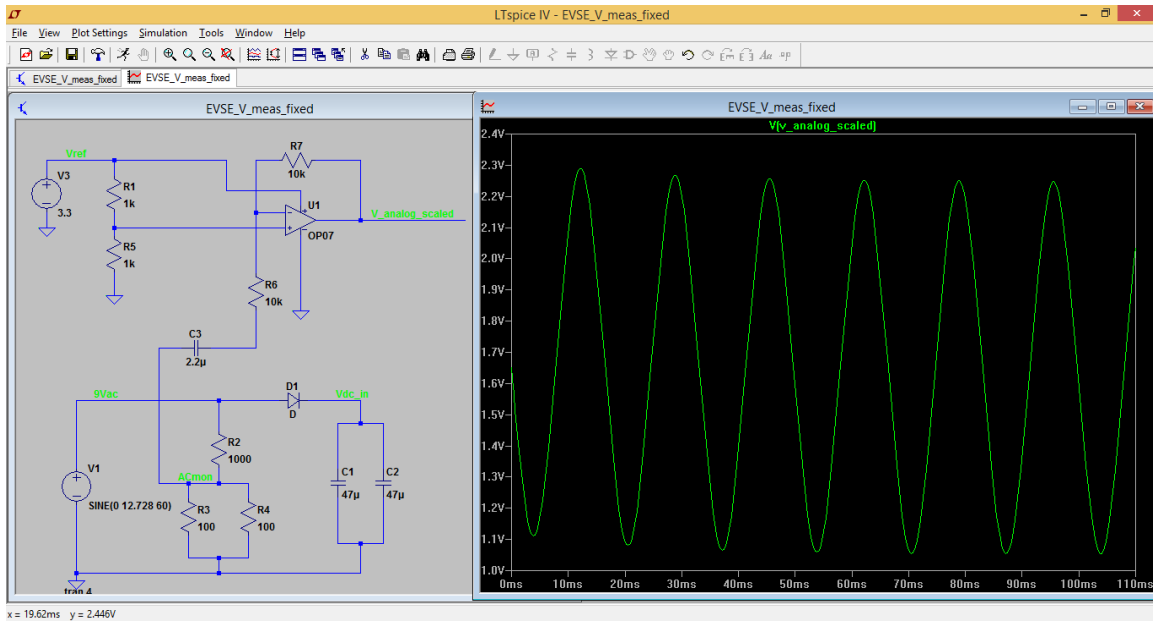


Figure 29: Voltage distortion repair in the modified circuit, with inverting op-amp

Current input and processing

The hardware design leverages a 50 Amp CT, placed across L1 on the EVSE, in order to measure the current footprint of the vehicle charging (note that for ease of installation, some of the parasitic current drain of the EVSE are included in this measurement). The circuitry converts the input from the 50-amp CT (where $0.33 V_{RMS}$ corresponds to $50 A_{RMS}$) and scales to $3.73V_{PP}$. Due to the $3.3V_{Ref}$ of the Arduino Due, this leads to a maximum amperage of 40A at 220V, which is well above the $\sim 33A$ maximum expected from the current highest-kW charging vehicle (Tesla Model S) at the installation site. In order to protect the circuitry, the board is also configured to provide the EV with a maximum PWM signal of 50% duty cycle (30A), and has automatic relay shutoff protection should that exceed 35A, in firmware.

The circuit design utilizes a single-supply differentiator op amp with difference amplifier to receive the input, and bias up to the midpoint of the voltage reference (1.65 or 2.5V depending on the jumper configuration). The amplifier circuitry is designed to provide a -3 dB cutoff at 1.59Hz. The design of the current amplification and buffering are shown in Figure 30.

The scaled and properly-biased current inputs are connected to the Arduino's analog input A4.

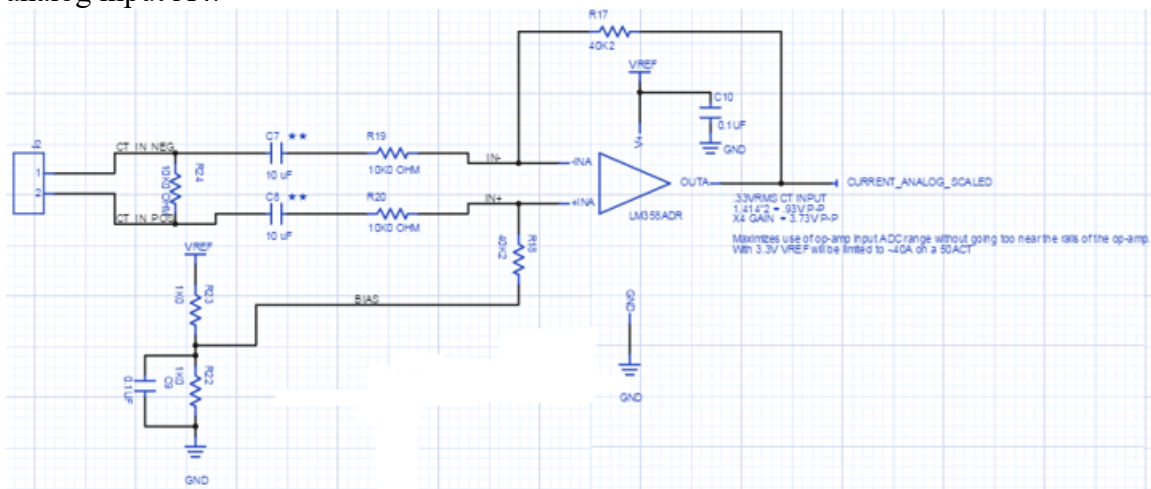


Figure 30: Current measurements on the J1772 intercept board

EVSE to board PWM signal input and processing

The resistance/PWM inputs from the EVSE to the hardware board are connected to the analog input A1. This input is wired to read the signal from the EVSE, and incorporate the resistors that would signal to the EVSE that the vehicle is connected and ready (State B; $2.74\text{k}\Omega$ and $V_{\text{POS}}=9\text{V}_{\text{DC}}$) or ready to charge (State C; 882Ω and $V_{\text{POS}}=6\text{V}_{\text{DC}}$). In order to comply with the J1772 specification, these resistors set the positive peak voltage for the current state, while the negative peak voltage is always at -12V.

The J1772 specification also includes a third state, with a resistance of 246Ω , or $V_{\text{POS}}=3\text{V}_{\text{DC}}$. This state indicates to the EVSE to turn on a connected vent fan, because of

hydrogen release associated with lead-acid battery charging. Because none of the vehicles participating in this research use lead acid batteries (and no commercially-available EVs using J1772 do), this state is ignored. The circuit design for the board to EVSE communications, including Arduino PWM out on digital pin D3, and resistance relays for ready (D6) and connected (D5) are highlighted in Figure 31.

Setting the connected state (D5) to high brings the resistance level as seen by the EVSE to State B, and having both ready state (D6) and connected state high sets the resistance to State C.

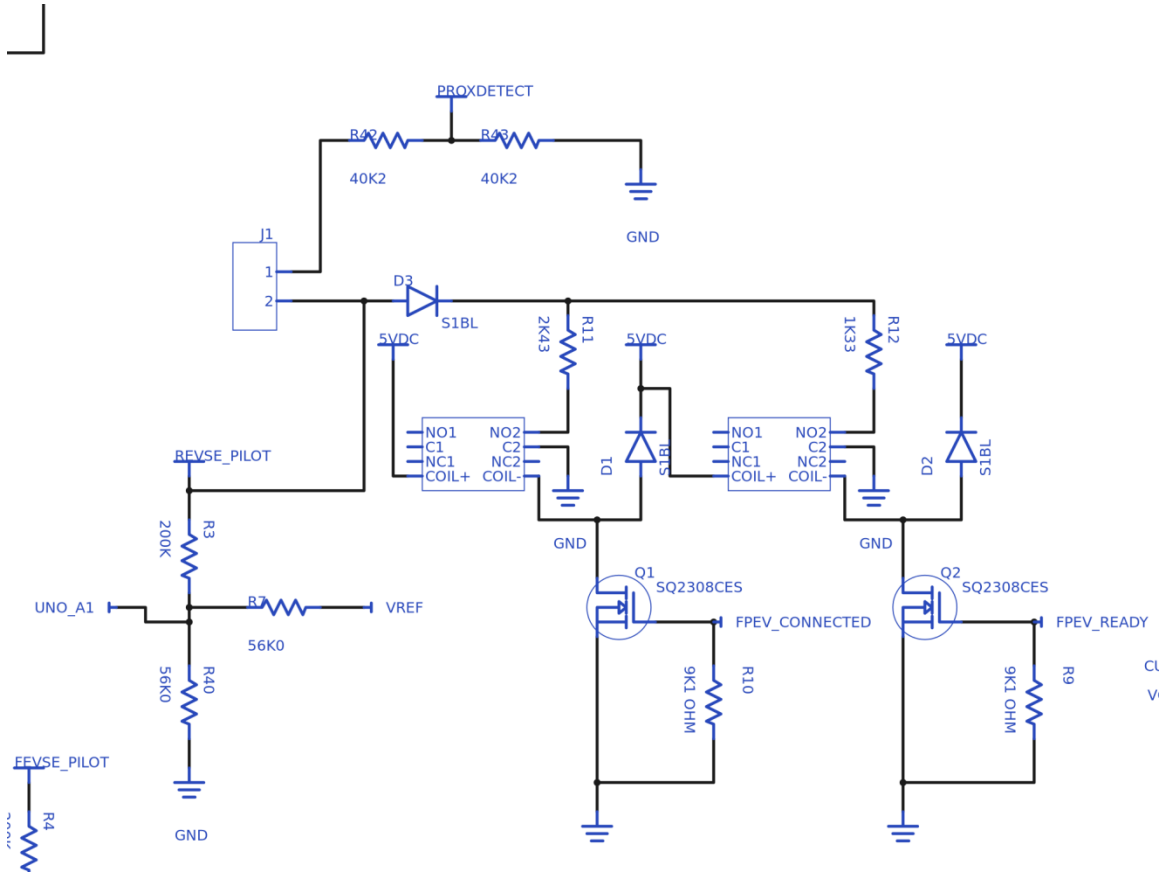


Figure 31: Circuit design for the communications between board and EVSE

EV to board PWM signal input and processing

The analog pin A0 provides the Arduino with the resistance levels provided from the EV, combined with the output PWM signal generated from the J1772 intercept board. This allows the A0 pin to provide a scaled view of the PWM signal as received by the EV, as well as to read the vehicle's state based on the positive peak voltage.

Printed Circuit Board Design

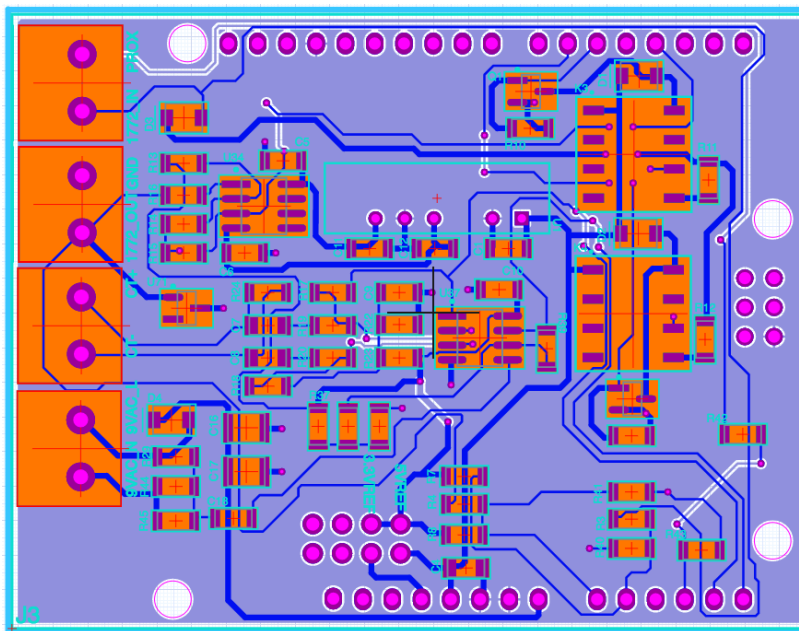


Figure 32: The PCB layout of the J1772 intercept board.

FIRMWARE DESIGN

The firmware for the application was developed by the author, designed to provide several features to support the research. The architecture for the firmware was developed to interface with an EV research server, running additional software, communicating via UDP.

Clock synchronization

During the initial setup of the firmware when it comes online, and every 10 minutes, the device sends a “time request” message to the IP address of the research server. The research server responds by broadcasting (to all clients) the current time, which is synchronized against a GPS time reference. The firmware then tracks the incoming packet and the time (against the Arduino’s internal millisecond counter) when it was received. For all communications back to the server, these numbers are shared back with the server. Given that the Arduino does not have an intrinsic architecture for handling 64-bit unsigned long integers, these data are sent instead as the 64-bit number last received from the server, and the millisecond differential between the current time and time reference receipt.

Waveform Capture

Every 330 microseconds, analog samples are taken and converted from the voltage, current, pilot to EV, and pilot to EVSE registers, and stored in their appropriate arrays. These arrays are designed to be sized as powers of two (e.g., 256 samples), to facilitate fast Fourier transformations at set intervals. By default, due to the large amount of bandwidth that would be taken up by transmitting these waveforms, only high level data are presented every 250 ms (e.g., VRMS, IRMS, EV and EVSE duty cycle and positive peak voltage). However, individual waveforms can be turned on or off, which would be transmitted as well. When these waveforms are transmitted, the time differential is also passed, to ensure that any appropriate computational algorithms have the needed tuning parameter.

Data computation

At the end of every waveform capture, the collected waveforms are analyzed to produce several values that are compared to previous ones. When the delta between the

recent and prior ones passes a certain threshold, a delta notification is logged and passed to the server. The following values are computed:

- RMS Voltage (off the Voltage waveform)
- System frequency (through signal analysis of the voltage waveform)
- RMS Current (off the Current waveform)
- Real Power
- Apparent Power
- Power Factor
- EV V_{MAX}
- EVSE V_{MAX}
- EV PWM Duty Cycle (0-255; for internal validation of the PWM generator)
- EVSE PWM Duty Cycle (0-255)

Once a second, the voltage and current waveforms are ran against a fast Fourier transform (FFT) to convert the sample into the frequency domain. This data are analyzed to compute the total harmonic distortion (THD), relative to the fundamental. The Fourier waveform can also be transmitted to the server, on request, and is logged.

Finite State Machine

In order to ensure the proper functioning of the device, and compliance with the 1772 specification, the firmware uses a finite state machine. The parameters of the finite state machine are highlighted in Table 4. There are two main modes for the system; the finite state machine is designed to step through the appropriate handshaking so that the timing parameters can be determined, and the vehicle charged. However, a simple bypass mode also exists to attempt to recreate whatever resistance level is offered to the board to

the EVSE, and whatever pilot signal duty cycle is presented to the board to the EV. This special diagnostic mode is intended only for testing purposes.

Index	Description	Condition for exit	State after Exit	Changes
0	Initialization		1	PWM=100% Ready=false Charging=false
1	Wait for EV plug-in	$V_{EV,Max} = +9\text{ V}$	2	
2	Signal EVSE plug-in		3	Ready=true Charging=false (EVSE sees 9V)
3	Wait for EVSE to provide a PWM	$V_{EVSE, Min} = -12\text{ V}$	4	
4	Start generating a PWM signal to EV	-	5	PWM=Min(50%, DR rate)
5	Wait for EV signal ready to charge	$V_{EV,Max} = +6\text{ V}$	6	
6	Signal to EVSE, ready to charge		7	Ready=true Charging=true (EVSE sees 6 V)
7	Charging underway	$V_{EV,Max} = +9\text{ V}$	8	PWM=Min(50%, DR rate)
		$V_{EV,Max} = +12\text{ V}$	10	
8	Charging session completed, EV plugged in		9	Ready=true Charging=false (EVSE sees 9V)
9	Wait for EV to be unplugged or charge restarted	$V_{EV,Max} = +12\text{ V}$	10	
		$V_{EV,Max} = +6\text{ V}$	6	
10	Signal EV disconnection		11	Ready=false Charging=false (EVSE sees 12V)
11	Wait for EVSE reset	$V_{EVSE, Min} > -9\text{ V}$	12	
12	Reset PWM		1	PWM=100%

Table 4: J1772 Intercept Board Finite State Machine (excluding diagnostic and test modes)

Appendix C: Institutional Review Board (IRB) Proposal

As of March 2015, the University of Texas Institutional Review Board (IRB) has approved this research as an exempt study, under study number 2015-01-0073. This proposal covers the interface with the EVSEs for control of electric vehicle charging, presenting EV drivers with different pricing models and occasional survey questions, protecting the identities of the drivers, and ensuring the drivers are protected should adverse events (e.g., insufficient BEV charge) occur. The IRB proposal is presented in the following pages.

1. Title

Zero to sixty hertz: Electrifying the transportation sector while enhancing the reliability of the bulk power system

2. Principal Investigator

Legatt, Michael E., MEL2373, Department of Electrical and Computer Engineering

3. Purpose

This project explores electric vehicles (EVs) from the energy systems engineering, economic, environmental and psychological perspectives. EV Drivers have the capacity to opt in to the research project on a daily basis at the Electric Reliability Council of Texas (ERCOT)'s Taylor, TX campus. In exchange for participation in the study, drivers will be given a reduced rate for charging their vehicles, with options tailored around their preferences. The charging stations (EVSEs) are configured to throttle vehicle charging in order to ensure vehicles are charged within the timeframe specified by the drivers, but optimized on one or more areas:

- Reducing peak demand (e.g., not charging near end of day on a hot summer day)
- Reducing output of vehicle-associated emissions (e.g., charging at higher rates when wind/solar generation are higher).
- Providing controlled reliability support to the grid (e.g., curtailing charging for periods of time of peak demand or insufficient generation reserves)
- Providing local reliability support to the grid (e.g., curtailing charging when system frequency drops below a set point, an indication of a sudden generation or transmission outage)
- Providing cost minimization based on locational marginal price (LMP), a measure of the cost of purchasing energy in the bulk power market at the vehicle's location.
- Providing coordination between multiple EV drivers, such that more than one driver can charge their vehicle during a typical workday

4. Procedures

A participant would pull up to one of the several Electric Vehicle Supply Equipment (EVSE)s located in ERCOT's Taylor, TX parking lots, and plug in the charging cord to their electric vehicle. They would be presented by signage that would instruct them to either use a QR code-enabled smartphone to navigate to the research's mobile website, run a device-specific mobile application, or navigate to a URL after entering the premises.

For the participant's first connection to the system, the website would present the user an electronic consent form (see Appendix C), clearly explaining that they may choose to charge their vehicles without participating in the research. If the user consents to participate in the research, they would be queried for demographic information, information about their electric vehicle, distance to home and other after-work destinations, cell phone number and email address (for notification purposes). If they choose not to participate in the research, they would be transferred to a merchant account site to collect payment for their one-time vehicle charge, at which point their vehicle would start charging.

Furthermore, drivers will be queried for their habitual information in order to support vehicle charge, including access request to their vehicles' battery state of charge, estimated distance to travel home after work, whether they anticipate driving out to lunch, etc. Drivers will provide demographic information and data linkages into their vehicle.

Appropriate precautions will be taken to ensure battery electric vehicles (e.g., Nissan Leaf, Tesla S) will always have additional buffer charge, while plug-in hybrid electric vehicles with gas backups (e.g., Chevrolet Volt, Ford C-Max Energi) may have reduced or eliminated buffers due to their integrated gas backups.

Drivers will, on occasion, receive surveys on their impressions of their electric vehicles, economic preferences in selecting charge rates and test messaging to identify means of maximizing driver situational awareness (SA) about the state of the power grid, and the role they can play in supporting reliability and reducing energy costs.

a. Location

All data collection and study activities will occur at ERCOT's Taylor, Texas facility, at the research test site. The charging stations are in the gated/access-secured TCC-1 and TCC-2 parking lots of the ERCOT facility. The data storage system is an access-secured and file-encrypted server located in one of the Primary Investigator's offices, either at UT Austin, or ERCOT Taylor.

Agencies involved in the research are Electric Reliability Council of Texas, Inc., University of Texas at Austin. Additional participants may have access to anonymized data due to their participation in the collaborative research, such as Pecan Street Project, Austin Energy, Intel Labs, CURB, and Circular Energy.

b. Resources

This research will be supported primarily through ERCOT, with additional support for equipment and expertise provided by UT.

c. Study Timeline

The project will take approximately one year from data collection to published results.

5. Measures

All study measures will be collected electronically via the research mobile application, in the form of surveys and free-form questions. There will be no formal interviews with participants. Upon beginning the project, the participant will answer no more than 5 survey questions focused on their perceptions of electric vehicles, cognizance of the bulk power system, understanding of impacts on their driving behaviors (whether gas or electric vehicles) on the environment and their spending. In addition, the participant will fill out profile information about their personal life and their electric vehicle. At later points in the project, surveys consisting of no more than five questions will be answered by the participant in order to see if any behavioral changes occur. In Appendix A, several examples of life cycles are shown in order to demonstrate how participants would use the application and/or website. In Appendix B, a list of all possible survey questions are shown. No questions other than the ones explicitly defined in the research proposal Appendix B will be presented to users. Should any additional questions be determined to be appropriate to the research, they will be proposed to the IRB in the form of an amendment.

“Free-form questions” refers to demographic data collected that cannot be measured in a multiple-choice question. For example, “How many miles do you drive from your home to this office?” All of these free-form questions will be asked during the initial signup in the demographic data collection of the process

6. Participants

a. Target Population

The target population is ERCOT, Inc. employees and visitors who drive and park electric vehicles in its Taylor, TX parking lots.

It is unknown how many participants will be included in the study. All electric vehicle drivers who utilize ERCOT Taylor’s EV charging infrastructure will be invited to participate. The goal would be to maximize participation, but changing trends in EV driving may lead to changes in the number of participants or charging sessions that the research acquires. Because the system is electronic, there are no additional resource implications of increased participation.

It is unknown what participant ages will tend to be. It is estimated that ERCOT EV drivers will be at the lower end in their mid-twenties (presuming college plus potentially graduate school, paired with the resources necessary to purchase an electric vehicle), up to a retirement age, which is estimated at 65. At the time of this writing, EV drivers charging at ERCOT’s Taylor site range from mid-thirties to mid-fifties.

b. Inclusion/Exclusion

Any EV-driving participant who wishes to participate in the research project may do so, and any EV driver who opts not to participate is able to bypass the research in order to charge their vehicle.

c. Benefits

Participants can expect a net positive economic benefit from participating in the study, as the cost of charging their vehicles will be reduced relative to the base price for non-participants. Participants will also receive documentation at the close of the study, indicating the conclusions of the study that will help them optimize driving and charging decisions.

If users would like, they are welcome to link their home systems (thermostats, smart meters, circuit breaker-level telemetry, home EV charger and PV panels) in order to view a total-home or per-circuit estimated total energy consumption footprint, which can help in situational awareness, and help inform decisions about shaping energy behaviors based on various preferences. Similarly, real-time grid conditions, including system generation/load balance and congestion will be integrated into the research. Participants can also choose to provide their home location, which in turn will give additional situational awareness about the adjacent transmission system's state.

d. Risks

There are no anticipated psychological or physical risks for a participant participating in this study. The only known potential risk to an EV driver is that their car will not be sufficiently charged at the moment they depart ERCOT's parking lot. To mitigate this, controls are put in place in the management software in order to ensure that vehicles have sufficient charge half an hour before the estimated departure time. Furthermore, battery electric vehicles (with no backup generation) will be charged before extended range EVs.

Due to the protective systems built into electric vehicle charging stations, no commands can be sent to vehicles that would induce harm to the vehicle, void its battery warranty, etc. Power flow will always be unidirectional, from the grid to the vehicle.

In the event that an EV driver needs to depart and has insufficient charge due to some component of the study, alternative and timely transportation will be provided to the driver at the expense of the project.

e. Recruitment

Known ERCOT employees who drive electric vehicles will be invited to sign up for the research project via an email. Anyone wishing to charge his or her EV will be invited to participate in the research project at the point of sale.

f. Obtaining Informed Consent

Informed consent will be provided and signed electronically, as part of the EV research site. No deception is involved in this study.

Due to ERCOT market rules, sensitive market data such as the real-time state of Texas' power plants cannot be displayed to non-ERCOT employees. Therefore, they will be displayed grid-status data from one-year prior, with a clear indication this is being done in order to protect critical infrastructure data.

7. Privacy and Confidentiality

The project will ensure the privacy via a database system that maintains random tokens to represent drivers, and the driver demographic and information data will be stored in a separate database with separate encryption in place for each database. All communications between participants and the research system will be conducted over SSL, in order to reduce possibility of data interception.

Additionally, all user data will be stored on the server using asymmetric key cryptography, such that the demographic data can only be accessed or updated by the user in combination with their username/password for the research, which will be hashed to provide their private key.

Due to the architecture of the database system, the identifying information (name, email, etc.), as stored in encrypted separate tables, will be deleted one year after the termination of the study. This will allow anonymized data (with few demographics, including age, sex, household income and zip code only) to be retained indefinitely.

Electric vehicles have only begun entering the Texas mainstream in 2011, with the release of the Chevrolet Volt and Nissan Leaf electric vehicles. Since it is anticipated that EV market growth may lead to changes in consumer EV purchasing, scheduling, and driving behaviors, it would be helpful to have limited demographic information (age, miles driven, educational level, vehicle make and model) to provide a basis of comparison to future studies.

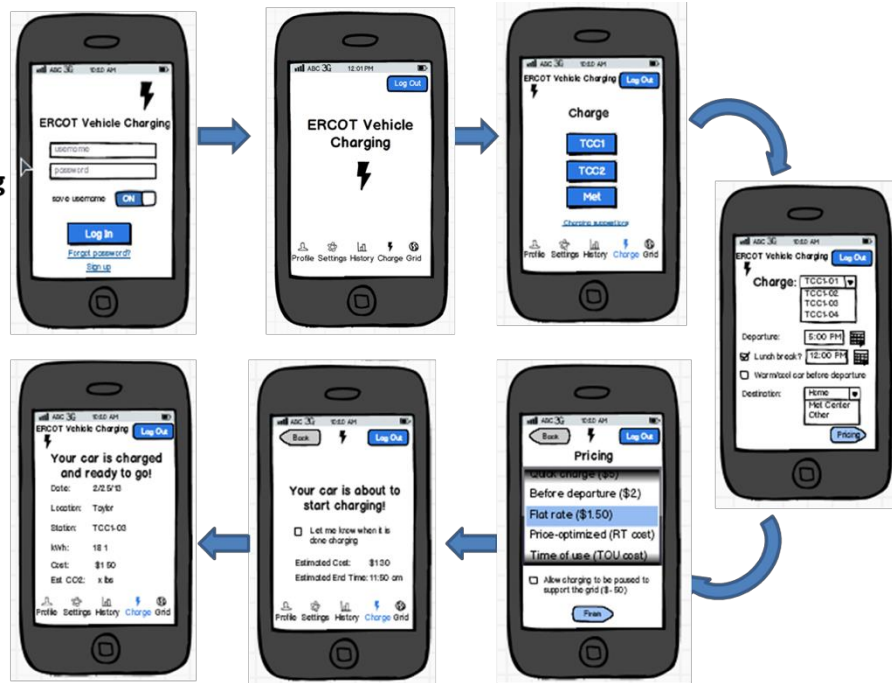
8. Compensation

Participants' only compensation will be in the form of reduced costs for charging their vehicles, in exchange for their participation in the research on a particular day.

Life Cycle Examples



Normal Charging



Waiting to Charge



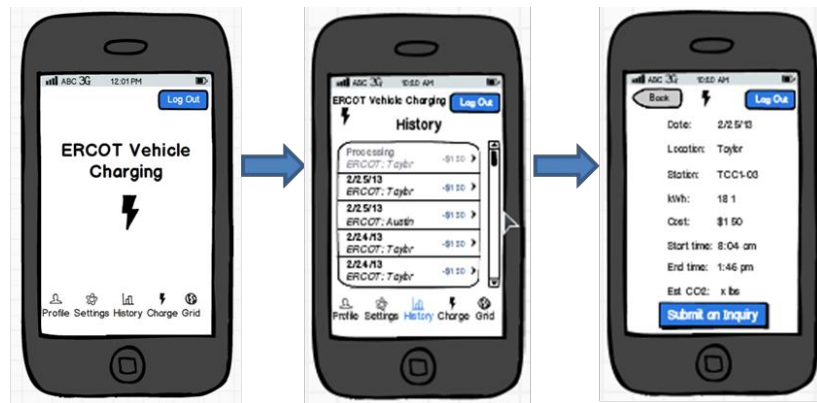
Check State of Grid or Weather



Change Notification or Critical Event Settings



Check Charging History and Payments



Normal Charging with Survey Questions



Survey Question Examples

- 1) I feel driving an EV creates less CO2 emissions than driving a gas vehicle.
 - a) Strongly agree
 - b) Agree
 - c) Disagree
 - d) Strongly disagree

- 2) I feel driving an EV costs less than a gas vehicle over the life of the vehicle.
 - a) Strongly agree
 - b) Agree
 - c) Disagree
 - d) Strongly disagree

- 3) What is your top motivator for purchasing an electric vehicle?
 - a) Environment
 - b) Saving money
 - c) Rebate(s)
 - d) HOV lane access
 - e) Other

- 4) What is your second highest motivator for purchasing an electric vehicle?
 - a) Environment
 - b) Saving money
 - c) Rebate(s)
 - d) HOV lane access
 - e) Other

- 5) What is your third highest motivator for purchasing an electric vehicle?
 - a) Environment
 - b) Saving money
 - c) Rebate(s)
 - d) HOV lane access
 - e) Other

- 6) I installed a Level II charger at my residence
 - a) Yes
 - b) No

- 7) Because of where I live, installing a charger at my residence is not possible
 - a) Yes
 - b) No
 - c) N/A

- 8) My residence already had charging stations installed

- a) Yes
 - b) No
 - c) N/A
- 9) I wish my vehicle had an increased electric driving range
- a) No
 - b) Yes - 10 additional miles
 - c) Yes - 20 additional miles
 - d) Yes - 30 additional miles
 - e) Yes - 40 additional miles
 - f) Yes - 50 or more additional miles
- 10) My current satisfaction level with public charging infrastructure
- a) Extremely satisfied
 - b) Somewhat satisfied
 - c) Somewhat unsatisfied
 - d) Extremely unsatisfied
- 11) I think about my car as a part of the power grid when I'm plugged in
- a) Never
 - b) Every now and then
 - c) Often
 - d) Always
- 12) I have set my vehicle charger to start charging
- a) Any time I plug it in
 - b) In the evening (5-8 PM)
 - c) Late evening (9-11 PM)
 - d) Early morning (12-4 AM)
- 13) Which way of charging your vehicle feels most comfortable to you?
- a) Immediately, when the car is plugged in
 - b) Start at a particular time
 - c) Be fully charged by a particular time
- 14) If you needed to travel 20 miles, what's the lowest estimated EV mile range you'd feel comfortable with today?
- a) 20 miles
 - b) 22 miles
 - c) 24 miles
 - d) 26 miles
 - e) Fully charged

- 15) How comfortable would you be setting your car to charge to [2,4,6,10,15] miles over the distance to your home, in terms of its electric range?
- a) Not at all
 - b) Somewhat comfortable
 - c) It depends on the weather
 - d) Totally comfortable
- 16) How much do changing gas prices make you feel about driving an electric car? (note - this should capture current median gas prices in the home city of the driver)
- a) Less glad you drive an EV
 - b) Neutral / doesn't affect
 - c) More glad you drive an EV

Additional Demographic Questions:

- 1) My current residence is:
- a) House
 - b) Apartment
 - c) Condo
 - d) Single family attached home (townhome, duplex, triplex, etc.)
 - e) Mobile Home
 - f) Other
- 2) I own my home
- a) Yes
 - b) No
- 3) The number of people that live in my residence:
- a) 1
 - b) 2
 - c) 3
 - d) 4
 - e) 5
 - f) 6 or more
- 4) Household income:
- a) \$49,999 or less
 - b) \$50,000 to \$99,999
 - c) \$100,000 to \$149,999
 - d) \$150,000 or more
- 5) I plan to install solar or wind on my home

- a) Yes
 - b) No
 - c) It is already installed
- 6) During working hours (8-5), where do you typically work?
- a) At a home office
 - b) In an office building
 - c) Mobile / traveling
 - d) Not working
 - e) At-home caregiver
- 7) If you have a partner, where do they typically work during business hours (8-5)?
- a) No partner
 - b) At a home office
 - c) In an office building
 - d) Mobile / traveling
 - e) Not working
 - f) At-home caregiver

Online Consent Form

***Informed Consent to Participate in Research
University of Texas at Austin***

You are invited to participate in a research study, entitled “Zero to sixty hertz: Electrifying the transportation sector while enhancing the reliability of the bulk power system”. This study is being conducted by Michael Legatt and Ross Baldick (Electrical and Computer Engineering) and Art Markman (Psychology) of the University of Texas at Austin.

Principal Investigator:

Michael E. Legatt
The University of Texas at Austin
Department of Electrical and Computer Engineering
University of Texas at Austin
Phone: (512) 248-4232

What is the purpose of this study?

The purpose of this research study is to examine your electric vehicle charging and your energy use, as it relates to the bulk power system. Your participation in the study will contribute to a better understanding of ways that electric vehicle charging can better be integrated with management of the power grid, and optimizing ways of communicating to energy consumers about the state of the power grid in order to enhance its reliability. You are free to contact the investigator at the above address and phone number to discuss the study. You must be at least 18 years old to participate.

If you agree to participate:

- The study will take approximately two minutes of your time on days when you charge your electric vehicle, at the time of charging.
- You will provide preferences on charging your vehicle, pick a pricing model that you want to use to charge your car, and respond to surveys on occasion.
- You will not be directly compensated for participation in the study. However, by participating in the study, you will be allowed to choose one of several charging pricing structures every day, and will benefit from a discounted charging rate.

Risks/Benefits/Confidentiality of Data

There are no known risks to participating in this study. By participating in the study, you can access lower rates for electric vehicle charging. Your name and email address will be kept during the data collection phase for tracking purposes only. A limited number of research team members will have access to the data during data collection. Identifying information will be stripped from the final dataset.

Participation or Withdrawal

Your participation in this study is voluntary. You may decline to answer any question and you have the right to withdraw from participation at any time. Withdrawal will not affect your relationship with The University of Texas in any way. If you do not want to participate either simply stop participating and do not access the research application or website further.

Contacts

If you have any questions about the study or need to update your email address contact the researcher, Michael E. Legatt, at (512) 248-4232, or send an email to mlegatt@utexas.edu. This study has been reviewed by The University of Texas at Austin Institutional Review Board and the study number is **2015-01-0073**.

Questions about your rights as a research participant.

If you have questions about your rights or are dissatisfied at any time with any part of this study, you can contact, anonymously if you wish, the Institutional Review Board by phone at (512) 471-8871 or email at orsc@uts.cc.utexas.edu.

If you would like a copy of this form emailed to you, please enter your email address here: [box for email address]

If you agree to participate, click on the OK button at the bottom of this window.

Thank you.

BIBLIOGRAPHY

- [1] Environmental Protection Agency, "DRAFT INVENTORY OF U.S. GREENHOUSE GAS EMISSIONS AND SINKS: 1990-2013," 2 2015. [Online]. Available: <http://www.epa.gov/climatechange/ghgemissions/usinventoryreport.html>. [Accessed 13 4 2015].
- [2] M. Legatt, "Electric Vehicles and Energy Storage: Growth Potentials," 13 July 2015. [Online]. Available: http://www.ercot.com/content/wcm/key_documents_lists/67259/MLegatt_LTSA_EV_EnergyStorage.pptx.
- [3] C. Meehan, "Estimating Emissions Impacts to the Bulk Power System of Increased Electric Vehicle and Renewable Energy Usage," 2013.
- [4] L. Alford, "Austin Energy Electric Transportation Program," in *American Mensa*, Austin, 2010.
- [5] Z. A. Needell, J. McNerney, M. T. Chang and J. E. Trancik, "Potential for widespread electrification of personal vehicle travel in the United States," *Nature Energy*, vol. 1, no. 1, p. 16112, 2016.
- [6] U.S. Department of Energy, "All-Electric Vehicles," 2011. [Online]. Available: <https://www.fueleconomy.gov/feg/evtech.shtml>.
- [7] D. Strohl, "Henry Ford and the Electric Car," 25 5 2010. [Online]. Available: <http://blog.hemmings.com/index.php/2010/05/25/henry-ford-and-the-electric-car/>.
- [8] Z. Shahan, "Henry Ford's Wife Wouldn't Drive Ford Model T, Kept Her Electric Car," 11 4 2014. [Online]. Available: <http://cleantechnica.com/2014/04/11/henry-fords-wife-wouldnt-drive-model-t-kept-electric-car/>.
- [9] M. Koerth-Baker, "Why Your Car Isn't Electric," 7 10 2012. [Online]. Available: http://www.nytimes.com/2012/10/07/magazine/why-your-car-isnt-electric.html?_r=0.
- [10] OpenEVSE Project, "OpenEVSE," 2014. [Online]. Available: <https://open-evse.googlecode.com/files/J1772.pdf>. [Accessed 10 7 2016].
- [11] J. Tomic and W. Kempton, "Using fleets of electric-drive vehicles for grid support," *Journal of Power Sources*, vol. 168, no. 20, pp. 459-468, 2007.
- [12] G. R. Parsons, M. K. Hidrue, W. Kempton and M. P. Gardner, "Willingness to pay for vehicle-to-grid (V2G) electric vehicles and their contract terms," *Energy Economics*, vol. 42, pp. 313-324, 2014.

- [13] X. Lu, L. V. Iyer, C. Lai, K. Mukherjee and N. C. Kar, "Design and Testing of a Multi-port Sustainable DC Fast-charging System for Electric Vehicles," *Electric Power Components and Systems*, vol. 44, no. 14, pp. 1576-1587, 2016.
- [14] J. Channegowda, V. K. Pathipati and S. S. Williamson, "Comprehensive review and comparison of DC fast charging converter topologies: Improving electric vehicle plug-to-wheels efficiency," in *IEEE 24th International Symposium on Industrial Electronics*, 2015.
- [15] M. Endlsey, "Toward a Theory of Situation Awareness in Dynamic Systems," *Human Factors*, vol. 37, no. 1, pp. 32-64, 3 1995.
- [16] R. Sexton, N. Brown Johnson and A. Konakayama, "Consumer response to continuous display electricity use monitors in a time-of-use pricing experiment," *Journal of Consumer Research*, pp. 55-62, Jun 1987.
- [17] K. A. Lattal, "Delayed reinforcement of operant behavior," *Journal of the Experimental Analysis of Behavior*, vol. 93, no. 1, pp. 129-139, 1 2010.
- [18] B. Khan, *Keynote, Energy Thought Summit*, 2015.
- [19] N. Rauh, T. Franke and J. K. Krems, "Understanding the impact of electric vehicle driving experience on range anxiety," *Human Factors: The Journal of the Human Factors and Ergonomics Society*, vol. 57, no. 1, pp. 177-187, 2 2015.
- [20] T. Franke and J. Krems, "What drives range preferences in electric vehicle users?," *Transport Policy*, vol. 30, pp. 56-62, 11 2013.
- [21] S. L. F. C. M. S. Saxena, "Quantifying EV battery end-of-life through analysis of travel needs with vehicle powertrain models," *Journal of Power Sciences*, pp. 265-276, 15 5 2015.
- [22] T. D. Chen, K. M. Kockelman and M. Khan, "The Electric Vehicle Charging Station Location Problem: A Parking-Based Assignment Method for Seattle," in *92nd Annual Meeting of the Transportation Research Board*, Washington DC, 2013.
- [23] I. Lunden, "Mozilla Extends Its Default Google Search Blockout, Signs Up Yandex In Turkey," *Tech Crunch*, 25 3 2015.
- [24] S. Sachdeva, R. Illiev and D. L. Medin, "Sinning saints and saintly sinners: the paradox of moral self-regulation," *Psychological Science*, vol. 20, no. 4, pp. 523-528, 4 2009.
- [25] G. R. Newsham, S. Mancini and B. J. Brit, "Do LEED-certified buildings save energy? Yes, but...," *Energy and Buildings*, vol. 41, no. 8, pp. 897-905, 8 2009.
- [26] U. Gneezy and A. Rustichini, "A fine is a price," *Journal of Legal Studies*, pp. 1-17, Jan 2000.
- [27] Platts, "ERCOT sets two new wind power records," 22 12 2015. [Online]. Available: <http://www.platts.com/latest-news/electric-power/houston/ercot-sets-two-new-wind-power-records-21655980>. [Accessed 17 1 2016].

- [28] Electric Reliability Council of Texas, Inc., "ERCOT Breaks Peak Record Again, Tops 71,000 MW for First Time," 11 8 2016. [Online]. Available: <http://www.ercot.com/news/releases/show/103663>. [Accessed 22 8 2016].
- [29] US Energy Information Administration, "Texas expected to keep breaking records for wind generation and wind capacity grows," 4 Nov 2015. [Online]. Available: <http://www.eia.gov/todayinenergy/detail.cfm?id=23632#>. [Accessed 17 Jan 2016].
- [30] ERCOT, Inc, "ERCOT Analysis of the Impacts of the Clean Power Plan," 16 Oct 2015. [Online]. Available: http://www.ercot.com/content/news/presentations/2015/ERCOT_Analysis_of_the_Impacts_of_the_Clean_Power_Plan-Final_.pdf. [Accessed 17 1 2016].
- [31] Modbus, "Modbus Application Protocol Specification v1.1b3," [Online]. Available: http://www.modbus.org/docs/Modbus_Application_Protocol_V1_1b3.pdf. [Accessed 10 7 2017].
- [32] IEEE, "1815-2012 - IEEE Standard for Electric Power Systems Communications-Distributed Network Protocol (DNP3)," 10 10 2012. [Online]. Available: <http://ieeexplore.ieee.org/xpl/articleDetails.jsp?arnumber=6327578>. [Accessed 10 7 2016].
- [33] C. Kriger, S. Behardien and J. Retonda-Modiya, "A Detailed Analysis of the GOOSE Message Structure in an IEC 61850 Standard-Based Substation Automation System," *INT J COMPUT COMMUN*, vol. 8, no. 5, pp. 708-721, Oct 2013.
- [34] J. Hoyos, M. Dehus and T. X. Brown, "Exploiting the GOOSE Protocol: A Practical Attack on Cyber-infrastructure," in *GC'12 Workshop: Smart Grid Communications: Design for Performance*.
- [35] R. Mackiewicz, "Technical Overview and Benefits of the IEC 61850 Standard for Substation Automation," [Online]. Available: https://www.controlglobal.com/assets/knowledge_centers/abb/assets/IEC61850_Overview_and_Benefits_Paper_General.pdf. [Accessed 20 7 2016].
- [36] G. Wood, "Ethereum: A Secure Decentralised Generalized Transaction Ledger. Homestead Revision.," 2014. [Online]. Available: <http://gavwood.com/Paper.pdf>. [Accessed 20 7 2016].
- [37] B. Schiller, "Is Brooklyn's Microgrid-On-The-Blockchain The Future Of The Electric System?," 18 4 2016. [Online]. Available: <http://www.fastcoexist.com/3058323/is-brooklyns-microgrid-on-the-blockchain-the-future-of-the-electric-system>. [Accessed 20 7 2016].
- [38] ERCOT, Inc., *ERCOT Load Case Study*, 2012.
- [39] NERC, "Reliability Assessment Guidebook," Atlanta, GA, 2012.

- [40] S. Schey, D. Scoffield and J. Smart, "A first look at the impact of electric vehicle charging on the electric grid in the EV project," in *EVS26 International Battery, Hybrid and Fuel Cell Electric Vehicle Symposium*, Los Angeles, CA, 2012.
- [41] W. M. Grady and D. Costello, "Implementation and Application of an Independent Texas Synchronphasor Network," *SEL Journal of Reliable Power*, vol. 2, no. 2, 5 2011.
- [42] S. Mohit, "Charging electric vehicles disrupts power grids less than exected," *ClimateWire*, 28 Oct 2013.
- [43] M. Kefayati, *Harnessing Demand Flexibility to Minimize Cost, Facilitate Renewable Integration, and Provide Ancillary Services*, Austin, TX: University of Texas at Austin, 2014.
- [44] B. Schneier, "Bruce Schneier on Trust," 23 2 2012. [Online]. Available: https://www.schneier.com/news/archives/2012/02/bruce_schneier_on_tr.html. [Accessed 20 8 2016].
- [45] N. Ferguson and B. Schneier, *Practical Cryptography*, Indiana: Wiley, 2003.
- [46] Electric Reliability Council of Texas, Inc., "2015 ERCOT Hourly Load Data," 7 1 2016. [Online]. Available: http://www.ercot.com/content/gridinfo/load/load_hist/native_Load_2015.xls. [Accessed 24 8 2016].
- [47] J. D. Glover, M. S. Sarma and T. J. Overbye, *Power Systems Analysis and Design*, Stamford: Cengage Learning, 2008.
- [48] A. Knight, "Electric Machines: Power and Torque," 15 9 2015. [Online]. Available: http://people.ucalgary.ca/~aknigh/electrical_machines/synchronous/design/power_torque.html. [Accessed 1 7 2016].
- [49] J. H. Yoon, "Demand response control of residential HVAC loads based on dynamic electricity prices and economic analysis," *Science and Technology for the Built Environment*, 2016.
- [50] Energy Star, "Room Air Conditioner," [Online]. Available: https://www.energystar.gov/products/heating_cooling/air_conditioning_room?qt-consumers_product_tab=2#qt-consumers_product_tab. [Accessed 10 7 2016].
- [51] akellyirl, "Reliable Frequency Detection Using DSP Techniques," [Online]. Available: <http://www.instructables.com/id/Reliable-Frequency-Detection-Using-DSP-Techniques/>. [Accessed 30 7 2016].
- [52] San Diego Gas & Electric, "EV Rates," [Online]. Available: <http://www.sdge.com/clean-energy/ev-rates>. [Accessed 10 7 2016].
- [53] Austin Energy, "Residential Service Pilot Programs," 1 4 2016. [Online]. Available: <http://austinenergy.com/wps/wcm/connect/2ec866e7-4556-407b-baed-207b227c9441/ResidentialPilotPrograms.pdf?MOD=AJPERES>. [Accessed 10 7 2016].

- [54] IEEE, "IEEE Standard 1901-2010, IEEE Standard for Broadband over Power Line Networks: Medium Access Control and Physical Layer Specifications," 30 Sep 2010. [Online]. Available: <http://grouper.ieee.org/groups/1901/>. [Accessed 20 7 2016].
- [55] Electric Reliability Council of Texas, Inc., "Fast Responding Regulation Service - Completed," 31 5 2016. [Online]. Available: <http://www.ercot.com/mktrules/pilots/frs>. [Accessed 10 7 2016].
- [56] L. Baird, "Overview of Swirls Hashgraph," 31 May 2016. [Online]. Available: <http://www.swirls.com/wp-content/uploads/2016/06/2016-05-31-Overview-of-Swirls-Hashgraph-1.pdf>. [Accessed 20 7 2016].
- [57] F. L. Weisstein, K. B. Monroe and M. Kukar-Kinney, "Effects of price framing on consumers' perceptions of online dynamic pricing practices," *Journal of the Academy of Marketing Science*, vol. 41, no. 5, pp. 501-514, 2013.
- [58] C. Lamadrid, "Hispanics and Energy: An Insight into Beliefs and Behaviors," 9 2015. [Online]. Available: http://becconference.org/wp-content/uploads/2015/10/presentation_lamadrid.pdf. [Accessed 20 7 2016].
- [59] Electric Reliability Council of Texas, Inc., "January 6 2014 EEA," 7 3 2014. [Online]. Available: http://www.ercot.com/content/meetings/ros/keydocs/2014/0306/ROS_Jan_6_EEA_Report.pdf. [Accessed 20 7 2016].
- [60] M. Legatt, "When Altruism Begins at Home: It Takes a Community of Energy Users," 20 Oct 2015. [Online]. Available: http://becconference.org/wp-content/uploads/2015/10/presentation_legatt_web.pdf. [Accessed 20 7 2016].
- [61] EPA, "Integrated Science Assessment for Particulate Matter (Final Report)," EPA.
- [62] A. Charron and R. M. Harrison, "Primary particle formation from vehicle emissions during exhaust dilution in the roadside atmosphere," *Atmospheric Environment*, vol. 37, no. 29, pp. 4109-4119, 9 2003.
- [63] J. F. Pearson, C. Bachireedy, S. Shyamprasad, A. B. Goldfine and J. S. Brownstein, "Association Between Fine Particulate Matter and Diabetes Prevalence in the U.S.," *Diabetes Care*, pp. 2196-2201, 13 July 2010.
- [64] A. Peters, E. Liu, R. L. Verrier, J. Schwartz, D. R. Gold, M. Mittleman, J. Baliff, J. A. Oh, G. Allen, K. Monahan and D. W. Dockery, "Air Pollution and Incidence of Cardiac Arrhythmia," *Epidemiology*, vol. 11, no. 1, pp. 11-17, 1 2000.
- [65] E. Wong, "Scale of 0 to 500, Beijing's Air Quality Tops 'Crazy Bad' at 755," *New York Times*, 12 1 2013.
- [66] R. Chen, Z. Zhao and H. Kan, "Heavy Smog and Hospital visits in Beijing, China," *Respiratory and Critical Care Medicine*, vol. 188, no. 9, pp. 1170-1171, 2013.
- [67] Y. Chen, A. Ebenstein, M. Greenstone and H. Li, "Evidence on the impact of sustained exposure to air pollution on life expectancy from China's Huai River

- policy," *Proceedings of the National Academy of Sciences of the United States of America*, vol. 110, no. 32, pp. 12936-12941, 5 2013.
- [68] M. Schneiderman, C. K. Cohn and G. Paulson, "Air pollution and urban freeways: Making a record on hazards to health and property," *Catholic University Law Review*, 1970.
- [69] H. C. Frey, A. Unal, N. M. Rouphail and J. D. Colyar, "On-Road Measurement of Vehicle Tailpipe Emissions Using a," *Journal of the Air & Waste Management Association*, pp. 992-1022, 22 feb 2012.
- [70] Austin American Statesman, "Skipping out on inspection sticker costs you, Texas," 15 5 2011. [Online]. Available: <http://www.statesman.com/news/news/local/skipping-out-on-inspection-sticker-costs-you-texas/nRZ5Q/>.
- [71] J. Ewing, "Volkswagen Memos Suggest Emissions Problem was Known Earlier," *New York Times*, 18 2 2016.
- [72] Minnesota Pollution Control Agency, "Mobile Sources of Air Pollution," 31 10 2013. [Online]. Available: <http://www.pca.state.mn.us/index.php/air/air-quality-and-pollutants/general-air-quality/motor-vehicle-pollution/health-effects-of-motor-vehicle-pollution.html>.
- [73] S. Cohen, D. C. Glass and J. E. Singer, "Apartment noise, auditory discrimination, and reading ability in children," *Journal of Experimental Social Psychology*, pp. 407-422, 1973.
- [74] jag9889, "Flickr," [Online]. Available: <https://www.flickr.com/photos/jag9889/2393178733/sizes/l/in/photostream/>. [Accessed 4 2013].
- [75] "Western Hemisphere," [Online]. Available: <http://sjp-apes.wikispaces.com/Western+Hemisphere>.
- [76] L. Calderón-Garcidueñas, M. Kavanaugh, M. Block, A. D'Angiulli, R. Delgado-Chavez, R. Torres-Jardon, A. Gonzalez-Maciel, R. Reynoso-Robles, N. Osnaya, R. Villarreal-Calderon, R. Guo, Z. Hua, H. Zhu, G. Perry and P. Diaz, "Neuroinflammation, Hyperphosphorylated Tau, Diffuse Amyloid Plaques, and Down-Regulation of the Cellular Prion Protein in Air Pollution Exposed Children and Young Adults," *Journal of Alzheimer's Disease*, pp. 93-107, 1 2012.
- [77] L. T. Johnson and C. Hope, "The social cost of carbon in U.S. regulatory impact analyses: an introduction and critique," *Journal of Environmental Studies and Sciences*, pp. 205-221, 12 9 2012.
- [78] US Government Accountability Office, "Update on Agencies' Monitoring Efforts and Coal-Fueled Generating Unit Retirements," GAO, 2015.
- [79] Arduino.org, "Arduino Due," [Online]. Available: <http://www.arduino.org/products/boards/arduino-due>. [Accessed 10 7 2016].

- [80] Arduino.org, "Arduino Ethernet Shield 2," [Online]. Available: <http://www.arduino.org/products/shields/arduino-ethernet-shield-2>. [Accessed 10 7 2016].
- [81] E. Howland, "What data centers' growing energy use means for utilities," *Utility Dive*, 10 4 2014.
- [82] Pecan Street Project, "South-Facing Solar Cut Peak Demand from Grid 54% – West-Facing Systems, 65%," Austin, 2013.
- [83] Electric Reliability Council of Texas, Inc., "Distributed Resources Energy and Ancillaries Market Task Force," 19 8 2015. [Online]. Available: http://www.ercot.com/content/wcm/key_documents_lists/72724/TAC_Dream_Report_Draft__2016_01_22_DREAMTF.docx. [Accessed 20 7 2017].

VITA

Michael E. Legatt is the CEO and founder of ResilientGrid, Inc., whose mission is to grow resilient infrastructures by optimizing the human side of the infrastructure management, including situational awareness, decision making support and collaboration tools in normal and emergency operations, and in fostering the kinds of organizational culture (high reliability, just culture) that empower humans to work more efficiently and effectively, lowering human error rates. Dr. Legatt has been a programmer for over 20 years, and worked in the energy, financial, medical, neuroscience research and educational sectors. He has M.A. and Ph.D. degrees in clinical health psychology/neuropsychology from the Ferkauf Graduate School of Psychology/Albert Einstein College of Medicine, and M.S.E. and Ph.D. degrees in energy systems engineering from the University of Texas at Austin, and is a Certified Performance Technologist.

As an amateur (ham) radio operator, he received a commendation for helping to provide emergency communications during the 2003 blackout in the northeastern United States, which sparked his interest in the psychology of energy management. He works to build systems designed to provide operators with needed information, optimizing for perception, speed, comprehension, and stress management. He also works at the organizational level to support the growth of the industry's high reliability culture.

Prior to founding ResilientGrid, Michael spent ten years as the principal human factors engineer for the Electric Reliability Council of Texas (ERCOT), which manages the flow of electricity to over 24 million Texas customers, about 90% of Texas' load. There, his development of the Macomber Map® has been featured in the New York Times, National Public Radio, T&D World, and Forbes. The Macomber Map was credited as being instrumental in helping ERCOT operators maintain grid reliability during several record-

setting wind generation levels since 2010, and through several severe weather events since 2009. Macomber Map is now freely available as an open-source application.

He also works on the behavioral aspects of consumer electric use, researching electric vehicle to grid integration, behavioral aspects of conservation and consumer awareness in grid management, and the cybersecurity, behavioral, and reliability issues that arise with integration of new technologies across layers of the grid. He was ERCOT's lead on a collaborative project with the University of Texas at Austin, EV-TEC and the Pecan Street Project to study integrating electric vehicle charging and driver behavioral patterns with the bulk electric system, and still serves as its principal investigator. This research project looks at the viability of EVs to intelligently charge in a distributed fashion and provide ancillary services.

Permanent address: mlegatt@utexas.edu

This dissertation was typed by the author.